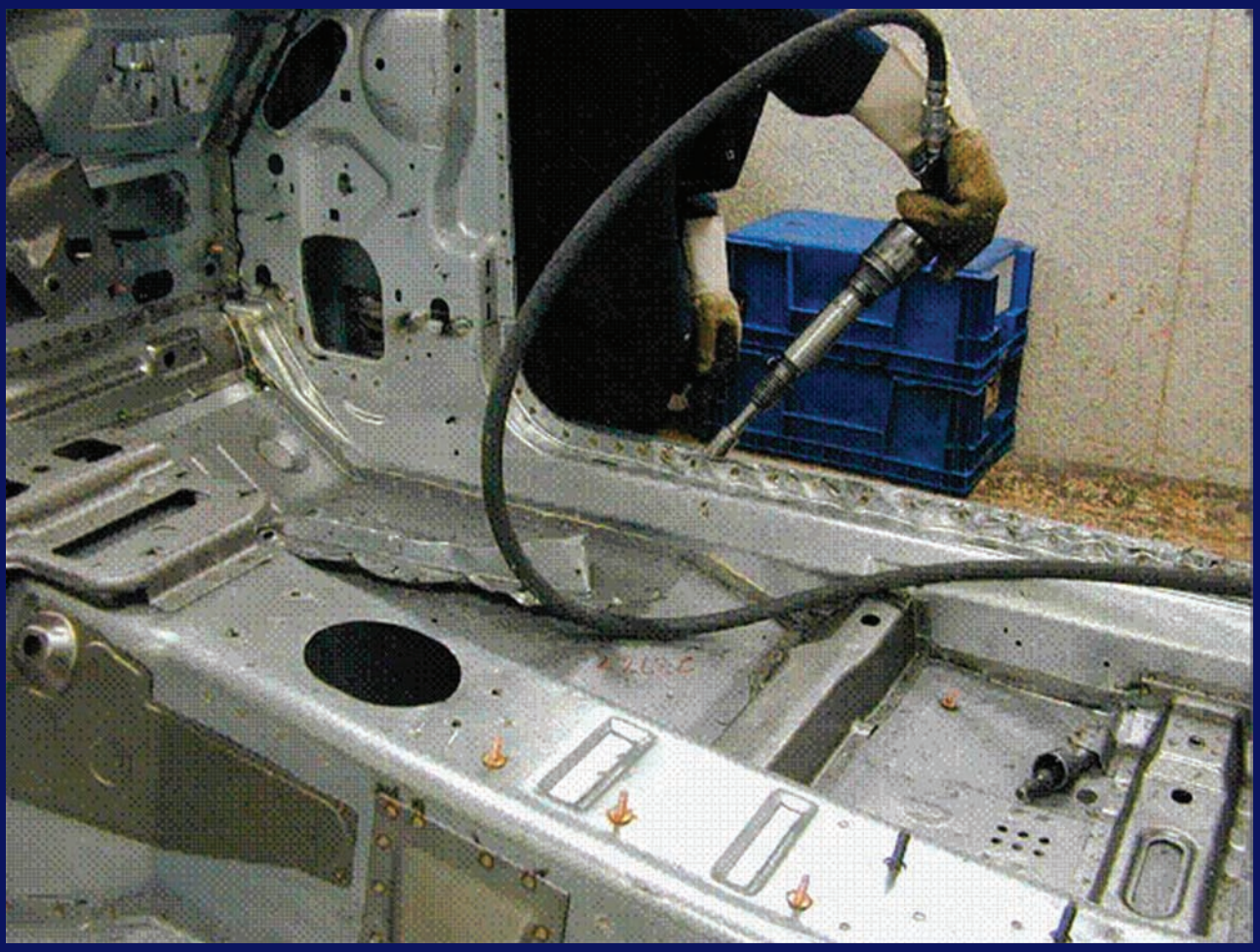

• Figure 1: One lot of samples after testing

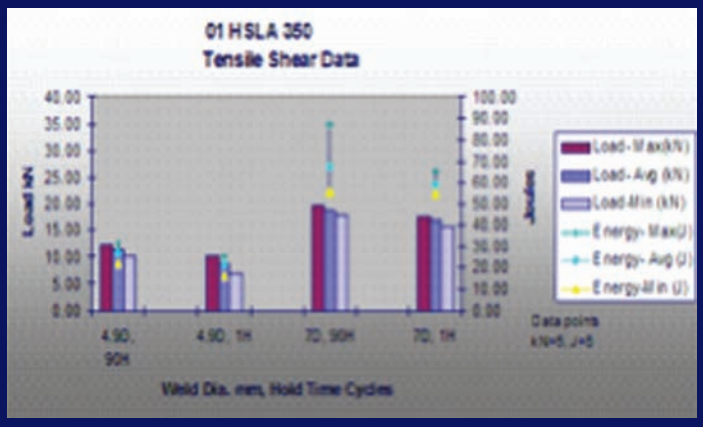

An Investigation of Resistance Welding Performance of Advanced High-Strength Steels

A/S/P Auto/Steel Partnership

www.a-sp.org

Auto/Steel Partnership

2000 Town Center
Suite 320
Southfield, MI 48075-1123
Phone 248.945.4777
Fax 248.356.8511
www.a-sp.org

An Investigation of Resistance Welding Performance of Advanced High-Strength Steels

Viewing this Document. on your computer:

When viewing this document, you can turn on the document map to quickly find any indexed item by clicking on the index in the map. You also can access any item listed in the table of contents by clicking on that item. Activate the "web" tool bar to allow using the forward and back arrows for navigating within this document.

Project Problem Statement

1. Sheet steels that exhibit interfacial fractures (partial or full) in spot welds have been unacceptable to automotive customers for many years for various reasons. As reported by Mitchell and Chang[1] from Ford Motor Co., welds with interfacial fractures have lower direct tension strength, and interfacial fractures lower impact properties of the welds. Sawhill and Furr[2] report similar findings and also report that partial interfacial fractures reduce current range because the weld button can be significantly smaller than the fused area, requiring higher minimum welding current to achieve the minimum button size.

2. Interfacial fracture modes also cause problems in meeting existing weldability qualification standards.[3,4] They are an unacceptable fracture mode in the establishment of minimum current levels and in the hold-time sensitivity test. Because interfacial fractures may prevent a material from passing automotive welding qualification standards, it is essential to know which factors promote such fractures and how to avoid or minimize them.

3. The issue facing the producers using resistance welding is to determine if interfacial fracture concerns with lower grades of steel are applicable for AHSS materials. Generally, all standards existing as of 1999 are based on welding of mild steels. The diminished performance of welds exhibiting interfacial fracture was generally accepted for steel grades below 420 MPa. Even in the low strength materials, interfacial fracture is accepted when welds are made in thick materials and in structures having mechanically stiff sections. These requirements for lower grades may not apply to AHSS grades.

Project Objectives

1. The objective of this work was to characterize AHSS weld properties produced using conventional processes. By collecting this data, designers can determine if the characteristics are suitable for use in specific automotive applications and be assured the welds can be achieved in their production environment. Much investigative work provides reports of welding performance that cannot be reproduced in production for various reasons, such as use of non standard sample design, laboratory equipment with unreported response characteristics and use of non standard testing practices.

2. Develop fracture classifications that can be used to grade welds related to their expected performance based on visual observations of destructive in process checks.

3. Determine if weld button pull requirements for lower grades of steel are a relevant strength indicator for resistance welds in AHSS.

4. Document and report all the testing equipment characteristics used to produce the test welds

5. Report the chemistry and physical characteristics of the base metal actually tested.

6. Determine static and dynamic properties and micro hardness of welds made using conventional welding processes and standard test methods where they exist.

7. Report fatigue characteristics of welds made with conventional weld practices.

Project Conclusions

1. Based on the test data that evaluated resistance welds using traditional production processes, AHSS materials are higher in static tensile shear strength, higher in impact tensile peak load and energy absorption than the baseline HSLA materials used in this study. AHSS are higher in static and dynamic loading gage-for-gage than DQS and other traditional low carbon steels with yield strength below approximately 400 MPa.

2. Weld lobes were developed for the range of materials studied in this project. The lobes represent a broad range of values that can be used with conventional automotive welding equipment such robotic welding, manual welding and machine welding processes.

3. A tip stabilization/preconditioning sequence was established that reduces variability of reported minimum and maximum weld lobe currents for weld times evaluated. The weld lobe data obtained using this improved procedure should be reproducible within measuring limits between other researchers using similar welding and measuring equipment.

4. Optimum flat sample width was determined for static and dynamic testing of spot welds to reduce the cost of fabricating special formed channels and using special grippers for the test equipment.

5. Using optimum flat sample width, welds were produced representing largest and smallest acceptable weld size and longest and shortest practical hold times.

6. Tensile shear and impact data was obtained for the range of materials and weld parameters studied in this project using a two level two factor experimental design.

7. A fracture classification matrix was established to enable standardize reporting of qualitative data for destructively tested welds. This classification matrix is being adopted by SAE/AWS.

8. Fatigue performance of resistance spot welds was obtained for all the materials in this project. Fatigue testing was performed at two load ratios R=0.1, R=0.3 for all the AHSS materials in this project and compared to base line materials of DQSK, IF, and HSLA. One additional test using full reverse loading (R=-1) was performed to demonstrate the effect of load mode and sample width on fatigue life.

9. Validation of AHSS resistance weld effectiveness was confirmed by applying welding processes developed in this investigation to a AHSS lightweight front structure. This confirmation test demonstrated that the AHSS resistance welded assembly performed to engineering requirements with no remarkable weld failures.

Standard terms and definitions

Terms related to weld test methods are standard terms found in AMERICAN WELDING SOCIETY publication A3.0-2001. Where appropriate for clarity, the text will include sufficient detail to make special terms and abbreviations clear to the reader.

REFERENCES

1. J. W. Mitchell and U. I. Chang, Ford Motor Co., "Resistance-Spot Welding of Microalloyed Steels for Automotive Applications," Proceedings from Micro-Alloying 75 Conference, Oct.1-3,1975, pages 599 - 605.

2. J. M. Sawhill and S. T. Furr, Bethlehem Steel Corp., "Weldability Considerations in the Development of High Strength Sheet Steels," Welding Research Supplement to the AWS Welding Journal, July 1984, pages 203-s to 212-s.

3. AWS D8.9-97, "Recommended Practices for Test Methods for Evaluating the Resistance Spot Welding Behavior of Automotive Sheet Steels," American Welding Society.

4. A/SP Weld Quality Test Method Manual, Rev. 1, 10/31/97.

Team Membership

Phil Coduti	Co Chairman	Ispat Inland Inc
James Dolfi	Chairman	Ford Motor Company
Tom Morrissett		Daimler Chrysler Corporation
Arnon Wexler		Ford Motor Company
Tom Mackie		Auto Steel Partnership
Ray Roberts		General Motors Corporation
Al Turley		General Motors Corporation
Chris Chen		General Motors Corporation
Min Kuo		Ispat Inland Inc/ RoMan Engineering Services
Andy Lee		Dofasco Inc
Eric Pakalnins		Daimler Chrysler Corporation
Maurali Tumuluru		United States Steel Corporation

Consultants

Wayne Chuko	Edison Welding Institute
Charles Orsette	RoMan Engineering Services
Warren Peterson	Ispat Inland Inc/ Edison Welding Institute
Hongyan Zhang	University of Toledo

Project Summary

Background

Phase 1 of this project focused on development of practical weld parameters that can be used in existing welding equipment throughout the automotive industry. Weld equipment representing a typical production resistance welding process was characterized and qualified. All welding was performed using the production type equipment**.** Additionally, welding was performed using the least complicated welding and process parameters. As an example of weld process simplification, all welding used single impulse resistance welding parameters. Single impulse welding represented a preferred process used in the automotive industry for the gages used in this study. Single impulse welds are also preferred for reasons of simplicity and maintainability in production.

Phase 2 of this project focuses on analysis of the mechanical performance of welds produced in phase 1 of this investigation.

The objective of Phase 1 work was to established laboratory techniques, produce welded samples perform mechanical testing and report data for static and dynamic tests. Techniques used to make the test samples were selected to reflect capability of existing automotive production facilities. Data for mechanical tests was collected and reported on individual run sheets for each material and weld condition.

Pre-test work was performed to determine effects of weld tip conditioning, effect of sample width on mechanical test results, and tip pre-conditioning effect on weld lobe current range.

Laboratory tests were used to develop welding lobes. Weld lobes delineate the boundary and range of welding parameters that produce welds exhibiting predictable and stable weld properties. Tests were performed to generate weld lobes on eight grades of steel having both hot dip and galvanneal coatings. Photographs of welds are superimposed on the weld lobes to illustrate weld appearance of the surfaces and cross sections at locations on the weld lobes. Tests were completed for grades of material shown in table 1. HSLA 340 MPa was selected as the baseline for comparison to the higher grades in the test plan. The testing program also produced data for static and dynamic strength and destructive weld test evaluation criteria.

All testing for weld lobe development used established A/SP sample preparation procedures; electrode conditioning and A/SP classifications for evaluation of weld fracture appearance. The equivalent American Welding Society Document D8-9-1998 was developed from ASP work and was the basis for parameter development for this study. During certain development stages, modifications and improvements to the standard procedures were developed. Specifically, the tip conditioning sequence for making accurate weld lobes was developed and verified. Effects of the weld tip conditioning for establishing weld lobes is reported.

The effects of machine characteristics and weld parameters on the nugget fracture and fusion zone were evaluated by physical tests consisting of conventional peel testing, cross sectioning through the fused zone of the welds, fatigue testing and impact testing.

Finally, a simplified DoE was performed to catalog physical test results and characterize quality of welds produced. The work for this project supported development of a fracture mode characteristic diagram and resistance welding quality standard proposal for the industry. This work also provided the basis for upgraded industry standards that establish requirements for material grades above 420 MPa yield strength. The run sheets for welding DoE are contained in the folder labeled source files on this CD.

Table 1 Material grades and coating of materials used in welding DoE test series. Detailed information of chemistry and physical properties is shown in Appendix H.

Material	Coating			Variants
Grade				Source/Heats
HSLA 340		GA	GI	2
DP 600		GA	GI	3/5
DP 800		GA		1/1
DP 980	BARE			1/1
RA 830			GI	1/1
MS 1300	BARE			1/1
TRIP 600	BARE			1/1
TRIP 800			EG	1/1

GA = GALVANNEAL, GI = HOT DIP GALVANIZED , EG = ELECTRO GALVANIZED

A valuable amount of knowledge has been obtained from the research activities on the effects of welding variables, steel variables, and sample preparation. The influence of the variables on static, dynamic and fatigue performance provided directional information on selection of welding and test methods. The result of this work produced general information that can be used by the design and process engineers to determine applicability of weld joint performance produced in a variety of Advanced High Strength Steels. Details of the tests will be found in the appendices of this report.

Two post-heat "hold" times were investigated to determine effects on destructive test results. Short hold time was determined experimentally and was considered minimum clamping time that did not produce characteristic change in peeling effort and weld appearance in setup peel tests. To obtain the short hold time,

the weld timer was set to zero ("0") hold. The actual "hold time" duration while the weld tip was in mechanical contact with the material was recorded. It should be noted that minimum hold time required for flat samples having only single welds can be significantly different that that needed on actual production parts. Unlike actual formed production parts, samples are essentially flat coupons with little tendency to separate due to spring back. Retained stresses in actual formed production parts and stresses caused by multiple welds can require longer hold time to avoid damage to a weld that is not sufficiently cooled before releasing the clamping force.

The long hold time was set to 90 cycles of the 60 Hz ac line current and was the time expected to represent the longest production line hold time and the time that would produce full quenching of the fused weld area. The schematic of a weld sequence is shown below to define portions of the resistance welding sequence. Measured hold time for one weld gun used in the production of test welds is shown in the appendix titled Effect of Gun Design . Note in the schematic of a weld sequence shown here, squeeze time is the total time programmed before heat is applied to the weldment. Hold time is the instrumental programmed time before the mechanical force is programmed to be released.

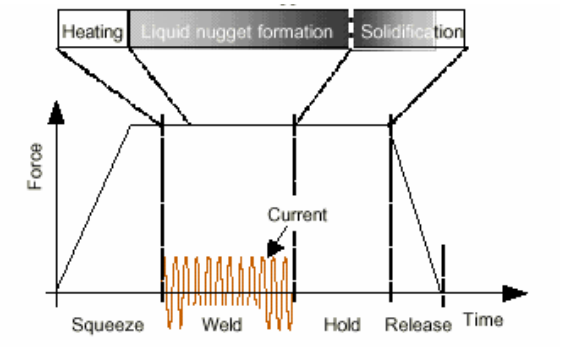

Figure 1 Schematic of a typical weld sequence

Correlation of peel tests fracture appearance to instrumented strength testing is the basis for acceptance of welds made in materials with yield strengths below 420 MPa. A peel test was used to setup each test run. This peel test can be thought of as similar in some respects to a chisel test that produces attribute data of fracture appearance, weld size and operator effort to separate the weld. The resulting joint appearance is subjectively evaluated and the welds are graded based on appearance standards and size measurements. Chisel testing (a destructive weld test shown in the Figure 14) represents an in process checking technique widely used throughout the automotive industry, due to its inherent simplicity and convenience. The issue of fracture appearance and size measurement is a major concern for defining acceptable welds from in-process chisel checks for AHSS and other high yield strength materials. Where button pull is desired as an indicator of weld process control, alternative methods may be needed.

Ultrasonic weld inspection techniques were performed to determine if weld size could be determined using this non destructive technique in AHSS. The results of a laboratory evaluation using a scanning type ultrasonic system are reported in Appendix F.

Weld Gun Characterization

Two weld gun designs, one a straight acting "C" gun, Figure 2 and one pinch/scissor gun, with electrode movement action typically used in production were characterized for gun arm deflection and overall effect on weld characteristics. The major effect of the gun design on weld performance was the nature of weld-tip contact to the steel sheet-tip interface. As expected, the scissor gun produced an initial non-parallel contact with the sheet as shown in Figure 3. The two guns were characterized for stiffness prior to performing tests. The performance and deflection characteristic of each gun are reported in Appendix A. Comparable total deflection was observed for both of the weld guns used in this series of tests.

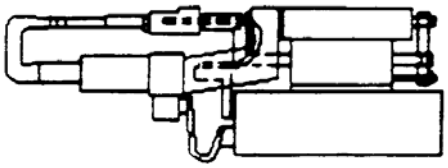

Figure 2 Straight Acting "C" Gun - Tips move in a straight line to contact the work piece. Deflection of the tip holders will cause some pinching as with the scissor gun

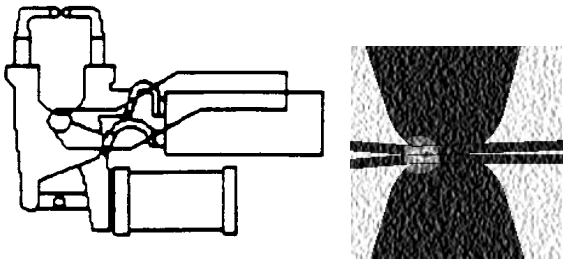

Figure 3 Scissor Gun. Tips move in an arc to contact the material being welded)

Inset shows possible condition of tip contact due to arc of arm movement. Tip will only be aligned to surface of metal when mechanical timing is perfect for a given thickness of metal and tip wear.

The two weld-gun tests confirmed that spot welding is a dynamic process in which the interaction of the local electrode-sheet and the welding machine has an influence on weldability and fracture face characteristics. The use of two weld guns and comparison of weld current phase shift also was evaluated and found to correlate with work performed in former studies done by the IRW[1] program.

Sample Design

Experimental evaluation and prior research data was used to determine the optimum sample width that would measure the weld characteristic. The development of sample width is discussed on Appendix H. Many prior tests used sample designs that profoundly influenced the indicated (observed) joint strength properties and did not accurately represent the weld strength. During physical testing, weld fracture modes were observed to change due to sample design and test load-mode when all other parameters for welding were held constant. The effect of sample stiffness on weld failure mode implies that actual car body welds located in "stiff sections" will also fail with either total or partial interfacial fracture (See fracture classifications in the Appendix J). Interfacial failure is influenced by weld size geometry and stiffness of the section and welds separating interfacially can be acceptable for performance and durability depending on service requirements.

Sample designs were intended to promote interfacial fractures by making the sample relatively resistant to bending during tensile loading. The samples used in this test were equivalent to stiffness of a U channel design shown in the Appendix G. To assure shear forces were evenly applied to the fused weld area, samples were gripped at a distance equal or greater than the sample width from the fused area of the weld. Welds were placed in the center of the overlap area of the specimens.

Note: This work could be extended to aid in establishing FEA modeling for future applications in simulation work for modeling. Samples will be retained for future evaluation by specialists in fracture mechanics and submitted for evaluation by our FEA team member.

[1] IRW Intelligent Resistance Welding program, performed under the DoE project of the Auto body Consortium

Effect of Sample width on impact

The effect of sample width was determined by laboratory experiments and is detailed in Appendix G. The standard width for weld samples is specified in AWS D8.9-97 for lower strength materials. A test was conducted to determine when maximum strength was obtained as sample width was increased. Wider samples produced higher breaking loads and promoted a higher proportion of interfacial failures in both static and dynamic tests of the joints. The objective of using a wider sample was to increase stiffness, and reduce twisting/rotating of the sample when loaded. This reduced the peeling action that promotes button pull-out during testing. The samples provided a better indication of the way welds would react when placed in body sections that typically have stiff section properties. The stiffer sample will show the strength of the weld and heat effected zone. All resistance welded samples for the static tensile and impact testing were made to a width of 125 mm to keep sample fabrication simple and accommodate the highest grade steels used in this project. Sample widths for other tests are noted.

Effect of sample width on Tensile Shear

Additional tests were performed to determine if a tensile shear test could be conducted using sample width that was less than that determined by simply increasing width to obtain highest weld loads. It would be desirable to use samples narrower than 125 mm to conserve material and avoid having to modify conventional sample grips used in many weld testing facilities.

An experiment was conducted using "strong-back" bearing plates to prevent tensile shear test samples from rotating under load and applying peeling action to the welds. Tests using the strong back bearing produced breaking load values similar to those obtained from the 125 mm wide specimens. Except for increased variation due to contact with the bearing plate, as the sample began to separate at the weld, narrower samples could be used as long as yielding does not occur in the sample. See Bearing Plate in Appendix G.

Effect of sample width on Fatigue

One experiment was conducted to determine the effect of loading fatigue specimens in tension-compression cycles. This mode is identified as R=-1 where both positive (tension) and negative (compressive) loads are cyclically applied to the test specimen. Almost all data reported for fatigue strength of weld joints is reported for tension-tension loads only. Typically, fatigue samples are cycled without reducing the tension loads to zero. AS/P fatigue tests use 38 mm wide samples with minimum loading of 10% and 30% of the maximum load (R=0.1, R=0.3). A series of tests was conducted on the

materials using AS/P standard practices where samples are subjected to a constant amplitude loading and a special spectrum loading sequence that varies throughout the test. (See AS/P spot weld fatigue project for detailed testing information and results)

One series of fatigue tests was conducted on the 125mm wide samples of DP-600 material using R=-1 loading. The outcome of the wide sample test at R=-1 was used to determine if additional tests should be performed on the balance of wide samples made for fatigue testing in this project. Since no significant difference in fatigue life was observed for the wide sample and load mode, further testing of the wide samples was not deemed necessary. The wide samples were able to take compression loads up to approximately 10kN before buckling at approximately 11kN. The 38 mm samples were not designed to take substantial compressive loading and were not subjected to compressive loading in any of the tests.

Figure 4 Appearance of 125 mm wide fatigue sample after exceeding 11kN compressive load.

The 125 mm specimens load displacement history. A photograph of the wide sample after testing at 11 kN is shown in Figure 4.

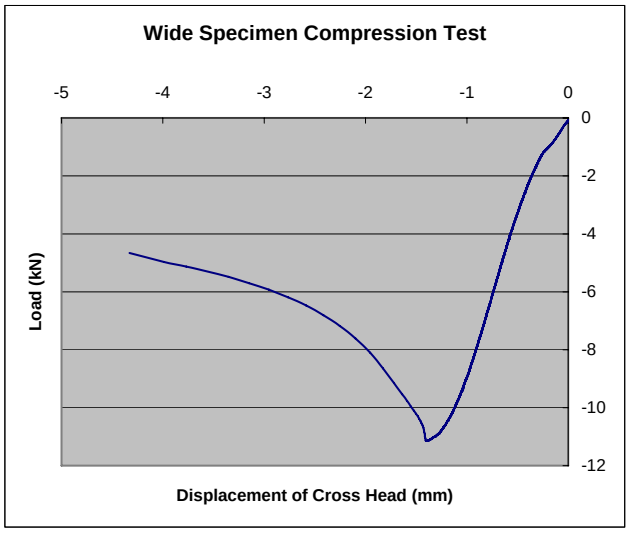

Figure 5 Displacement curve of 125 mm sample compression test

The specimen buckled at a load of 11 kN. The specimen did start showing signs of slight bowing out (or out of plane displacement) near 10 kN see Figure 5.

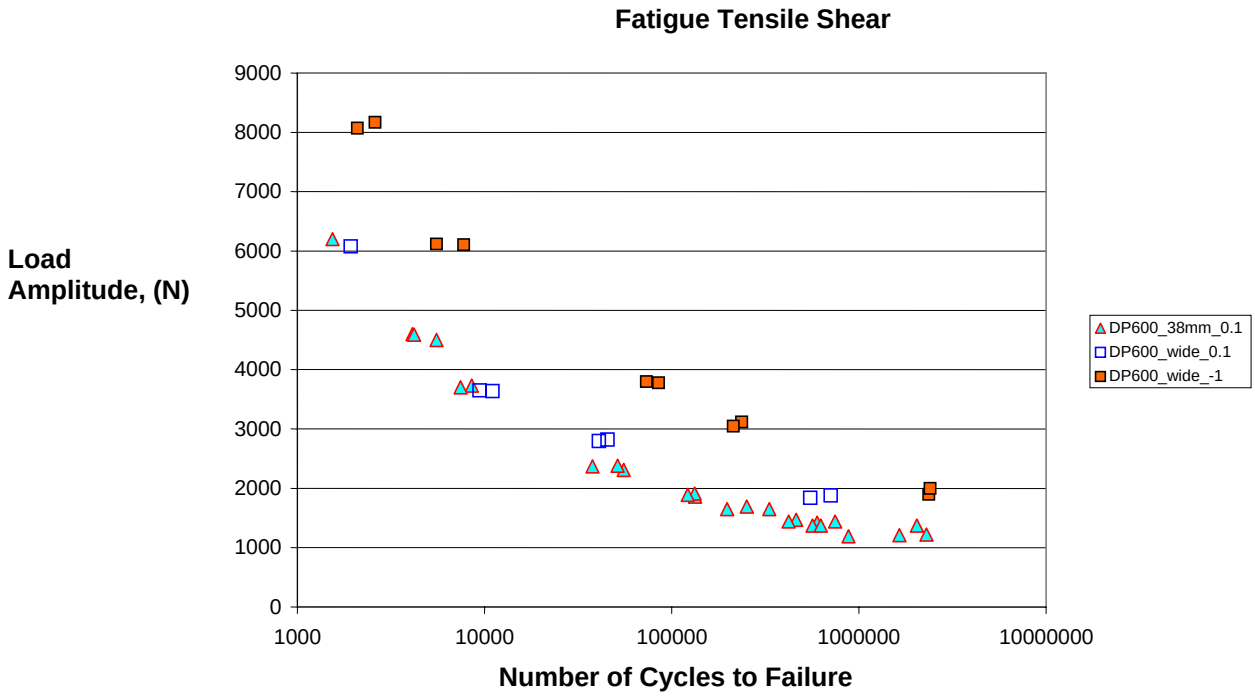

Figure 6 Test of 38 mm and 125 mm wide at R = 0.1

Figure 6 shows effect of sample width on L-N performance. The 125mm (wide) sample run at R = -1 is also compared to 125mm at R = 0.1.

The results of the R-1 wide sample test are compared with several other materials tested using the 38 mm wide samples at R=0.1. The wide sample performance was slightly better than the 38 mm samples. Since buckling was not present on the 38 mm samples and was minimized for wide samples, the mean stress on the wide samples (fully reversed loading) was assumed zero and accounted for the slight improvement in fatigue load-life.

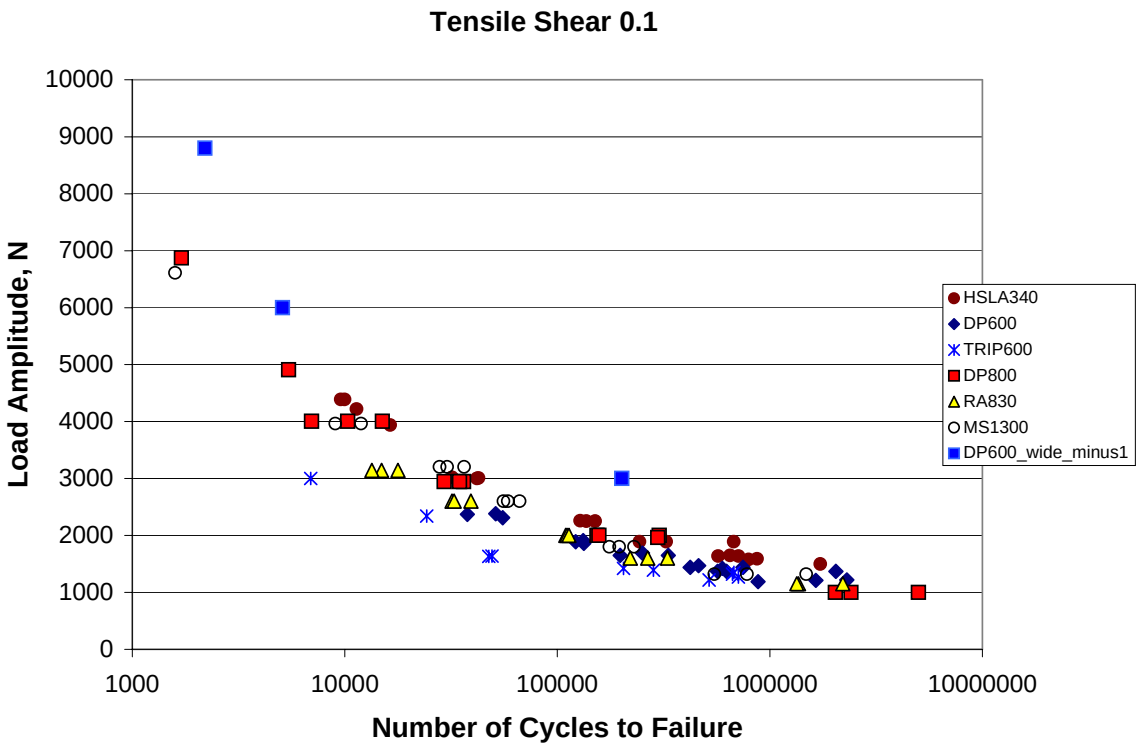

Figure 7 Comparison of fatigue of several 38 mm R=0.1 and 125 mm wide R=-1.

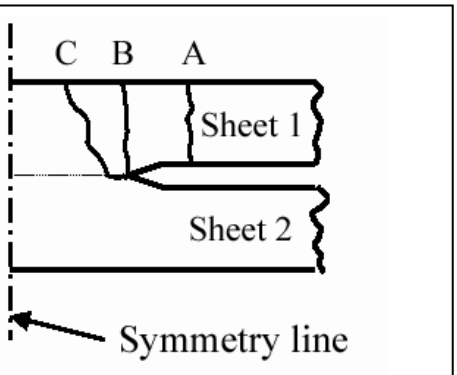

Figure 8 Schematic showing section of weld joint with typical fatigue cracks at failure

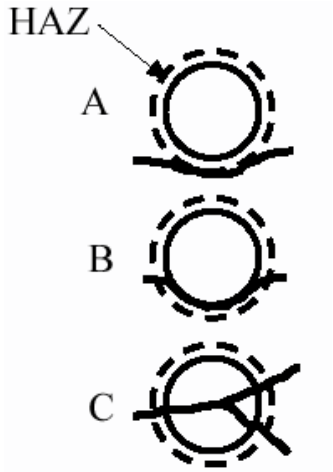

Figure 9 Plan view of typical crack locations produced in fatigue tests

These graphics illustrate typical failure locations seen of fatigue samples. The left graphic shows locations in the cross section of a sample. The right graphic shows a plan view of crack locations. In the detailed reports load levels generally determine where the typical failure will occur.

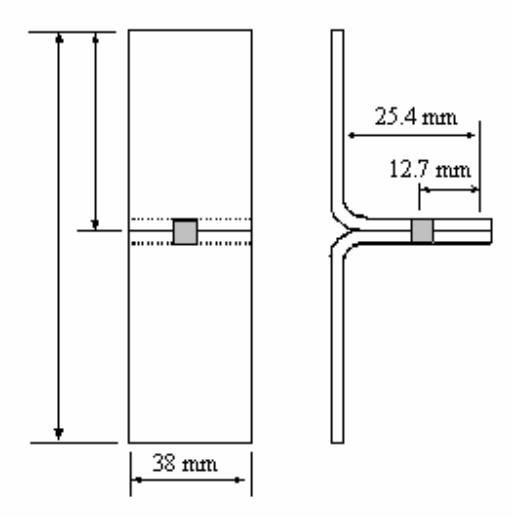

Figure 10 Schematic of coach peel specimen for fatigue testing

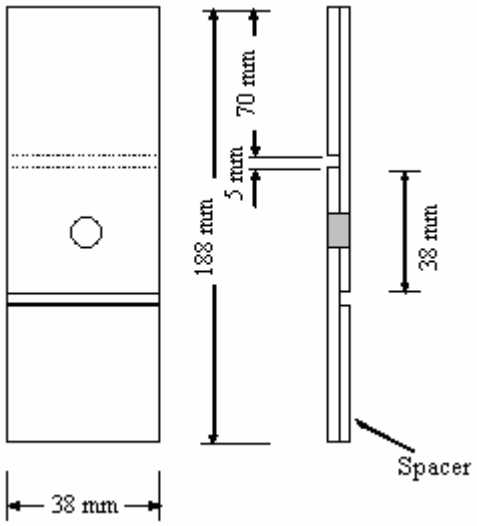

Figure 11 Schematic of tensile shear specimen for fatigue testing

(More fatigue information is contained in the CD file "FINAL-fatigue-phase1-05-28-04 jwd.pdf")

Weld Lobe Development

The purpose for this phase one study was to develop weld lobe windows for the eight grades of high strength steel used in the test series. Two types of weld-guns were using in this series. The two weld-guns are the styles typically used an automotive production resistance welding. The weld guns are identified as a straight acting C-gun and a pinch or scissor type gun. During this work, weld schedules using high and low phase-shift settings and transformer tap settings were used to explore the effect of weld current duty cycle.

Photographic documentation for each weld made during the weld lobe development is used to show the weld condition resulting from a particular weld schedule. Photo macrographs are shown for the welds in the plan view, cross section and as peeled condition.

Numerical material references refer to the coded material identification shown in the "material test matrix". Material 5, Dual Phase 600, was used for developing the weld-tip-conditioning sequence. Material 1,2, and 8 were also tested to explore for potential problems that may be encountered during subsequent development work.

Procedures used to develop the minimum and maximum welding currents reported are taken from AWS/SAE D8.9M:2002. There is no standard method for developing weld lobes in that or any other standard. Consequently, some work had to be performed to develop standard methods for generating weld lobes that were repeatable and cost-effective. Some of the procedures outlined in that standard are repeated here to avoid cross-referencing that standard.

General Conditions for All Weld Testing

Unless otherwise stated, all welding was performed with weld Cap No. 4 as defined in the AWS/SAE D8.9 M:2002 standard. This weld cap (electrode) is fabricated from RWMA class 2 copper. This cap is a 45 degree truncated cone having a flat contact face diameter of 7 mm and a body diameter of 19 mm. Well force is 6.7Kn (1500 pounds). Water flow is maintained at 3.8 liters per minute (1gpm). Temperature of incoming cooling water is below 27 degrees centigrade (81 degrees Fahrenheit). Unless otherwise stated electrode face and weld size stabilization procedures were used for all weld tests and weld hold time was 30 cycles for weld lobes.

Electrode-Face and Weld Size Stabilization Procedure

To compensate for the dynamic behavior of welding current vs. weld size that occurs when making welds on coated materials a stabilization procedure is performed at the start of any test. Details of the stabilization procedure and can be seen in section 9 of the reference AWS/SAE standard. Briefly stated, approximately 80 to 250 welds are made at a current level slightly under the minimum weld size level. The minimum weld size for this test is equivalent to four square roots of the thickness of the thinner material. For these tests, all materials welded together were the same grade and same thickness.

Tip conditioning represented a significant portion of time and cost for all of the tests in this series. One proposed method for developing the weld lobes suggested using one set of welding tips to complete the development of one weld lobe. Using a single weld tip would result in significantly fewer weld caps being conditioned to develop the lobe. It was recognized, that exposing the weld tip to expulsion weld current could significantly change the weld characteristic current levels reported for the following welds made by that tip. Two conditioning methods were used to determine the effect of expulsion on reported weld current.

During the weld lobe development phase of the project, two methods of electrode conditioning were evaluated to determine the effect of electrode conditioning on current levels for I_{min} , I_{max} reported for weld lobes. The comparison of tip conditioning method will aid in understanding variations reported in past literature for current range of a weld lobe boundaries.

Schematic drawing of Approach 1 - one tip used for complete lobe development (zigzag)

Approach No. 1 For Weld Tip Conditioning And Weld Lobe Development:

Perform electrode stabilization procedure. For weld cycles of 16, 22, and 28 cycles, determine minimum (Imin), determine nominal (Inom), determine face (Iface) then determine maximum (Imax) weld current. Using this process, the weld tip conditioning sequence only exposed the weld tip face to expulsion when determining I-maximum. For this sequence, the weld tip may be exposed to many expulsion events. Additionally, the tip would be exposed to many more weld heating cycles prior to making the last weld for the weld lobe.

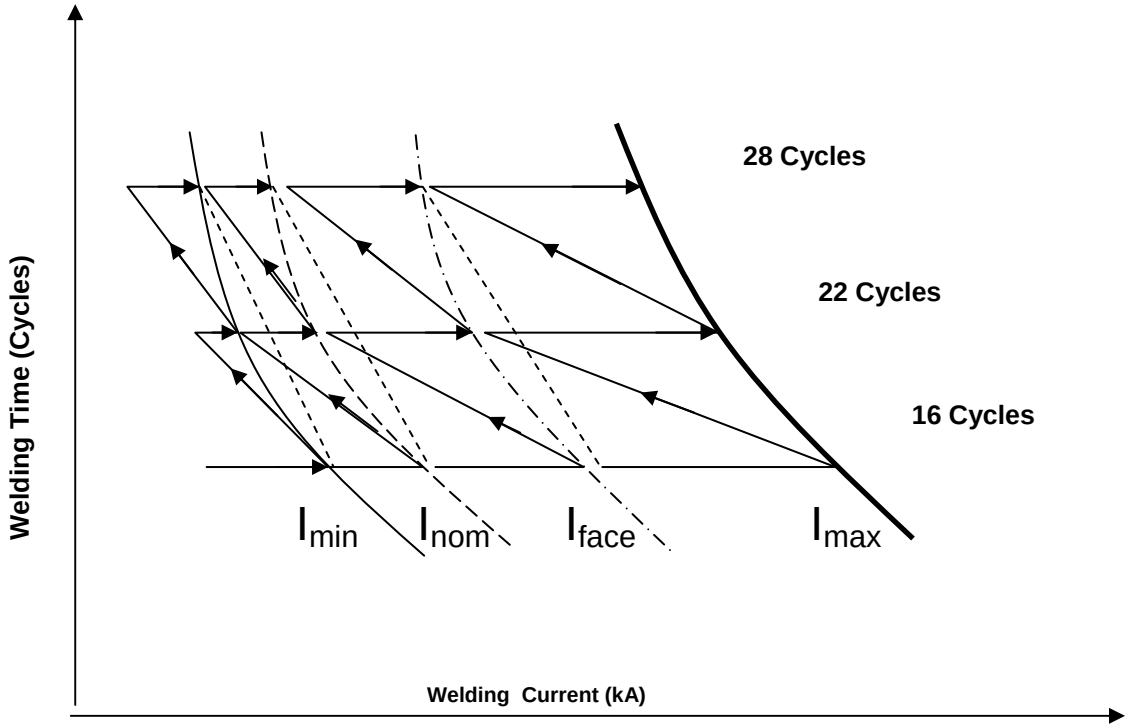

Figure 12 One weld electrode used for complete lobe development

Schematic drawing of Approach 2 – one set of caps for each weld time

Approach No. 2 for Weld Tip Conditioning and Weld Lobe Development

Perform electrode stabilization procedure, using one cap/electrode at each weld time, determine minimum, nominal, face, and maximum weld currents at one weld time. Using this sequence three conditioned weld caps are used, one for each weld time. The effect of using a new weld tip for each weld time improved duplicating the expulsion and minimum current limits.

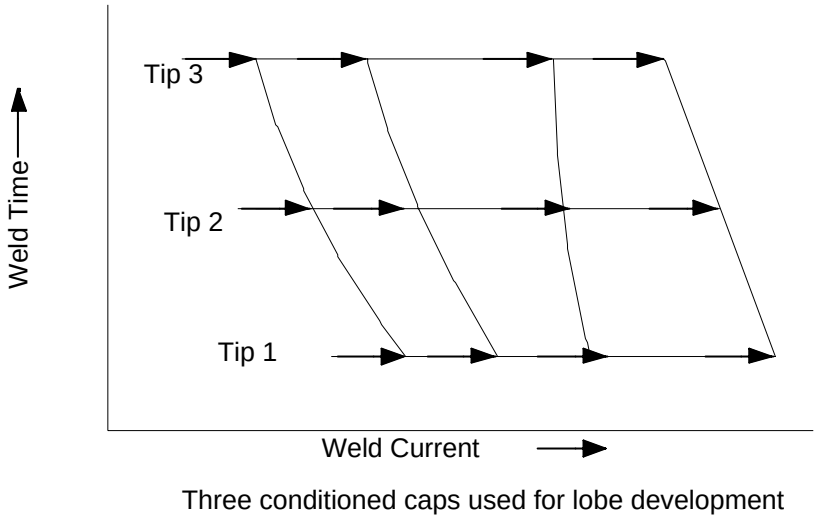

Figure 13 One weld cap used for each weld time for lobe development

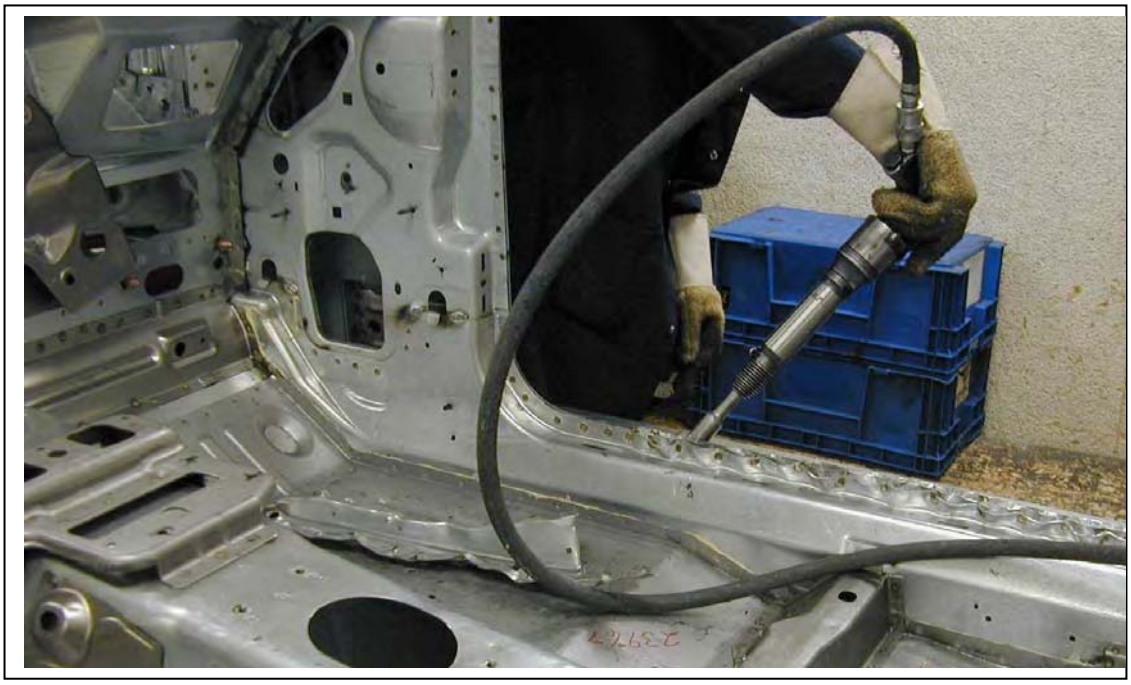

Figure 14 Typical manual chisel check for Autobody weld effectiveness

Destructive testing of actual production (Figure 14) is used to verify weld process effectiveness. Each element of the body is removed and weld size and appearance is recorded. Advanced High Strength Steels may require some modification of this technique to provide more peeling action in heavy or stiff sections. It can be seen that this method is not comparable to the peeling tests used for material acceptance tests (Shown in Appendix D). The manually applied chisel test will have more variation. The chisel is first applied to cause separation of the sheets between the welds causing substantial strain to the material. Finally material is pried apart using the chisel as a lever arm. Each weld tested is subjected to differing straining, impacting and prying. The method is effective for determining many of the weld process characteristics by a trained operator. Additionally, the operator may see that some welds are more easily separated than others leading to generation of remedial action reports.

While this process is costly, it presently has no alternative non destructive cost effective test that is capable of evaluating all the welds in the body. Selected welds that are classified as "non-pryable" are tested with non-destructive methods such as ultrasonic A-scan where cost savings can be realized.
Some manufacturers using AHSS have devised special fixtures that grip the material and peel the sheets from the body structure. This is done in an effort to produce the peeling action similar to that used in laboratory material acceptance tests. Using the peeling fixture, the body sheet metal is prepared by selectively cutting starting and gripping points at strategic locations for the test.

Weld Gun Characterization

Objective: To characterize the mechanical characteristics of welders used for A/SP weldability study, in order to obtain an insight understanding of the influence of welders on weldability of AHSS.

Modern resistance welders usually have good control of electric parameters such as weld current. However, due to mechanical response time, actual response may differ substantially from programmed values on the weld timer. One of the factors in the Joining Committee's project was hold time at two extreme values (0 cycles and 99 cycles). A test was performed to record the difference between programmed values in the weld timer and the actual force applied to the weldment and time the weld tip was in contact with the materials after weld current was stopped. Other mechanical system-related factors, such as response time, etc. were also investigated.

A fixture of three displacement sensors was made to measure the stiffness of the machines. The sensors measured the vertical displacement, rotation of the electrodes, and lateral displacement (skidding). A force sensor was placed between the gun arm and weld tip to record welding force during the weld sequence.

Dynamic response for gun follow-up behavior was determined by placing a 2-mm diameter steel ball between the electrodes. When the current is applied, the ball is heated or melted. This creates a sudden closing action of the electrodes. From the displacement signals, the speed of closing can be estimated. The rate of collapse of the ball for the "C" gun was 113 mm/sec, the "scissor" gun 121 mm/sec.

Test results show that the “C" gun appears stiffer in than the scissor-gun. Additionally, the follow-up experiments indicate these two guns have very similar follow up characteristics.. A chart of both gun arm deflection measurements is shown for a range of welding forces is below.

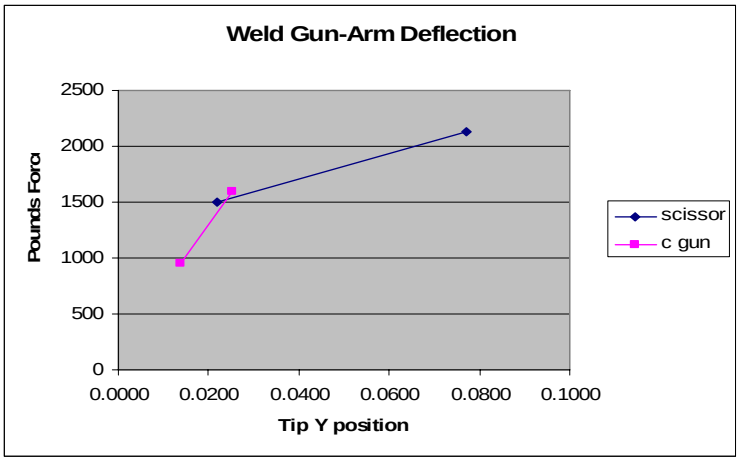

Figure A1 plot of gun arm displacement at tip vs. force

In Task 2, the setup values, input through a key pad on the weld controller, were compared with measurements using a force sensor which reveals the time needed for electrode force build-up, and the time after the current is shut off and electrodes move away from the sheets. In general, the mechanical system of a welder takes certain amount of time for it to react after receiving a command from a controller. The experiments show that the actual squeeze time is about 4 cycles shorter than the setup value for the C-gun, and the actual hold time is about 5 cycles longer than the setup. This observation means that according to the setup welding times, electric current could be applied, or welding would occur prematurely before electrode force is stabilized. The difference in hold time shows that the electrodes could be retracted at a different moment from the designated value, from the work piece after the current is shut off, and the just formed weld could be undercooled or overcooled. This could be a serious concern for high strength steels especially when Martensitic transformation is involved in strengthening the material.

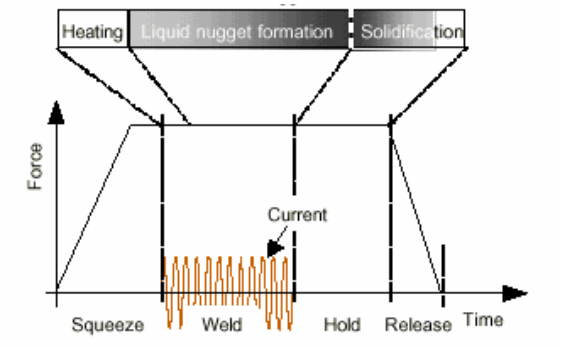

Figure A2 Schematic of a single pulse weld sequence

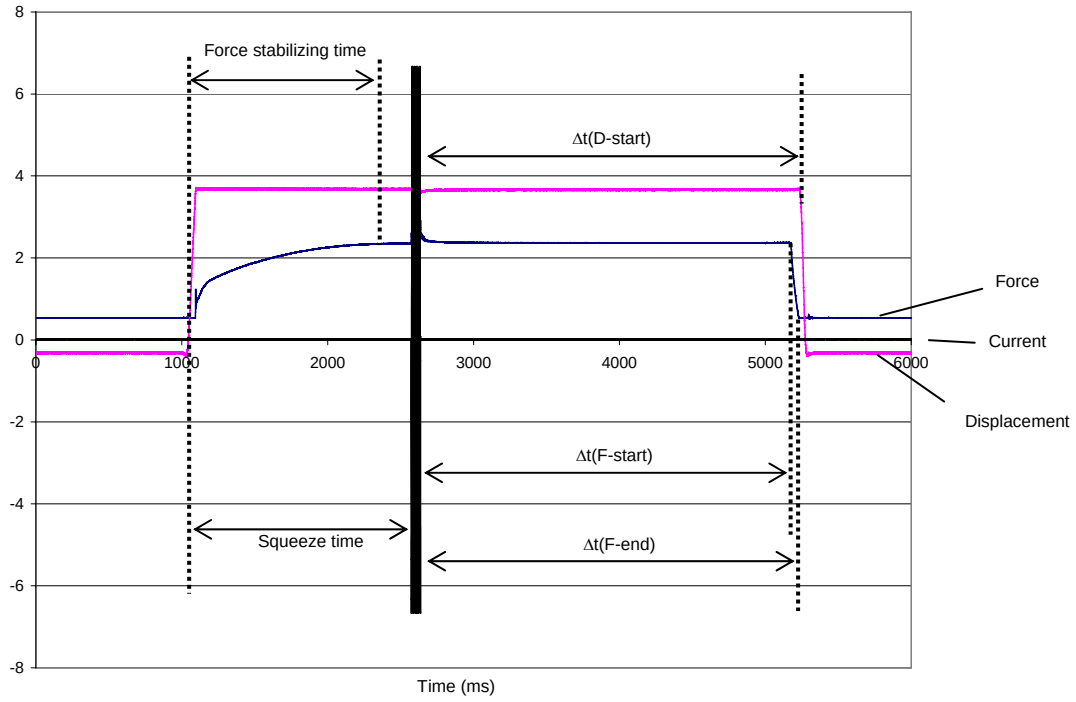

Figure A3 Plot of force, current and electrode displacement

Signals obtained for a typical welding cycle using the DAQ system. They are shown here as raw voltage signals (in volts) from the sensors, not in their respective engineering units.

First, the difference between the setup squeeze time and the measured squeeze time was calculated using the signals. Three sensors, force, displacement and electric current sensors were used for the study. The electric current signals were used to identify the end of the squeeze period (as the start of the current) and the start of the cooling period (as the end of the current). The measured squeeze time is defined as the period starting from the moment at which electrodes start to move, characterized by the start of increase of displacement value as shown in Figure A3 . The time ends when electric current is applied. Another period to be considered during squeezing is the time to stabilize the electrode force, when the electrode force reaches a steady level (or the preset value). The comparison between setup squeeze time and measured squeeze time, as well as the time needed for stabilizing the electrode force is presented in Table A1 for the C-gun.

Table A1 . Setup and measured squeeze time for the C-gun

Setup (cyc)	Measured (ms)	**Measured (cyc)**	Stable (ms)	**Stable (cyc)**	Diff. in squeeze (ms)	**Diff. in squeeze (cyc)**
35	505.8	**30.3**	320.7	19.2	-77.30	**-4.6**
40	590.3	**35.4**	333.6	20.0	-76.10	**-4.6**
45	674.3	**40.5**	341.1	20.5	-75.40	**-4.5**
50	755.6	**45.3**	335.5	20.1	-77.40	**-4.6**
60	920.6	**55.2**	335.5	20.1	-79.00	**-4.7**
70	1091.0	**65.5**	362.6	21.8	-75.20	**-4.5**
80	1263.0	**75.8**	361.2	21.7	-69.80	**-4.2**
90	1422.0	**85.3**	357.2	21.5	-77.40	**-4.6**
99	1573.5	**94.4**	343.4	20.7	-75.84	**-4.6**

Table A1 shows that there is an approximately constant difference between real (measured) squeeze time and the setup time. Being a negative value (~4 cycles) means that the measured time is shorter than the setup, which is not desirable as electric current would be applied, or welding would occur prematurely. Because welding could start before electrode force reaches desired level, additional squeeze time should be used. The time needed to reach stable electrode force appears fairly constant. The C-gun needs about 21 cycles to reach the preset force level. This is the minimum squeeze time needed for welding. Shorter time may result in unconformable welds or excessive electrode wear due to over-heating the contact interfaces.

The hold time response was analyzed for the C-gun using same signals. The hold time starts at the end of electric current application, but the end of the hold period can be defined in several ways. The start of electrode force drop (F-start) can be considered as the end of electrode cooling of the weldment. The moment when the electrode force drops to zero (F-end) and that when electrodes start to leave the workpiece (D-start, so the electrodes are not in contact with the workpiece) can also be defined as the end of cooling period. These periods are illustrated in Figure A3 . Table A1 lists various hold times (expressed as the differences between measured and setup hold times) measured according to different definitions on the C-gun.

Table A2. Setup and measured hold time for the C-gun

Setup (cyc)	Δt (F-start, cyc)	Δt (F-end, cyc)	Δt (D-start, cyc)
1	2.1	4.7	5.5
10	1.4	4.7	4.9
20	1.4	4.6	5.1
30	1.5	4.7	5.1
40	1.5	4.6	5.2
60	1.3	4.7	5.3
80	1.5	4.8	5.2
99	1.6	4.9	5.3

The hold time characterized by the start of electrode motion (defined as D-start in Figure A3) seems a reasonable choice as the physical separation of the electrodes from the workpiece marks the end of cooling. As shown in Table A2 the C-gun has fairly consistent larger hold times than the setup values. It has about 5 cycles more than the setup. As the cooling rate determines the microstructure, and therefore, the mechanical properties of a weldment after electric current is shut off, the discrepancies between true and setup hold times are of certain importance. Because hold time effect is different for mild steel, HSLA (high strength low alloy) steel and AHSS (advanced high strength steel), such effect deserves a systematic study and the deviation of real hold time from its setup value should be accounted for.

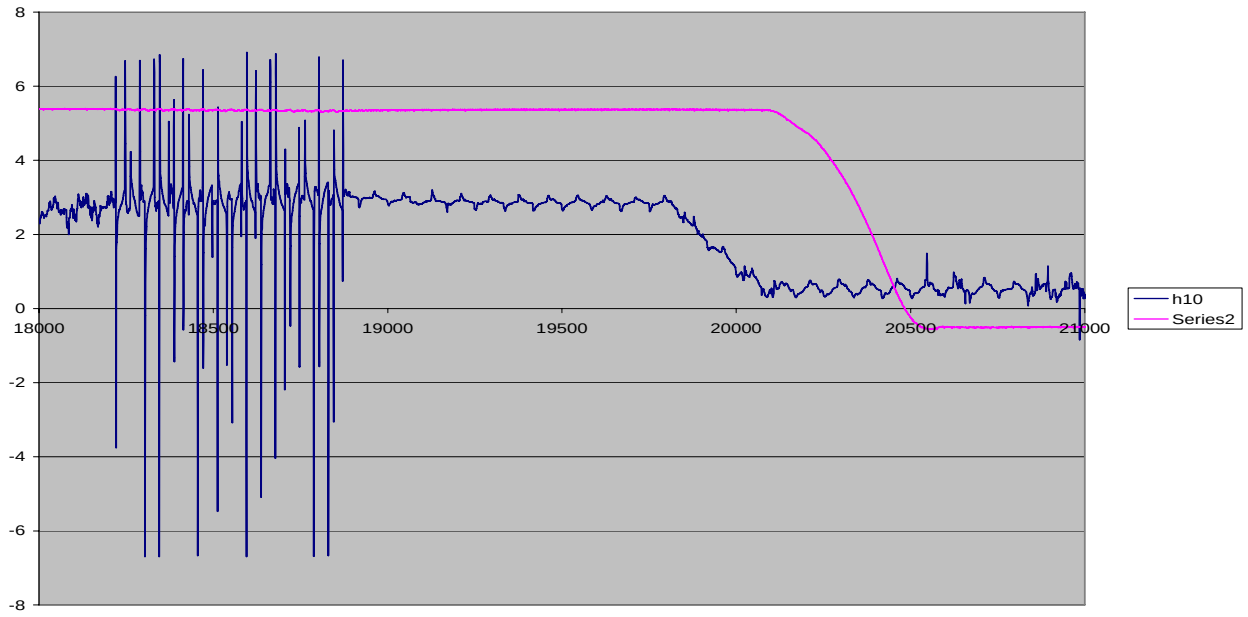

Figure A4 Programmed hold time was 10 cycles for this trace.

Values obtained for programmed hold times from 1 to 99 cycles.

Run #	Setup Time (ms)	**Setup Time (cyc)**	ΔT (F-start, ms)	**ΔT (F-start, cyc)**	ΔT (F-end, ms)	**ΔT (F-end, cyc)**	ΔT (D-start, ms)	**ΔT (D-start, cyc)**	ΔT (D-end, ms)	**ΔT (D-end, cyc)**
h1	16.66	**1**	35.1	**2.1**	77.5	**4.7**	90.9	**5.5**	180.5	**10.8**
h10	166.6	**10**	23.6	**1.4**	78.8	**4.7**	81.2	**4.9**	169.4	**10.2**
h20	333.3	**20**	22.8	**1.4**	77.0	**4.6**	85.2	**5.1**	176.0	**10.6**
h30	499.8	**30**	25.2	**1.5**	78.4	**4.7**	84.4	**5.1**	175.2	**10.5**
h40	666.4	**40**	24.8	**1.5**	77.2	**4.6**	86.0	**5.2**	180.0	**10.8**
h60	999.6	**60**	21.8	**1.3**	79.0	**4.7**	88.2	**5.3**	182.6	**10.9**
h80	1332.8	**80**	25.6	**1.5**	80.0	**4.8**	87.0	**5.2**	182.0	**10.9**
h99	1649.3	**99**	25.9	**1.6**	80.9	**4.9**	88.1	**5.3**	188.3	**11.3**

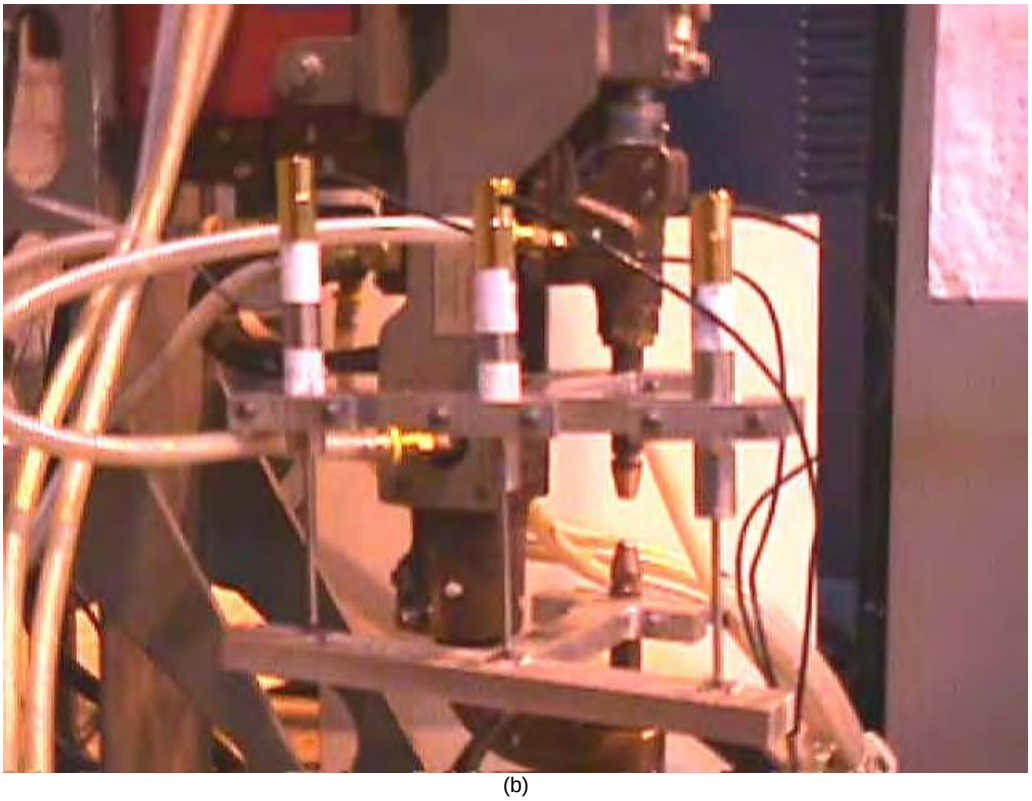

(b)

Sensor setup for the measurement

Appendix B Weld Machine Electrical Characteristics

Effect of Tap Switch Settings for Weld Guns

Testing was performed to determine if significant current range and weld performance effects are produced by using more of the AC waveform for producing a resistance spot weld. In general, acceptable welds could be produced using either high-tap (less conduction angle) or low-tap (more conduction angle) on the welding transformer. It was noticed that the current range was shifted by both the gun style used and the transformer tap setting. Welding current range was wider using the high tap setting on the transformer

Experimental results are listed in Table B1 and Table B2 for C Gun and S-Gun respectively. For C Gun, high tap setting exhibited wider weld current range compared to the low tap setting condition. In addition, low tap setting showed more than 10% difference between two test runs at Imax. Consequently, high tap setting is selected as the tap setting parameter throughout this project.

Table B1 Weld Lobes with Low and High Tap Setting (C Gun)

	Tap 1 (Low Tap Setting)			Tap 1 (Averaged)			
1-5-1	WT	I_{min}	I_{max}	WT	I_{min}	I_{max}	ΔI
	16	11.4	12.8	16	11.0	13.5	2.5
	22	10.2	11.0	22	10.2	11.6	1.4
	28	9.6	10.7	28	9.9	11.3	1.4
	Tap 1 (Low Tap setting)			Practical Tap 1 Setting			
	WT	I_{min}	I_{max}	WT	I_{min}	I_{max}	ΔI
1-5-2	16	10.6	14.3	16	11.4	12.8	**1.4**
	22	10.2	12.2	22	10.2	11.0	**0.8**
	28	10.1	11.9	28	10.1	10.7	**0.6**

	Tap 4 (High Tap Setting)			Tap 4 (Averaged)			
1-5-3	WT	I_{min}	I_{max}	WT	I_{min}	I_{max}	ΔI
	16	11.7	13.3	16	11.3	13.4	2.1
	22	10.6	12.0	22	10.3	12.0	1.7
	28	10.0	11.6	28	9.8	11.8	2.0
	Tap 4 (High Tap Setting)			Practical Tap 4 Setting			
	WT	I_{min}	I_{max}	WT	I_{min}	I_{max}	ΔI
1-5-4	16	10.9	13.5	16	11.7	13.3	**1.6**
	22	10.0	12.0	22	10.6	12.0	**1.4**
	28	9.5	11.9	28	10.0	11.6	**1.6**

AVERAGE IS THE AVERAGE OF THE TWO TEST RUNS.

PRACTICAL IS THE LARGER OF OBSERVED INDIVIDAUL RUN VALUES FOR I-MIN AND THE LOWEST VALUE OF I-MAX.

Percentage Difference between Test Run (Tap 1) Low		
WT	% ΔI_{min}	% ΔI_{max}
16	7.5	***11.7***
22	0.0	***10.9***
28	5.2	***11.2***

Percentage Difference between Test Run (Tap 4) High		
WT	% ΔI_{min}	% ΔI_{max}
16	7.3	1.5
22	6.0	0.0
28	5.3	2.6

For S Gun, high tap setting possesses wider weld current range compared to low tap setting conditions. There were no significant differences between two test runs on both tap-setting conditions. As a result, further weld lobe development was conducted with high tap setting simulating practices used in some auto body manufacturing.

Table B2 Weld Lobes with Low and High Tap Setting (S Gun)

	Tap 1 (Low Tap Setting)			Tap 1 (Averaged)			
2-5-1	WT	I_{min}	I_{max}	WT	I_{min}	I_{max}	ΔI
	16	10.9	11.9	16	10.8	12.0	1.2
	22	9.7	11.6	22	9.6	11.5	1.9
	28	9.3	11.0	28	9.1	11.0	1.9
	Tap 1 (Low Tap setting)			Practical Tap 1 Setting			
	WT	I_{min}	I_{max}	WT	I_{min}	I_{max}	ΔI
2-5-2	16	10.6	12.1	16	10.9	11.9	**1.0**
	22	9.4	11.3	22	9.7	11.3	**1.6**
	28	8.9	11.0	28	9.3	11.0	**1.7**

	Tap 5 (High Tap Setting)			Tap 5 (Averaged)			
2-5-3	WT	I_{min}	I_{max}	WT	I_{min}	I_{max}	ΔI
	16	10.1	11.9	16	10.0	12.0	2.0
	22	9.2	11.0	22	8.9	10.9	2.0
	28	8.9	10.7	28	8.6	10.5	1.9
	Tap 5 (High Tap Setting)			Practical Tap 5 Setting			
	WT	I_{min}	I_{max}	WT	I_{min}	I_{max}	ΔI
2-5-4	16	10.9	13.5	16	10.1	11.9	**1.8**
	22	10.0	12.0	22	9.2	10.8	**1.6**
	28	9.5	11.9	28	8.9	10.3	**1.4**

Percentage Difference between Test Run (Tap 1) Low		
WT	% ΔI_{min}	% ΔI_{max}
16	2.8	1.7
22	3.2	2.7
28	4.5	0.0

Percentage Difference between Test Run (Tap 5) High		
WT	% ΔI_{min}	% ΔI_{max}
16	3.1	1.7
22	7.0	1.9
28	3.5	3.9

AVERAGE IS THE AVERAGE OF THE TWO TEST RUNS.

PRACTICAL IS THE LARGER OF OBSERVED INDIVIDAUL RUN VALUES FOR I-MIN AND THE LOWEST VALUE OF I-MAX.

Appendix C Weld Lobe Charts Force: 1500 lbs ,Weld Time: 16, 22, 28 Cycles Hold Time: 30 Cycles

LINK TO AND

MATERIAL ID CHEMISTRY

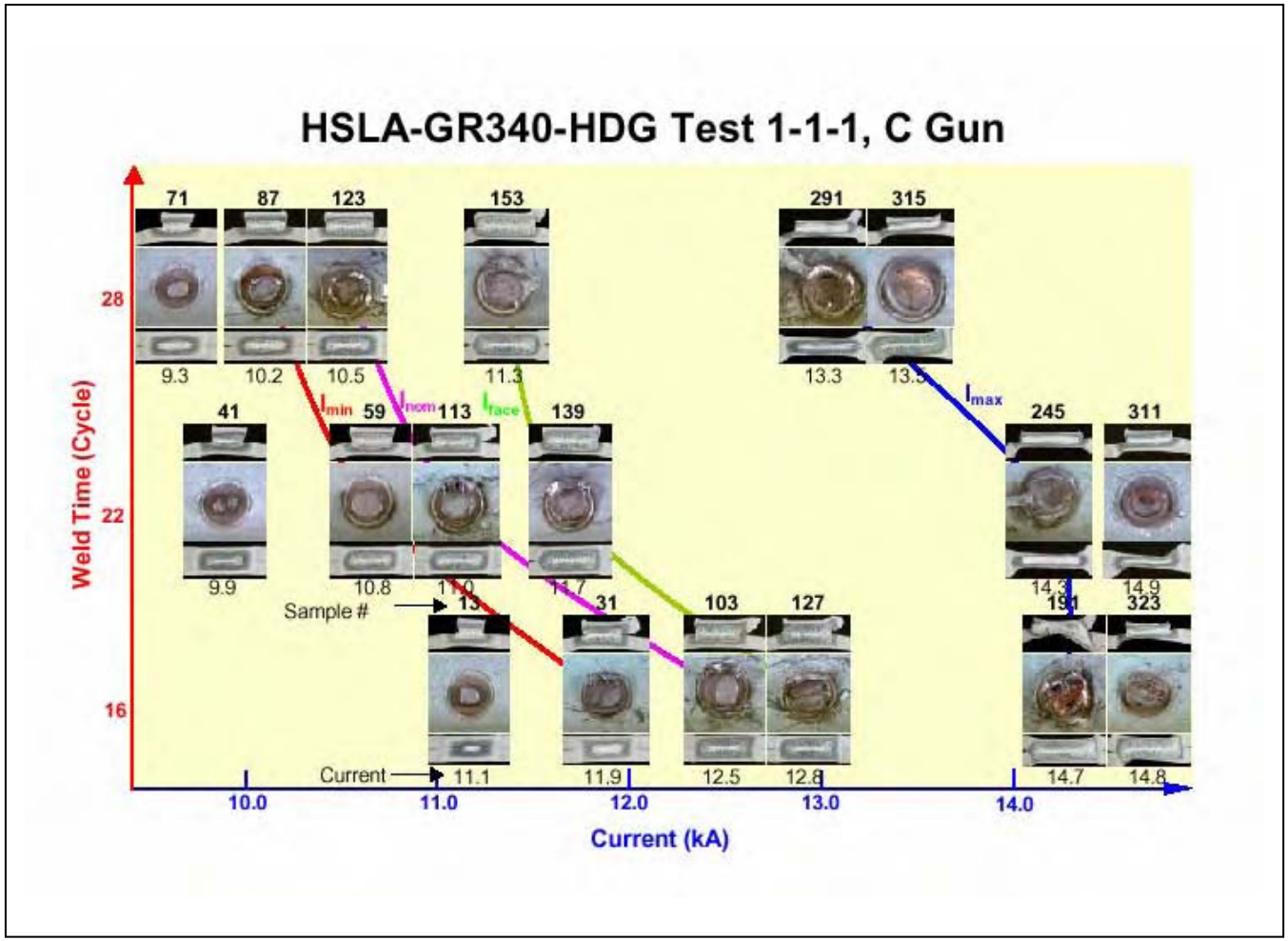

MATERIAL 01 HSLA 340Y GI , C-GUN

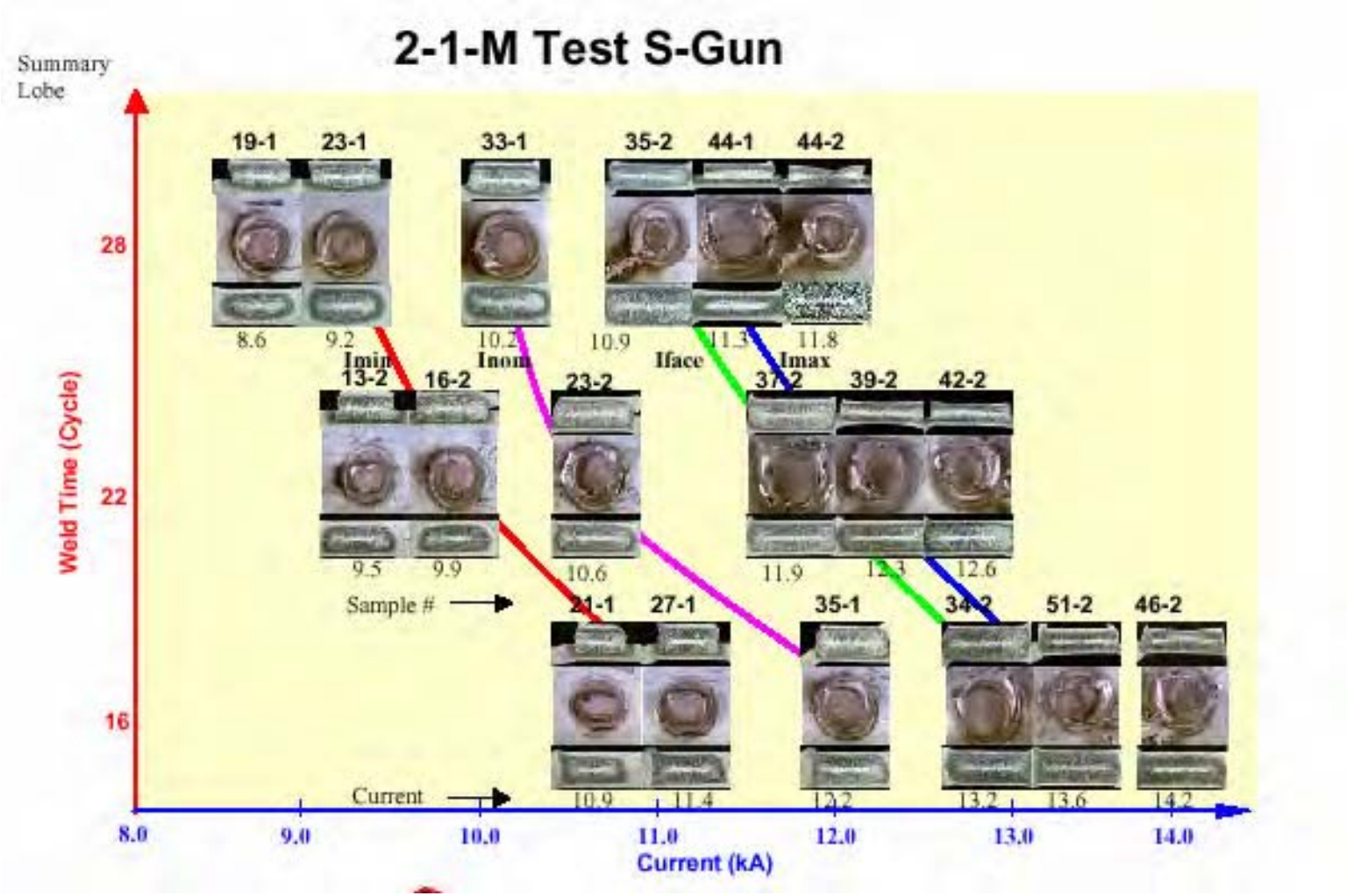

MATERIAL 01 HSLA 340Y GI, S-GUN

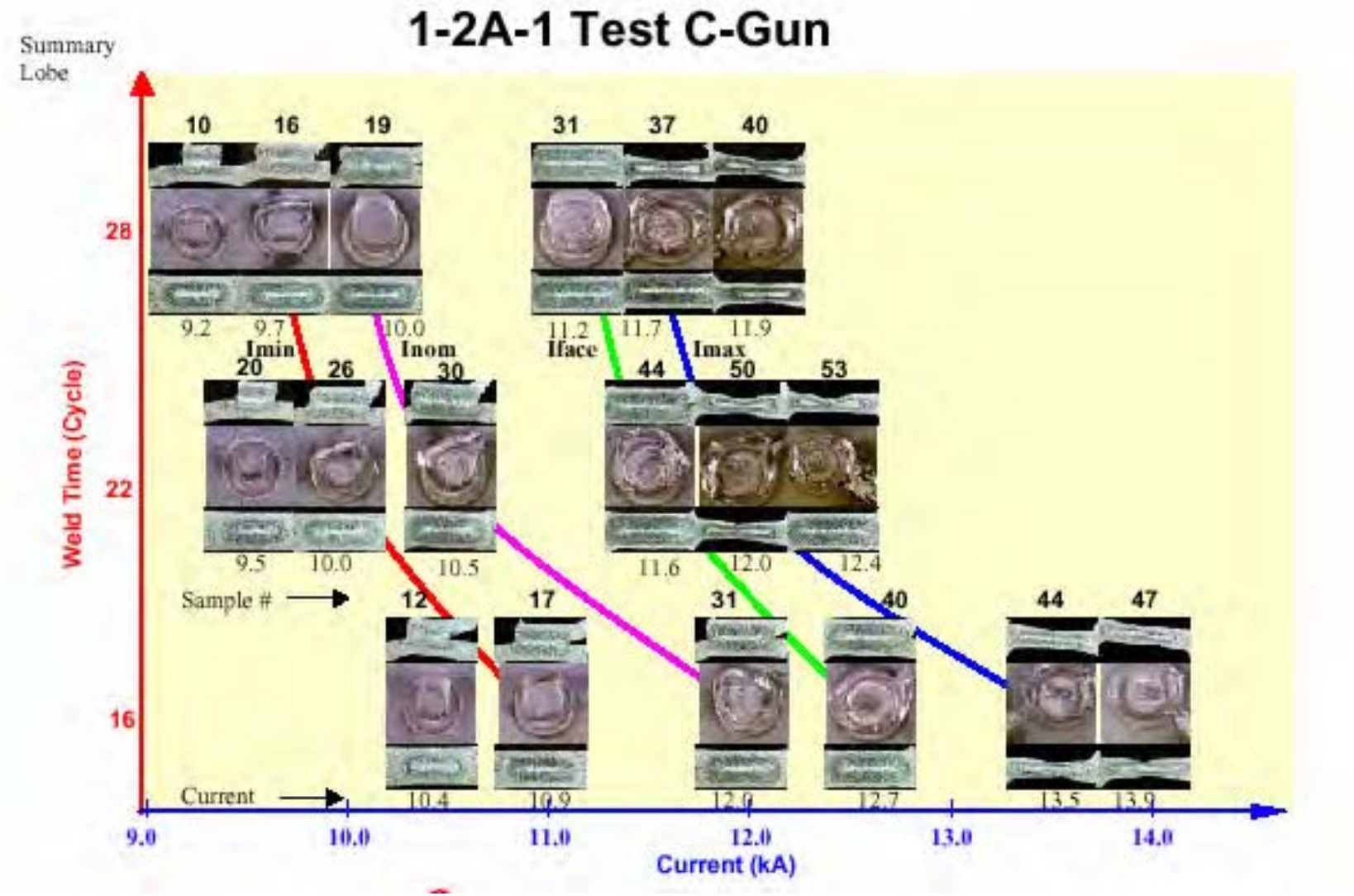

MATERIAL 02 HSLA 340Y GA, C-GUN

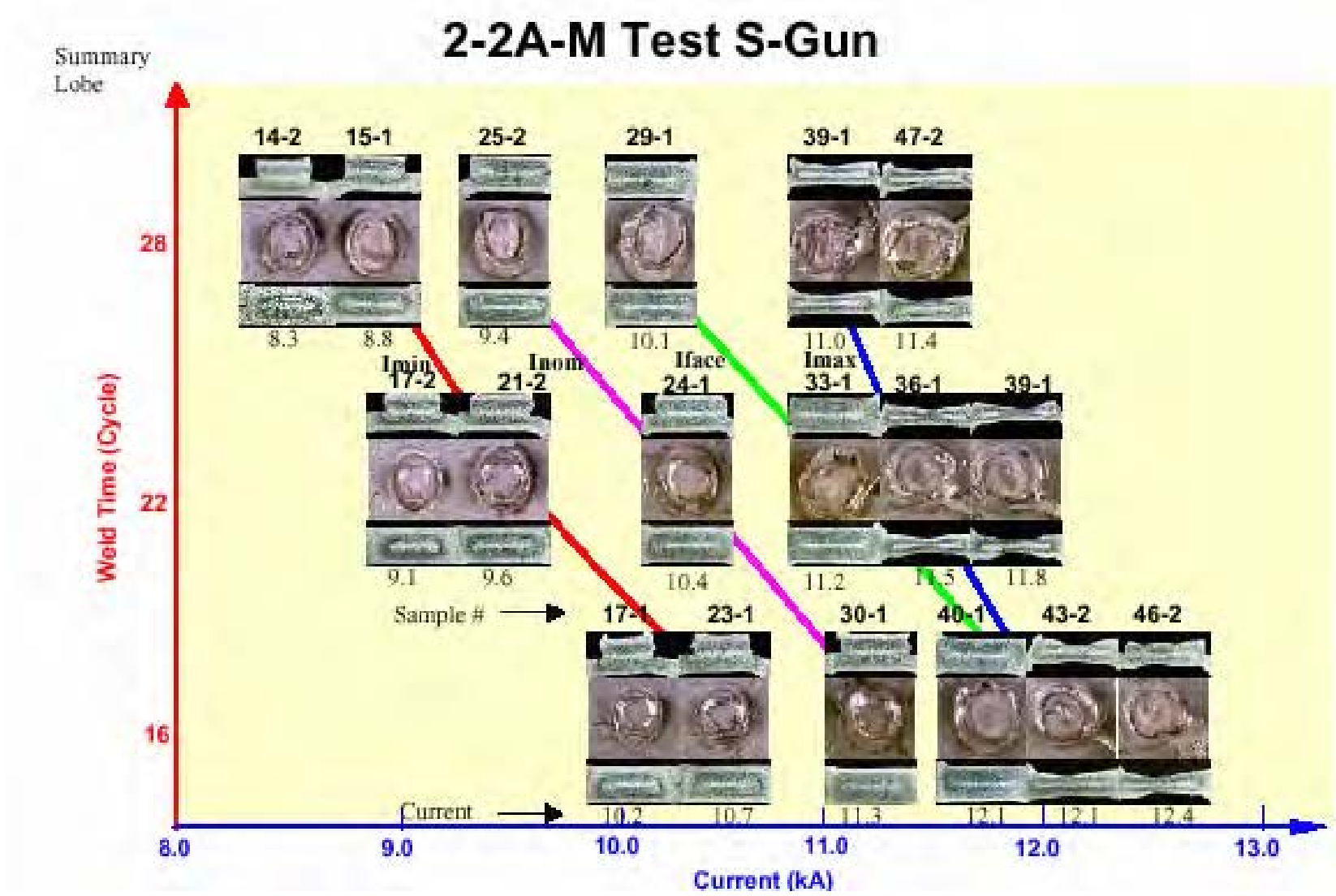

MATERIAL 02 HSLA 340Y GA, S-GUN

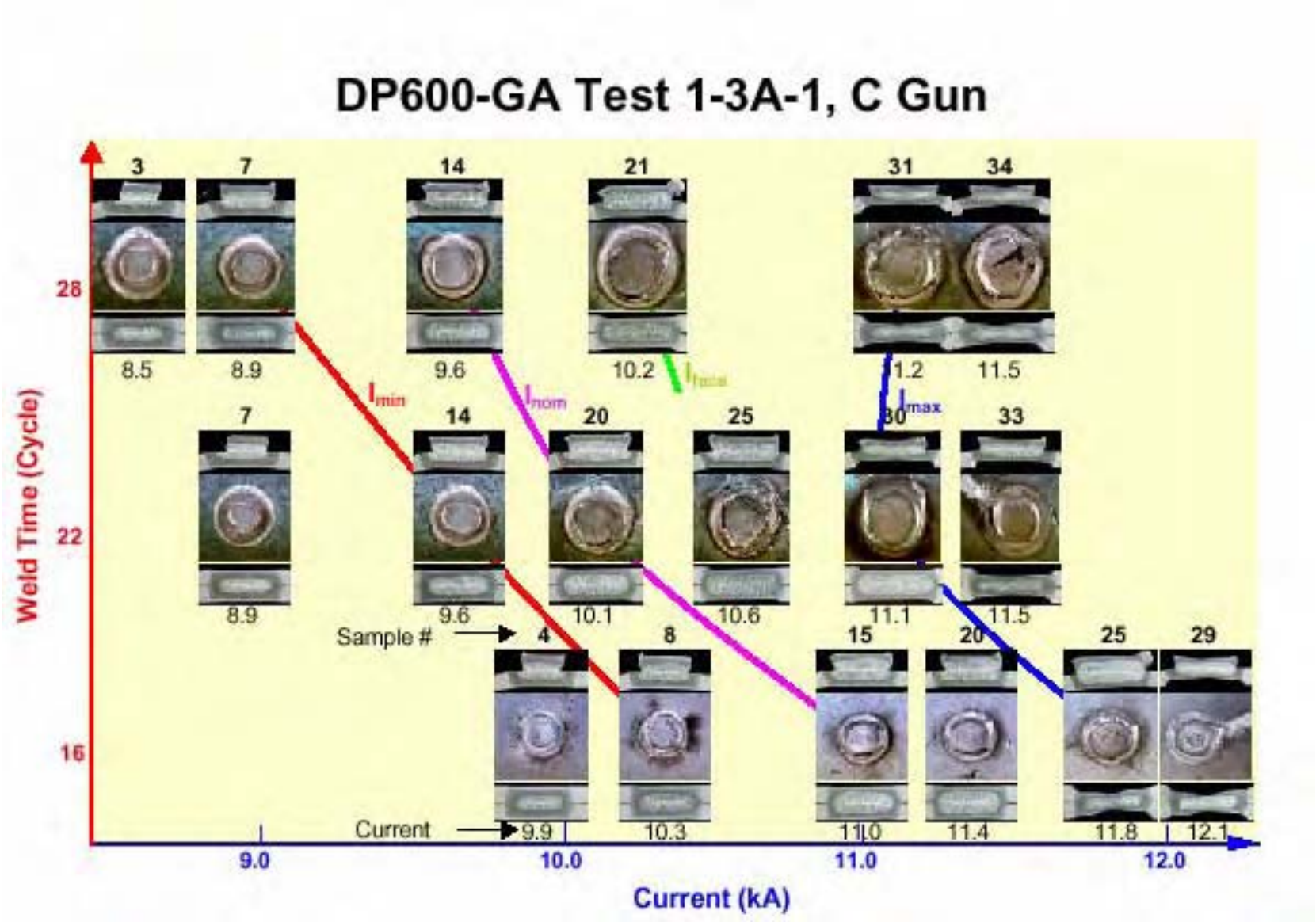

MATERIAL 3A DP 600 GA, C-GUN

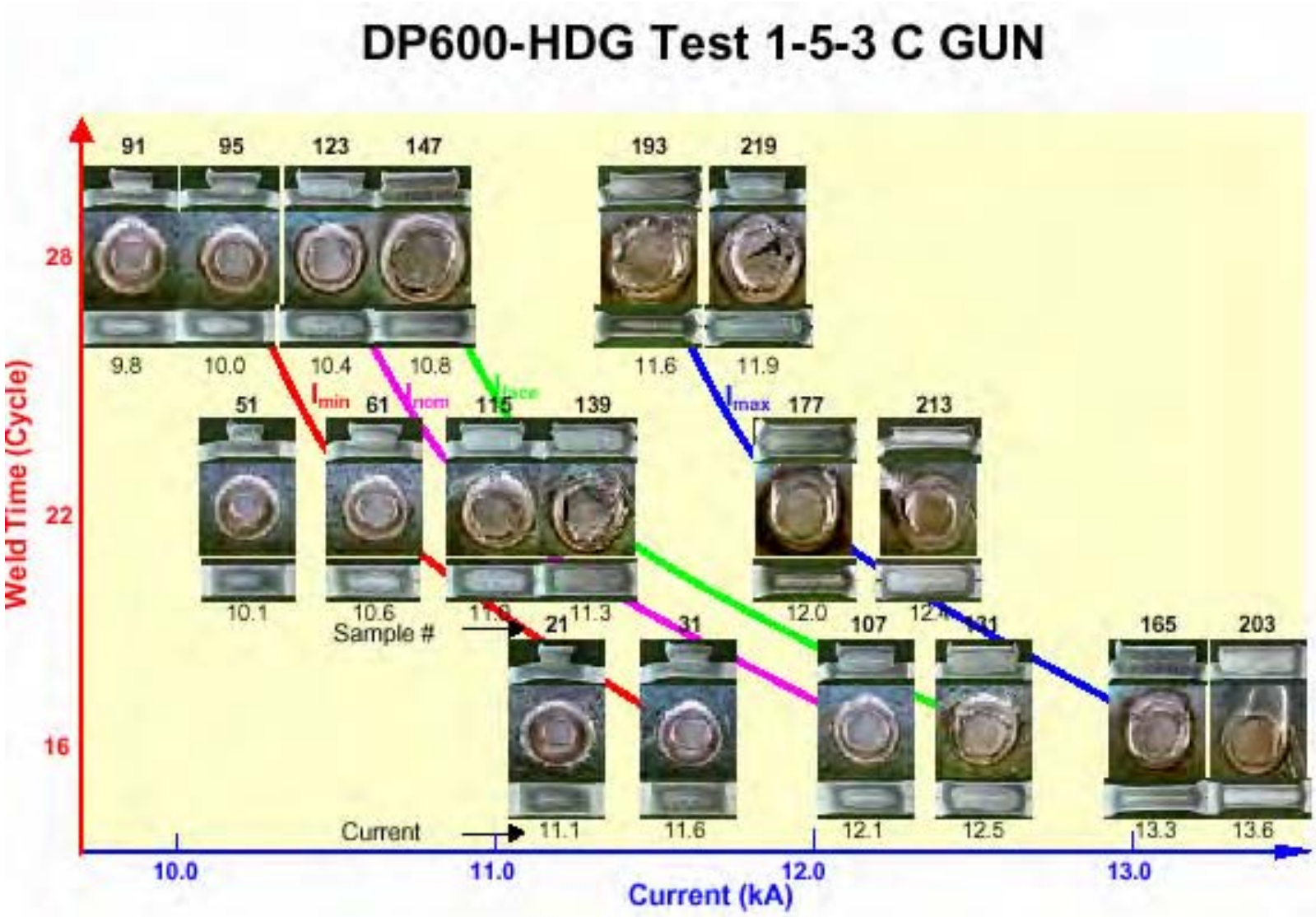

MATERIAL 5 DP600 GI , C-GUN

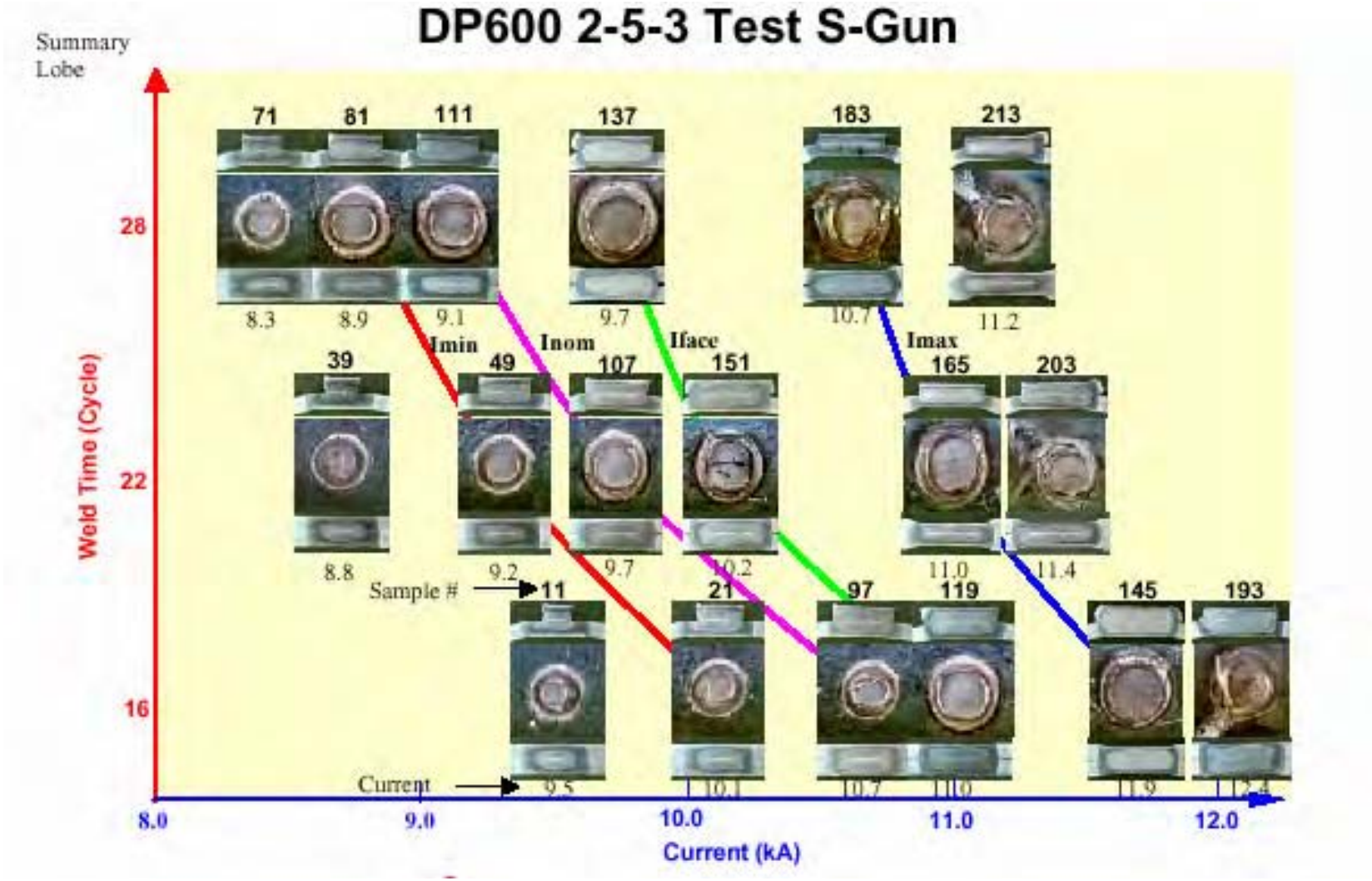

MATERIAL 5 DP 600 GI , S-GUN

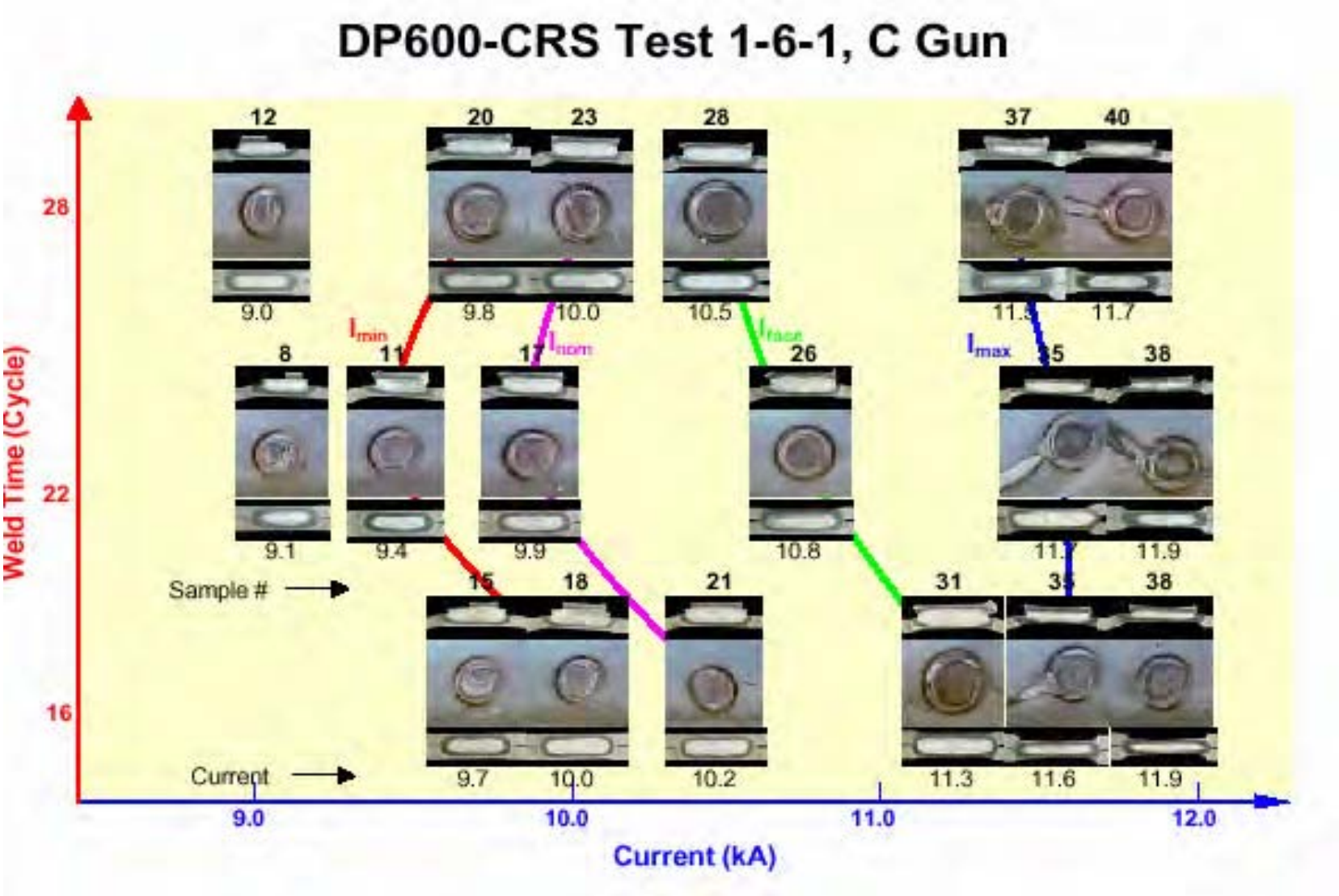

MATERIAL 6 DP 600 BARE, C-GUN

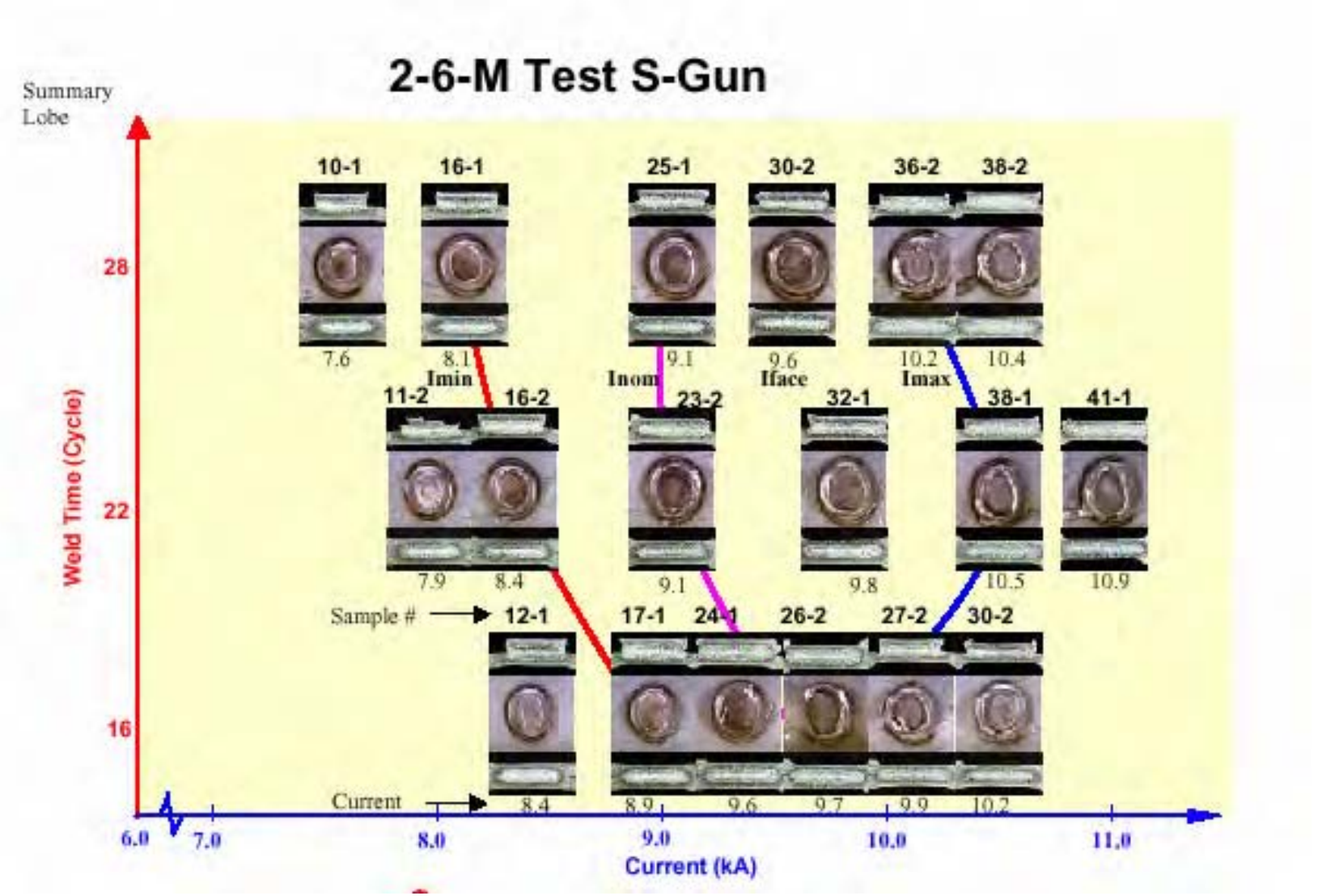

MATERIAL 6 DP 600 CRS, S-GUN

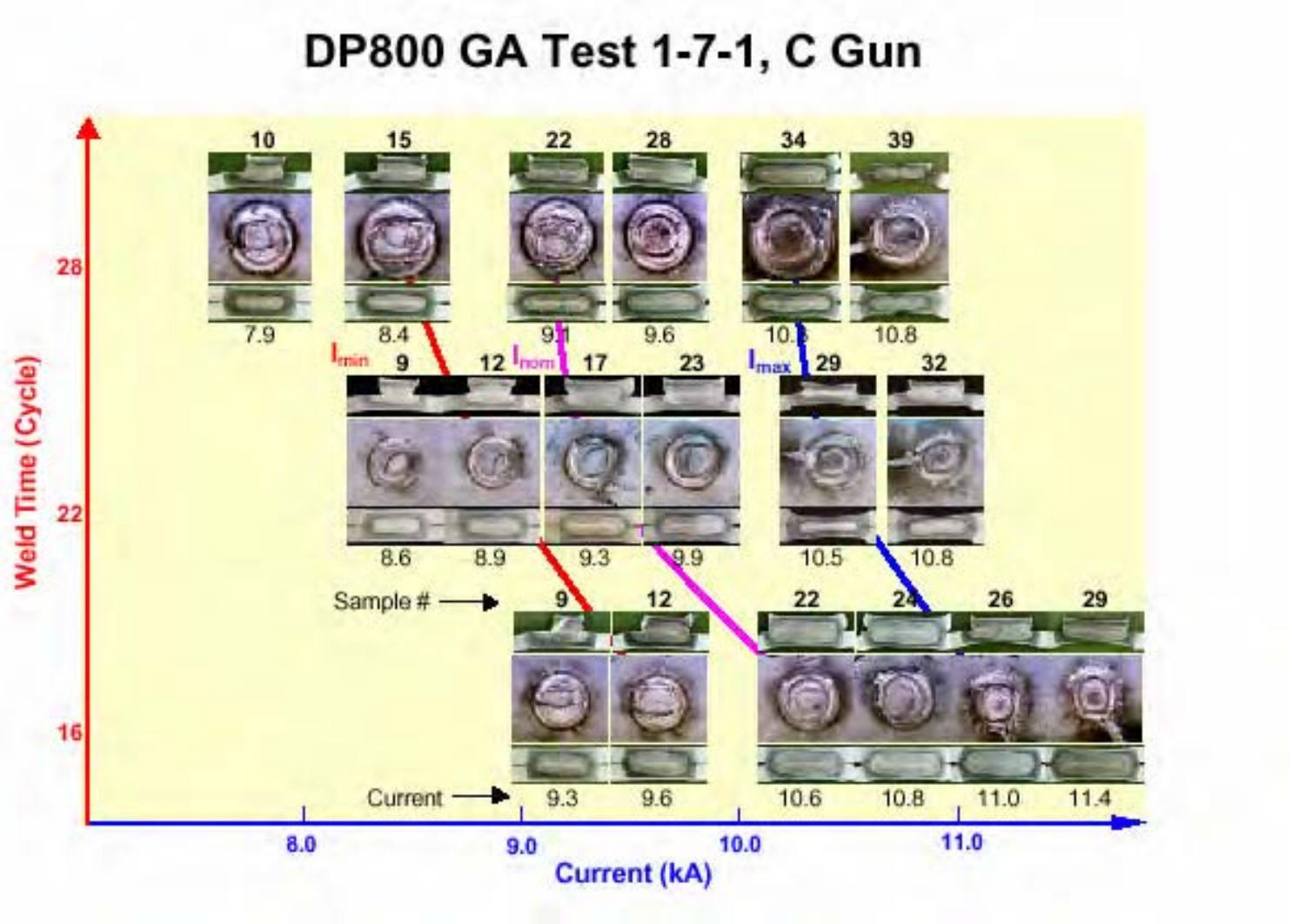

MATERIAL 7 DP 800 GA, C-GUN

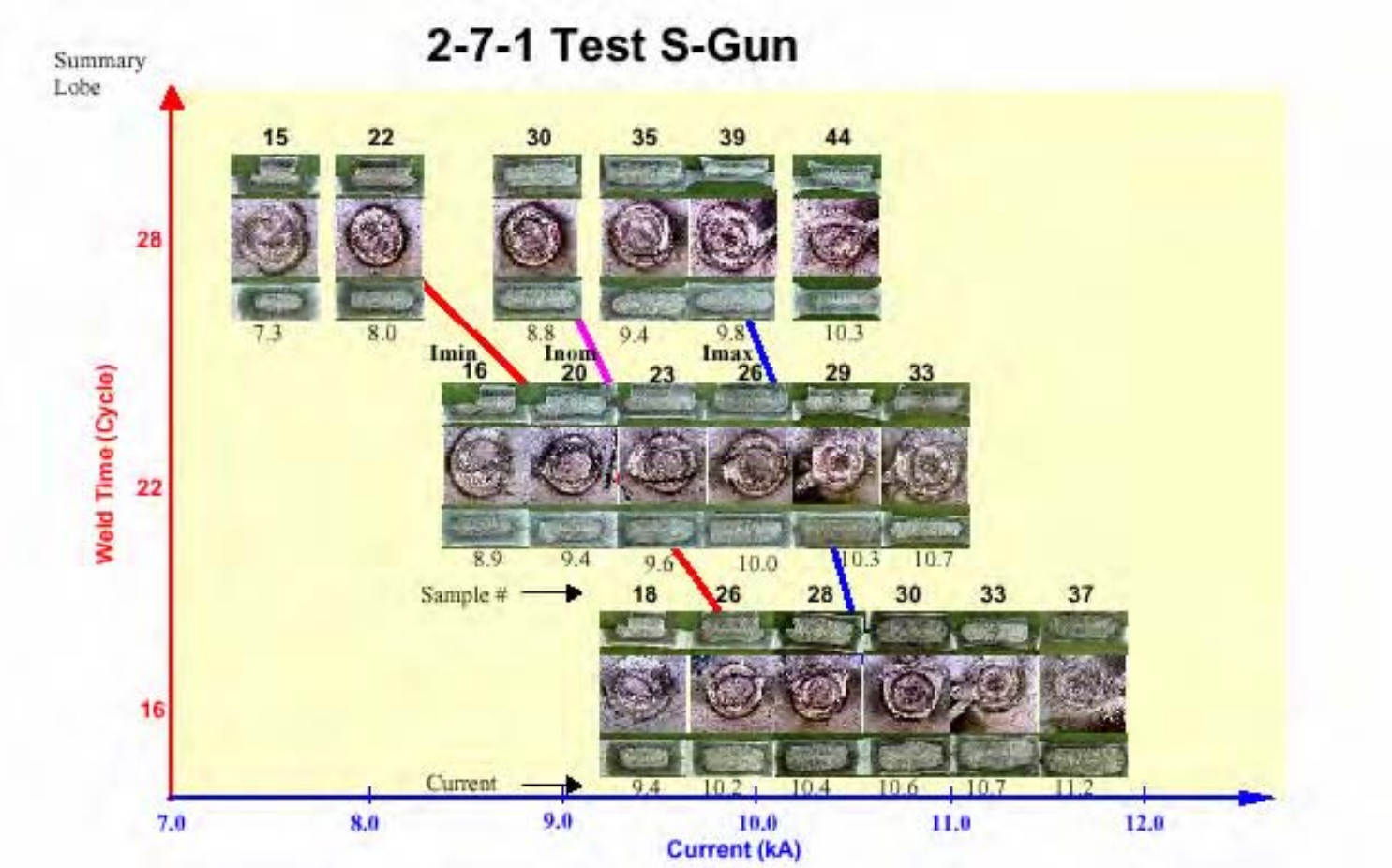

MATERIAL 7 DP 800 GA, S-GUN

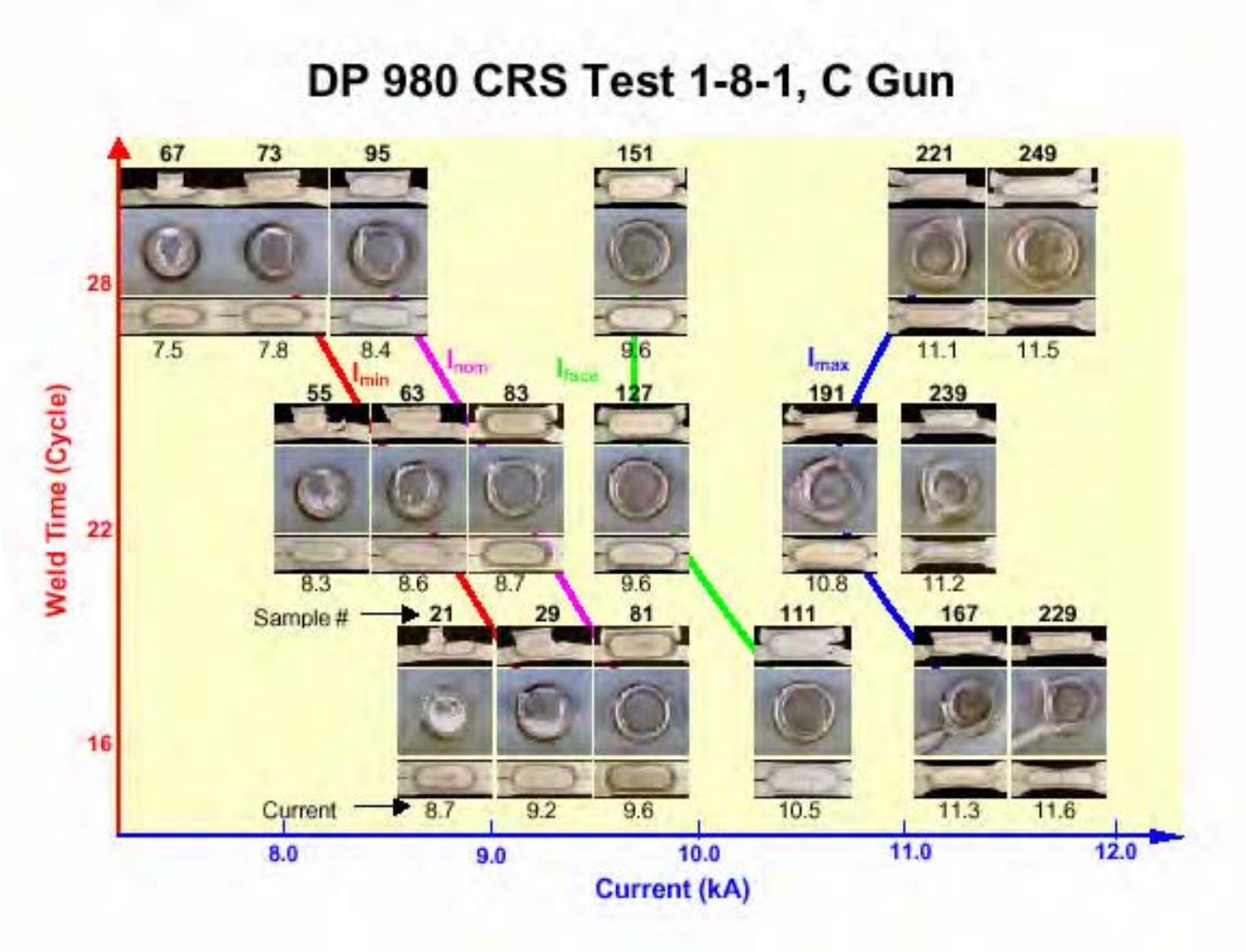

MATERIAL 8 DP 980 CRS, C-GUN

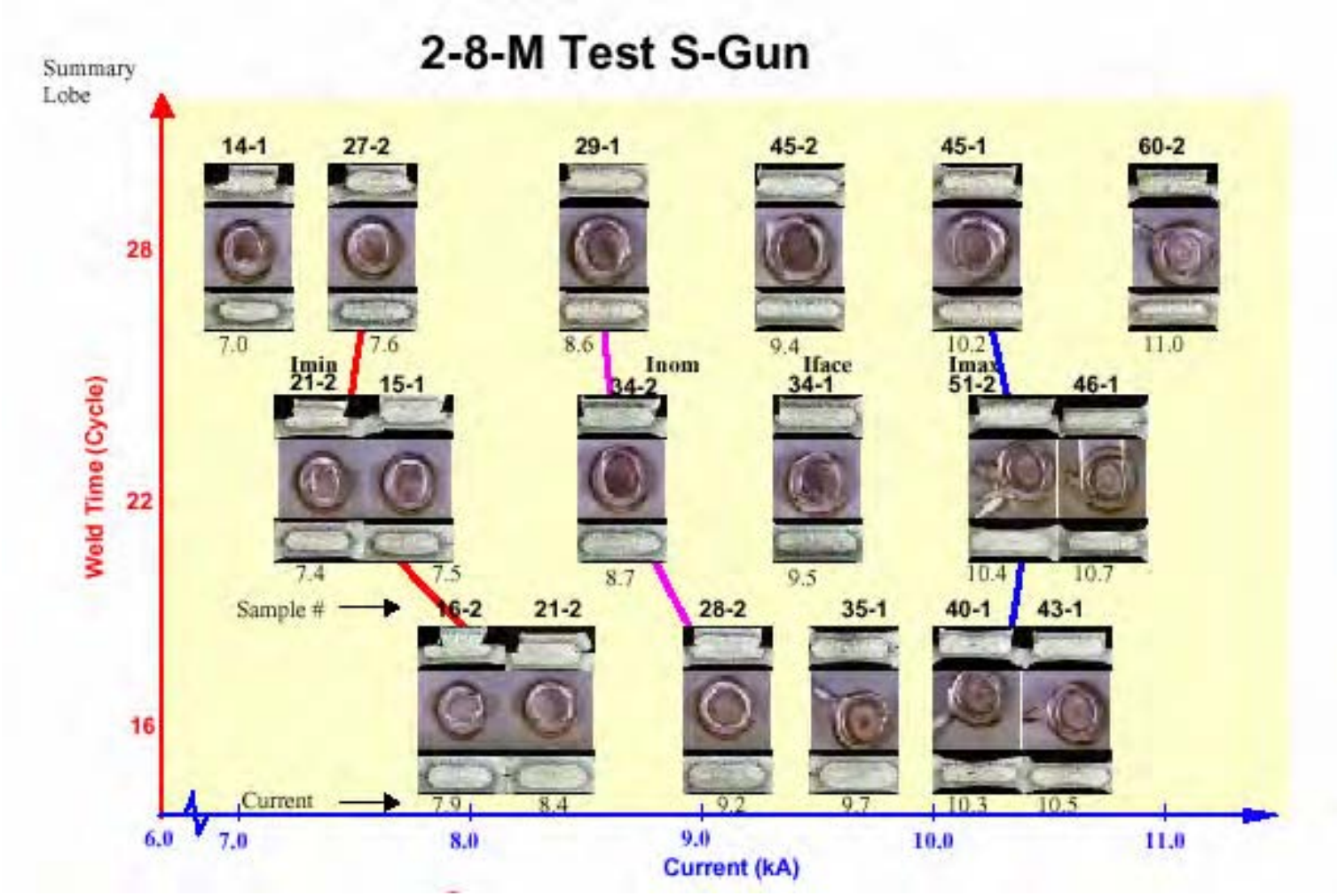

MATERIAL 8 DP 980 CRS, S-GUN

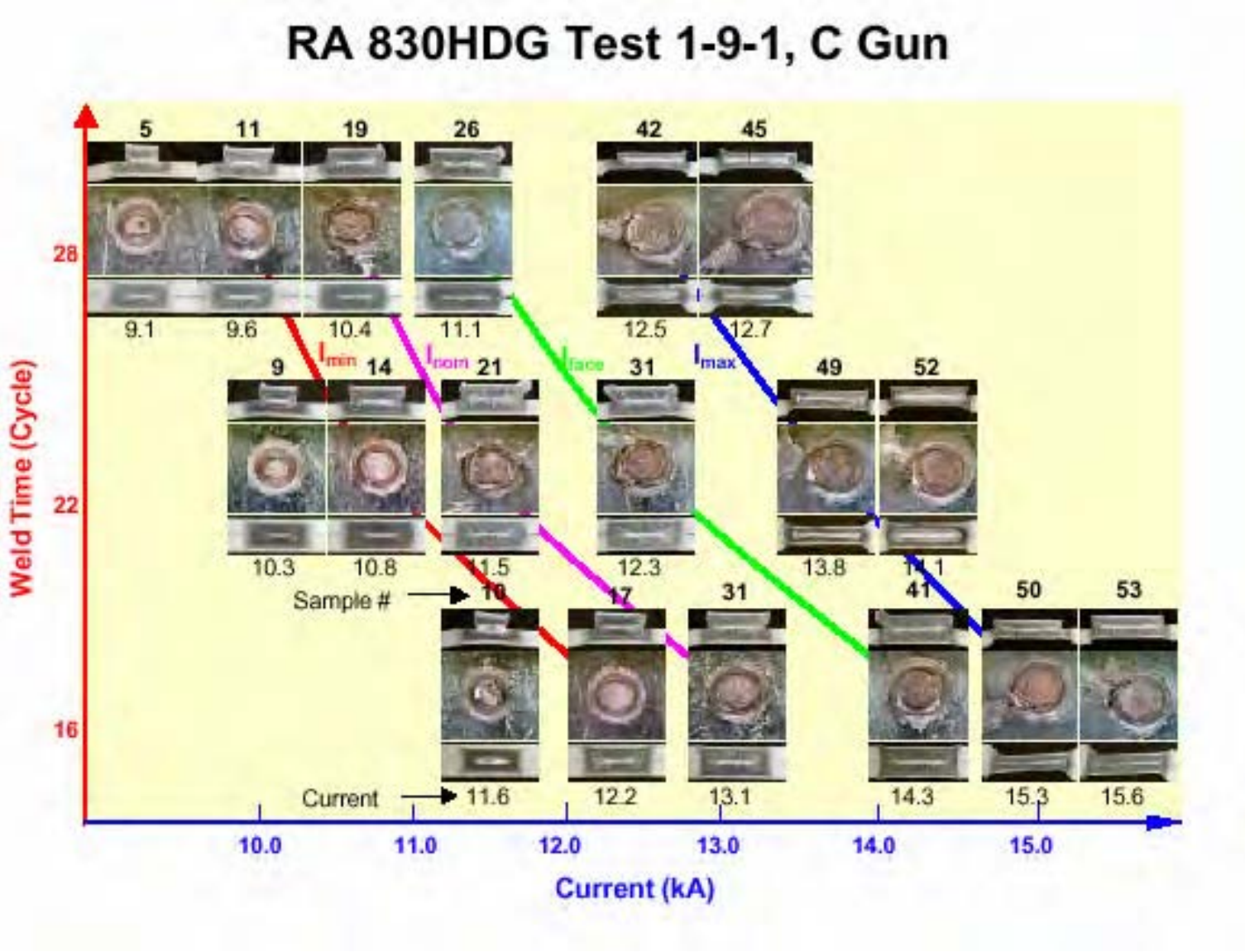

MATERIAL 9 RA 830 GI, C-GUN

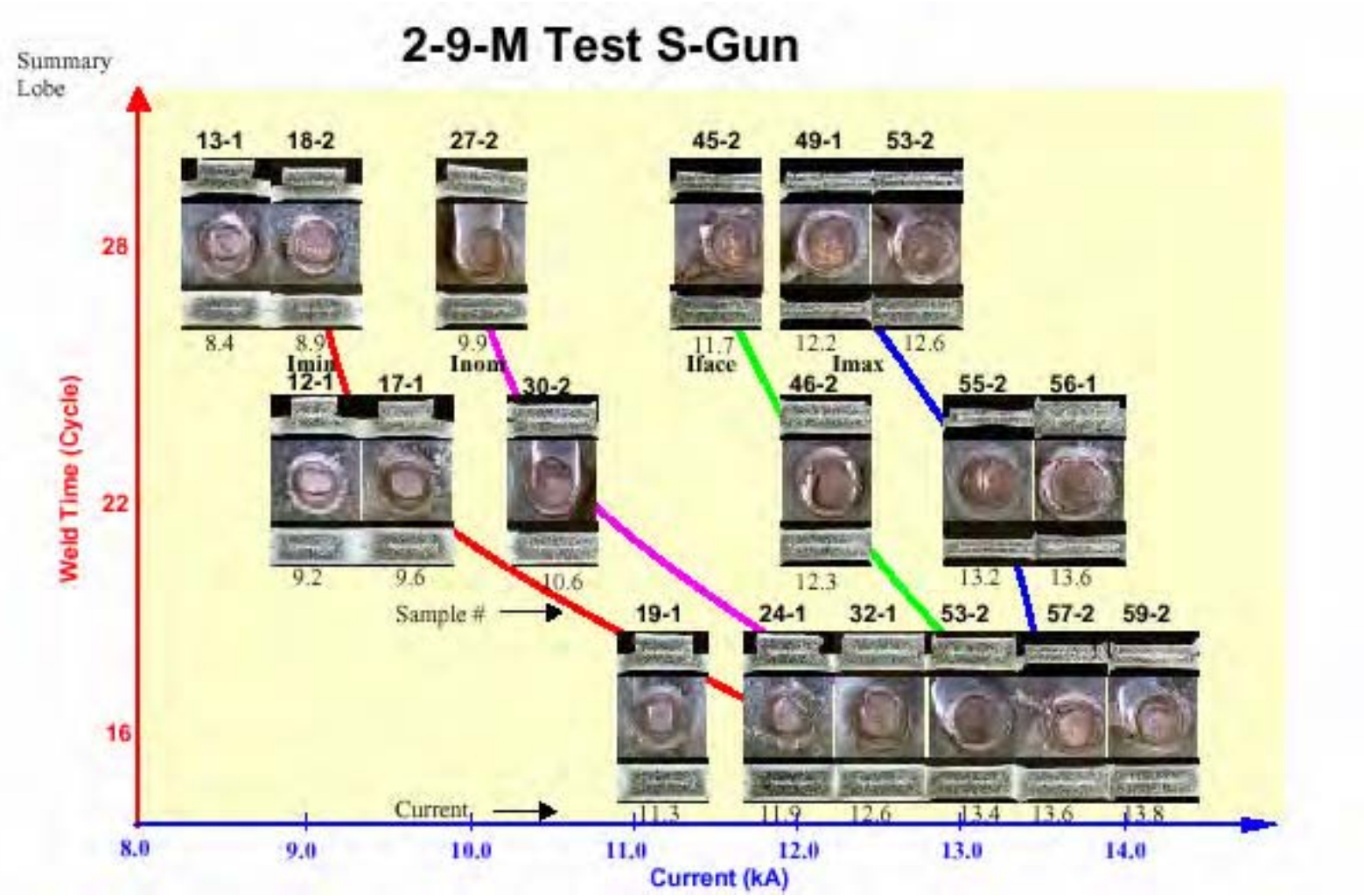

MATERIAL 9 RA 830 GI, S-GUN

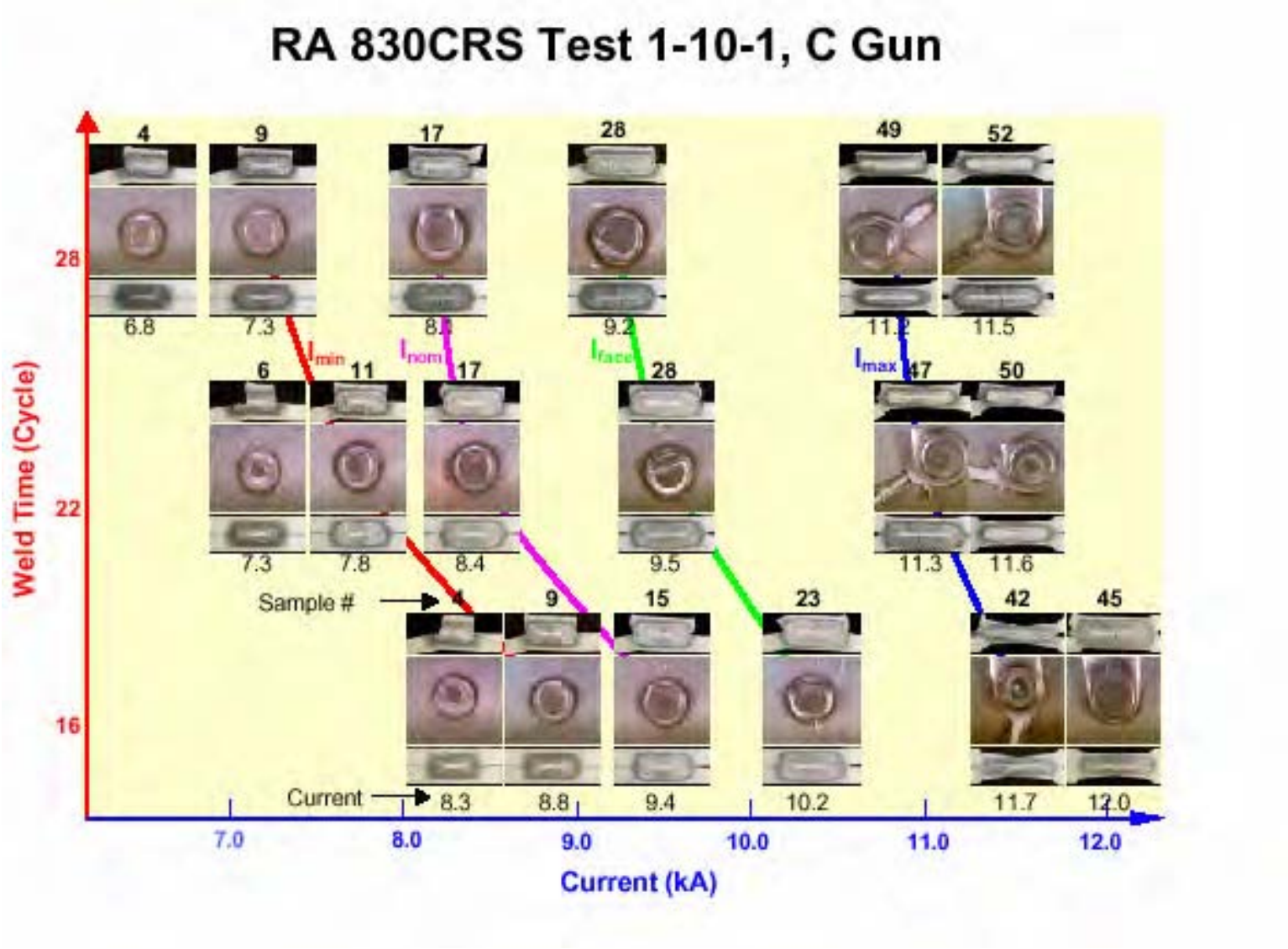

MATERIAL 10 RA 830 CRS, CGUN

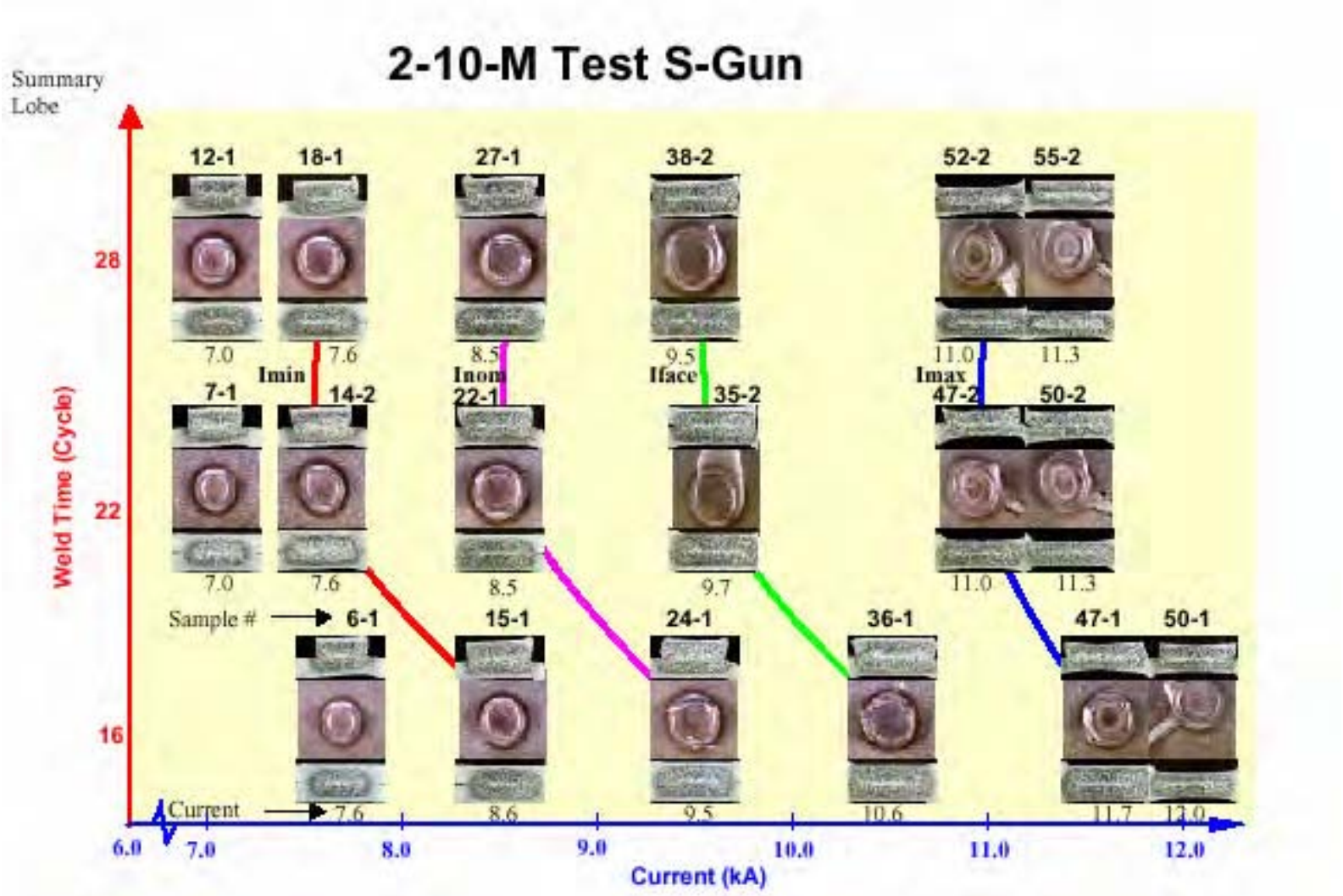

MATERIAL 10 RA 830 CRS, S-GUN

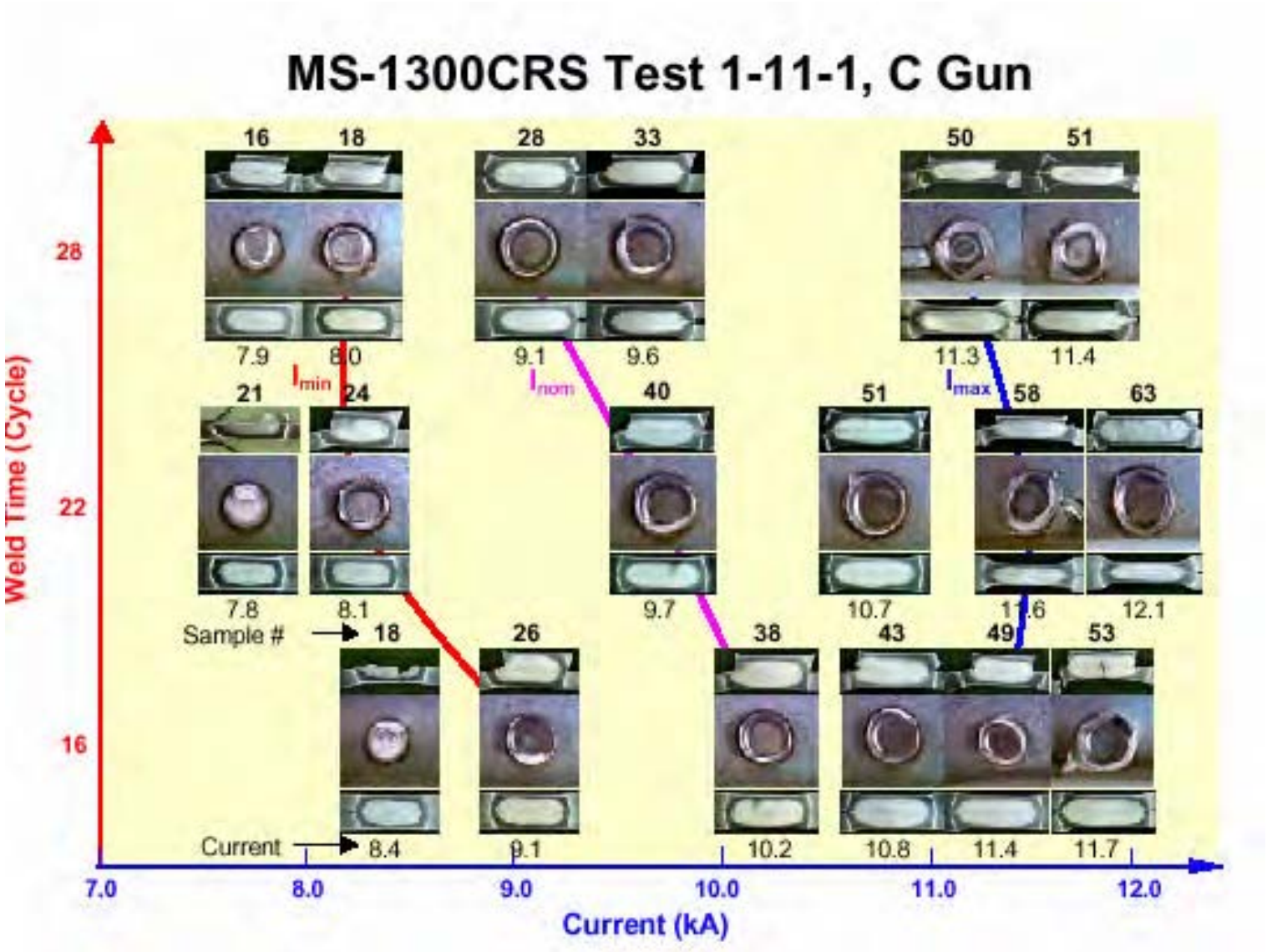

MATERIAL 11 MS 1300, C-GUN

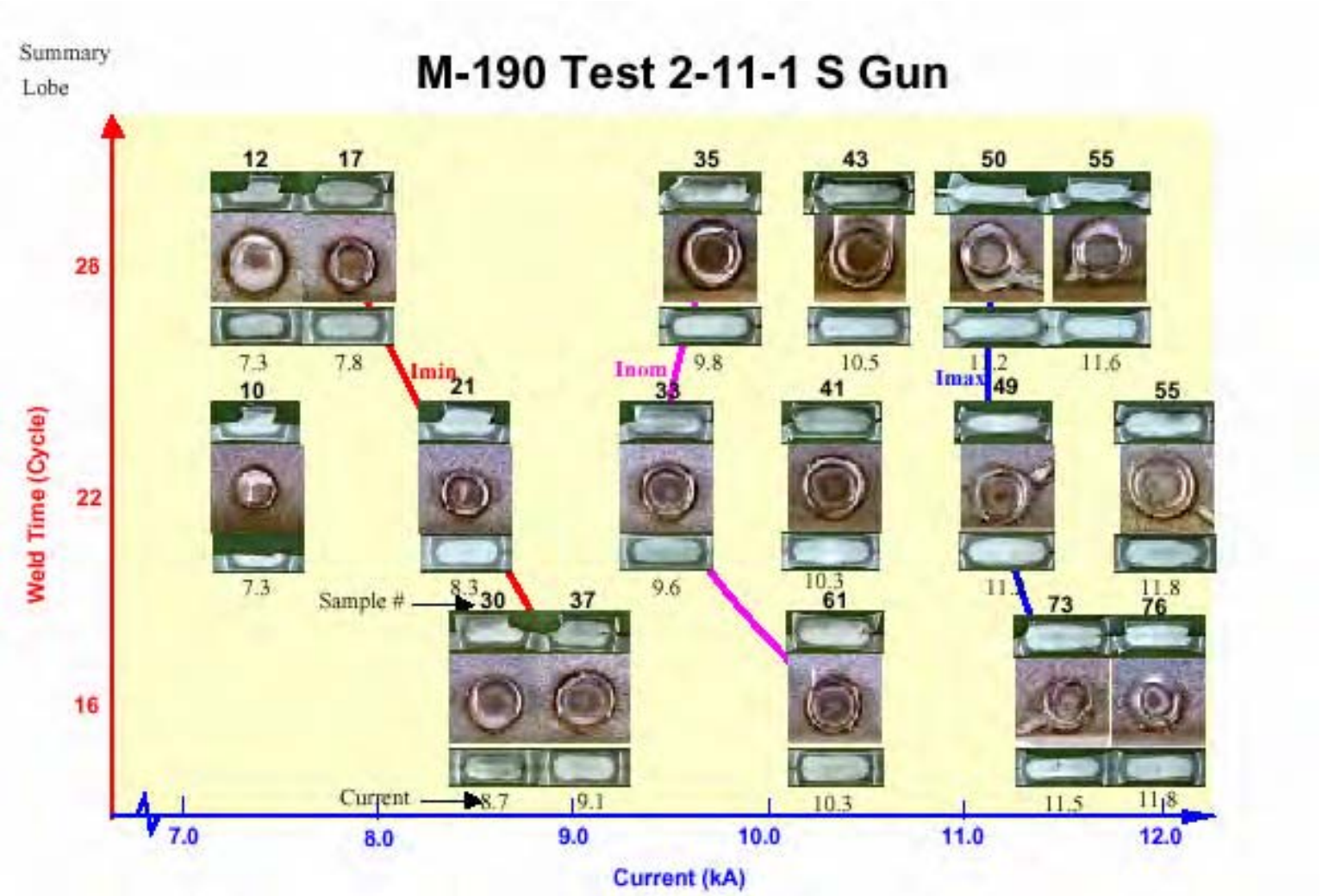

MATERIAL 11 MS 1300 , S-GUN

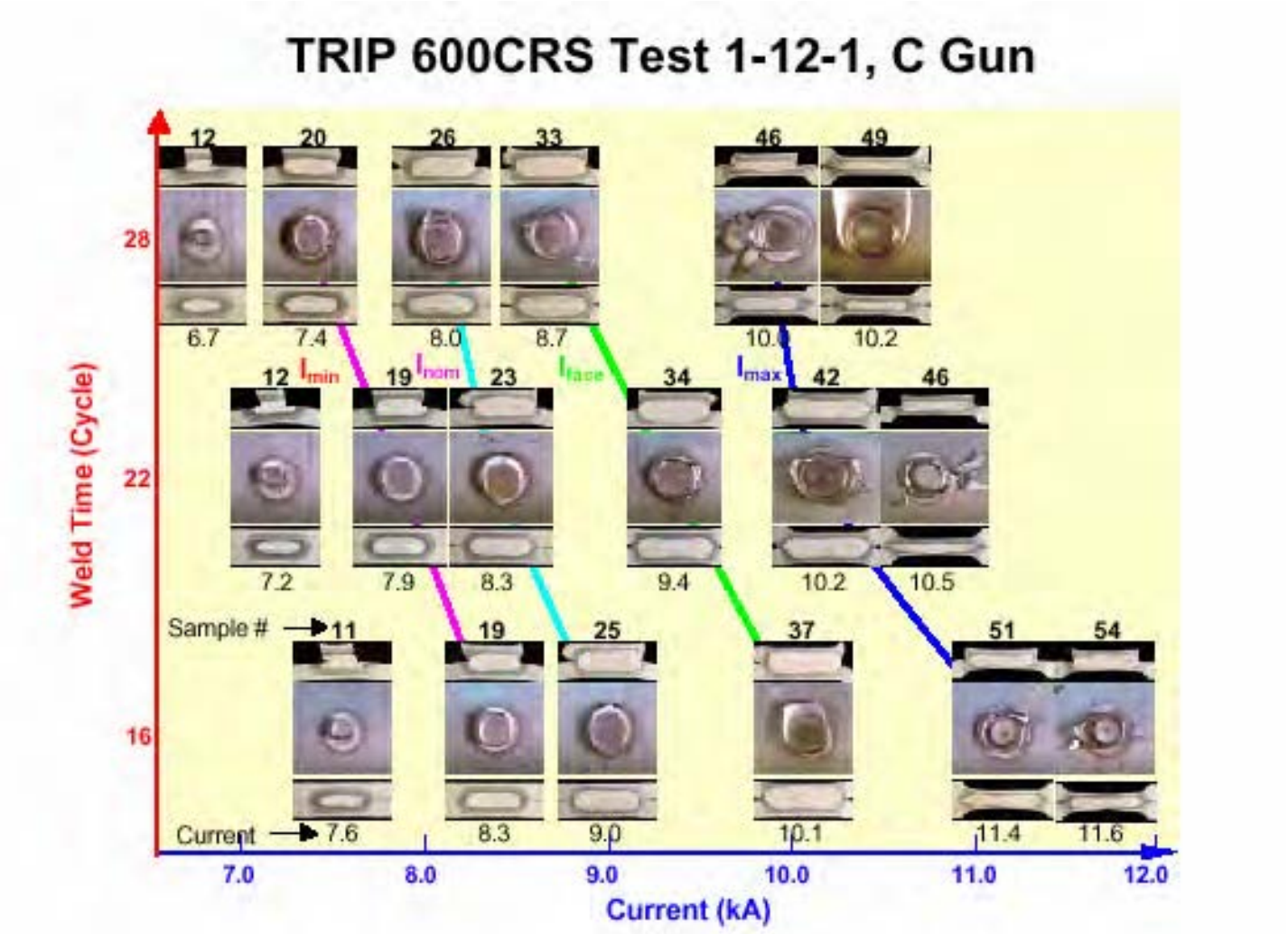

MATERIAL 12 TRIP 600 CRS, C-GUN

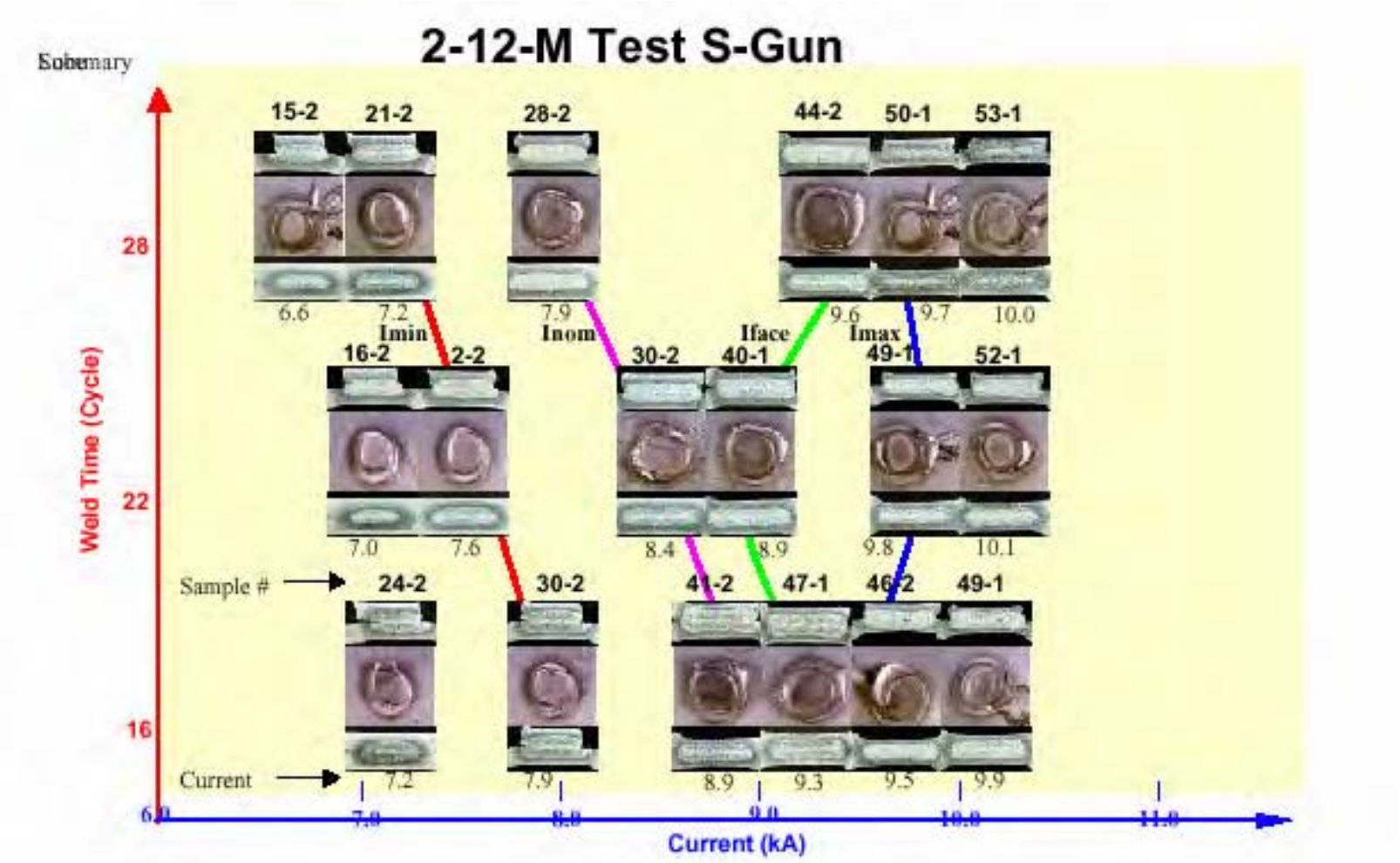

MATERIAL 12 TRIP 600 CRS, S-GUN

Material 13 with C-Gun

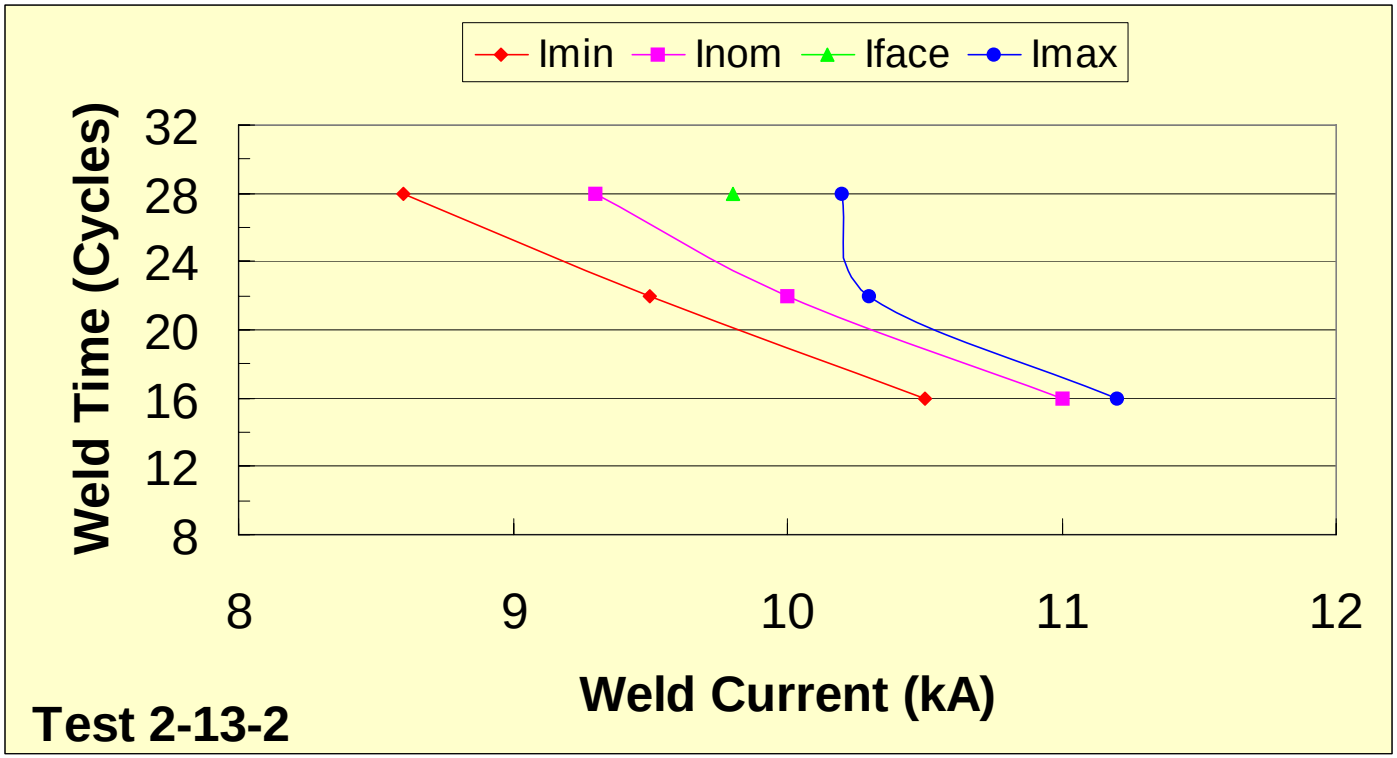

TRIP 800 EG, C-GUN

Appendix D Graphics of Peeled Welds for Weld Size Determination

After the weld tip conditioning sequence is performed, weld size is determined by peel testing samples. Each sample has two welds. The first weld "anchor weld" keeps the specimen together after peeling past the test weld. The first weld also provides a current shunt path typical of automotive welded assemblies. This the method for determining weld size for material acceptance standard AWS/SAE D8-9. The method tends to cause a button pull out of the material unlike the chisel check test which introduces a separating action between the welds as shown in the automotive teardown analysis

Figure D2 Sample bent for application of peeling tool

Figure D3 Peeling has initiated a button pull from one of the sheets.

Figure D4 Peel testing producing metal "teardrop"

Some lower strength materials designed for deep drawing may produce a teardrop that must be cut away from the button to allow button measurement.

Appendix E Weld Bonding Strength and Characteristics

DP 600 GI Matl # 005 Tensile Tests –Weld Bond

Test details for weld bond experiments

- Adhesive - EFTEC EFBOND WC 2309 (Courtesy of DaimlerChrysler) , Specification Number: MS-CD-457-TYPE A
- 0.010” Adhesive Bond Line Thickness (with glass beads)
- Sample size:
    - Coach Peel 150 mm (6 in) overall length x 38 mm (1.5 in) wide, with 38mm x 15 mm weld flange
    - Tensile Shear, 200mm (8 in.) overall length x 38 mm (1.5 in) wide, with 38 mm (1.5 in. overlap)
- Tensile Shear (Pull rate - 0.5” / min.)
- Coach Peel (Pull rate - 0.5” / min.)

Thermal treatment to cure adhesive used a simulated automotive paint bake cycle of:

20 min @ 350 F, Cool , 30 min @ 325 F , Cool, 30 min @ 270 F

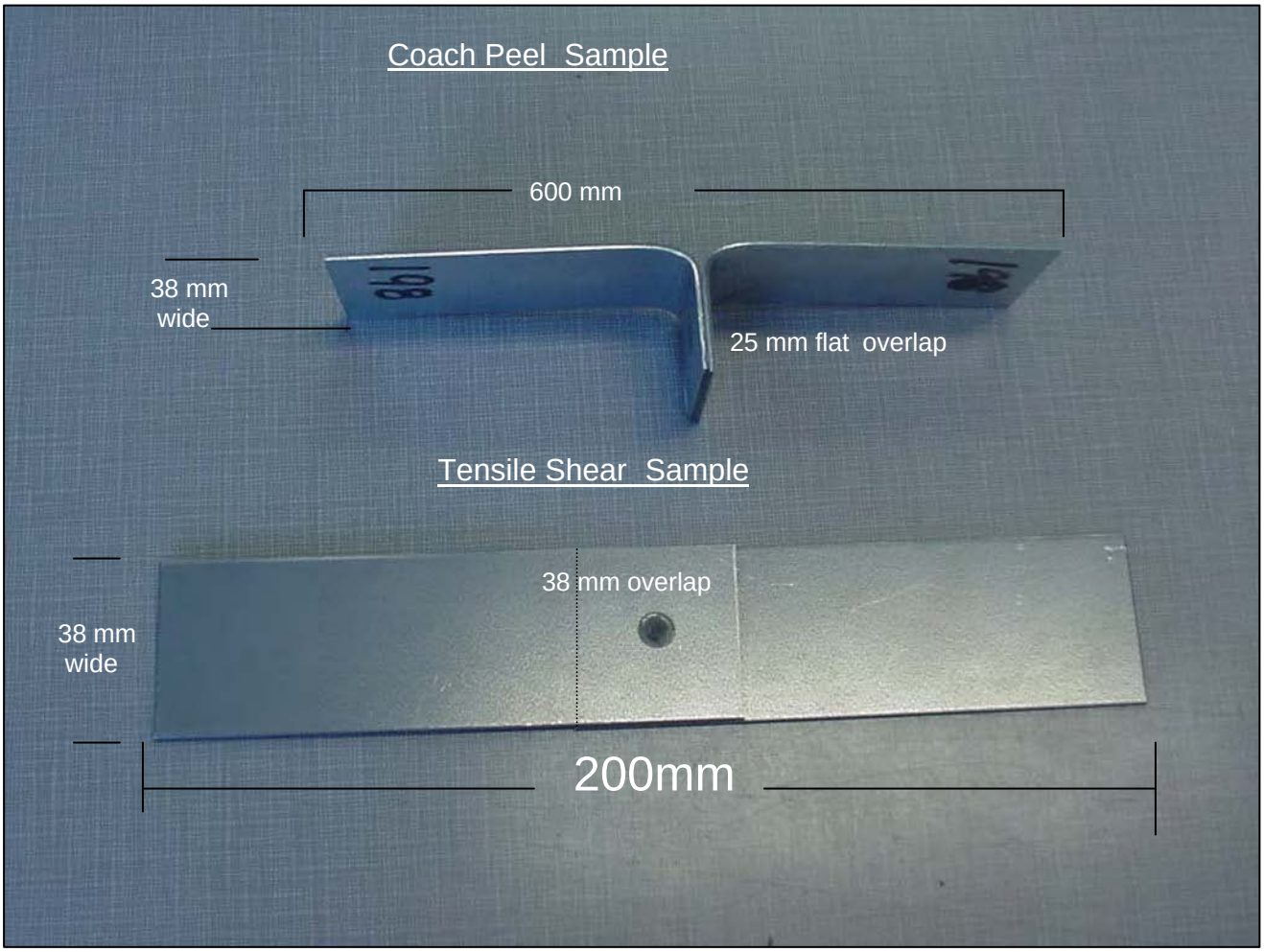

Figure E1 Graphic of weld bond samples

DP 600 GI Matl # 005 Tensile Strips

Base Metal		Adhesive Bond Only	
Max. Load	Max. Ext.	Max. Load	Max. Ext.
(kN)	(mm)	(kN)	(mm)
3476 ± .50	18.30 ± 3.33	28.69 ± .81	3.81 ± .43

1 cycle 4.9 mm	Peak One		Peak Two	
	(kN)	(mm)	(kN)	(mm)
Weld only	13.60 ± 1.37	1.40 ± .25	--	--
Weld Bond	27.79 ± .30	3.63 ± .15	16.50 ± 1.31	.48 ± .13
Weld & Heat Treat	12.75 ± .66	1.27 ± 0	--	--

1 cycle 7 mm	Peak One		Peak Two	
	(kN)	(mm)	(kN)	(mm)
Weld only	20.79 ± .30	3.50 ± .20	--	--
Weld Bond	21.58 ± 4.14	2.01 ± .64	21.02 ± .45	2.01 ± 0.28
Weld & Heat Treat	20.14 ± .15	3.50 ± .20	--	--

90 cycle 4.9 mm	Peak One		Peak Two	
	(kN)	(mm)	(kN)	(mm)
Weld only	12.98 ± 1.17	1.47 ± .20	--	--
Weld Bond	28.66 ± .46	4.01 ± .33	13.60 ± 1.82	.36 ± .08
Weld & Heat Treat	12.34 ± 1.27	1.42 ± .23	--	--

90 cycle 7 mm	Peak One		Peak Two	
	(kN)	(mm)	(kN)	(mm)
Weld only	20.76 ± .16	3.56 ± 0	--	--
Weld Bond	24.80 ± 1.96	2.69 ± .67	20.55 ± .18	1.70 ± .33
Weld & Heat Treat	20.82 ± .61	3.66 ± .23	--	--

DP 600 GA Matl # 003A Tensile Tests – Weld Bond

Base Metal		Adhesive Bond Only	
Max. Load	Max. Ext.	Max. Load	Max. Ext.
(kN)	(mm)	(kN)	(mm)
35.86 ± .04	26.16 ± .89	26.58 ± 1.26	2.18 ± .86

1 cycle 4.9 mm	Peak One		Peak Two	
	(kN)	(mm)	(kN)	(mm)
Weld only	13.71 ± 2.0	1.52 ± .017	--	--
Weld Bond	27.75 ± .89	1.93 ± .81	14.86 ± .87	2.79 ± .08
Weld & Heat Treat	14.06 ± .93	1.37 ± .25	--	--

1 cycle 7 mm	Peak One		Peak Two	
	(kN)	(mm)	(kN)	(mm)
Weld only	20.10 ± .31	3.61 ± .10	--	--
Weld Bond	17.47 ± 1.60	1.14 ± .08	20.73 ± .17	2.08 ± .127
Weld & Heat Treat	20.53 ± .089	3.25 ± .10	--	--

90 cycle 4.9 mm	Peak One		Peak Two	
	(kN)	(mm)	(kN)	(mm)
Weld only	16.01 ± .93	1.83 ± .10	--	--
Weld Bond	26.67 ± .43	2.69 ± .13	16.86 ± .36	.46 ± .15
Weld & Heat Treat	15.67 ± .54	1.57 ± .10	--	--

90 cycle 7 mm	Peak One		Peak Two	
	(kN)	(mm)	(kN)	(mm)
Weld only	21.25 ± .10	3.81 ± .18	--	--
Weld Bond	18.21 ± 1.02	1.22 ± .13	21.33 ± .17	2.16 ± .08
Weld & Heat Treat	21.35 ± .20	3.45 ± .13	--	--

HSLA 340 GI Matl # 002 Tensile Tests – Weld Bond

Base Metal		Adhesive Bond Only	
Max. Load	Max. Ext.	Max. Load	Max. Ext.
(kN)	(mm)	(kN)	(mm)
27.59 ± .040	28.19 ± .71	24.73 ± 1.30	6.99 ± .43

1 cycle 4.9 mm	Peak One		Peak Two	
	(kN)	(mm)	(kN)	(mm)
Weld only	10.91 ± .72	2.24 ± .41	--	--
Weld Bond	25.53 ± .88	6.70 ± .96	8.90 ± 0	1.14 ± .21
Weld & Heat Treat	10.62 ± .44	2.03 ± .94	--	--

1 cycle 7 mm	Peak One		Peak Two	
	(kN)	(mm)	(kN)	(mm)
Weld only	18.20 ± .18	5.28 ± .58	--	--
Weld Bond	26.00 ± .68	6.53 ± 2.11	17.09 ± .96	3.86 ± 1.40
Weld & Heat Treat	17.69 ± .23	4.98 ± .81	--	--

90 cycle 4.9 mm	Peak One		Peak Two	
	(kN)	(mm)	(kN)	(mm)
Weld only	12.71 ± .45	1.83 ± .20	--	--
Weld Bond	26.14 ± .32	7.19 ± 1.29	11.70 ± .47	.84 ± .10
Weld & Heat Treat	13.06 ± .15	2.64 ± .13	--	--

90 cycle 7 mm	Peak One		Peak Two	
	(kN)	(mm)	(kN)	(mm)
Weld only	18.52 ± .24	1.82 ± .51	--	--
Weld Bond	25.55 ± .20	8.03 ± .97	18.34 ± .24	3.66 ± .56
Weld & Heat Treat	18.37 ± .29	5.99 ± .76	--	--

DP 600 GI Matl # 005 Coach Peel Samples

Adhesive Bond Only	
Max. Load	Max. Ext.
(kN)	(mm)
5.11 ± .37	.25 ± .25

1 cycle 4.9 mm	Peak One		Peak Two	
	(kN)	(mm)	(kN)	(mm)
Weld only	2.25 ± .07	21.59 ± 4.01	--	--
Weld Bond	2.22 ± .30	.15 ± .05	2.66 ± .32	24.38 ± 4.82
Weld & Heat Treat	2.57 ± .21	17.0 ± .76	--	--

90 cycle 7 mm	Peak One		Peak Two	
	(kN)	(mm)	(kN)	(mm)
Weld only	3.69± .22	24.13 ± 1.78	--	--
Weld Bond	1.45 ± .28	.15 ± .05	4.07 ± 1.06	13.21 ± 5.08
Weld & Heat Treat	3.53 ± .45	16.00 ± 1.27	--	--

DP 600 GA Matl # 003A Coach Peel Samples

Adhesive Bond Only	
Max. Load	Max. Ext.
(kN)	(mm)
2.76 ± .39	.10 ± 0

1 cycle 4.9 mm	Peak One		Peak Two	
	(kN)	(mm)	(kN)	(mm)
Weld only	2.64 ± .27	19.30 ± 1.27	--	--
Weld Bond	1.16 ± .21	.15± .1	3.09 ± .34	11.43 ± .76
Weld & Heat Treat	2.48 ± .12	20.83 ± .51	--	--

90 cycle 7 mm	Peak One		Peak Two	
	(kN)	(mm)	(kN)	(mm)
Weld only	3.11 ± .27	16.23 ± .25	--	--
Weld Bond	1.60 ± .09	.08 ± .02	3.32 ± .31	14.22 ± 2.29
Weld & Heat Treat	3.34 ± .38	15.24 ± 2.54	--	--

HSLA 340 GI Matl # 002 Coach Peel Tensile Samples

Adhesive Bond Only	
Max. Load	Max. Ext.
(kN)	(mm)
2.86 ± .42	.15 ± .05

1 cycle 4.9 mm	Peak One		Peak Two	
	(kN)	(mm)	(kN)	(mm)
Weld only	3.43 ± .63	19.56 ± 4.06	--	--
Weld Bond	1.94 ± .64	.46 ± .13	3.43 ± .26	16.76 ± 1.78
Weld & Heat Treat	3.48 ± .16	16.51 ± .25	--	--

90 cycle 7 mm	Peak One		Peak Two	
	(kN)	(mm)	(kN)	(mm)
Weld only	4.41 ± .78	20.07 ± 2.54	--	--
Weld Bond	2.38 ± .93	.30 ± .13	5.41 ± .18	16.51 ± 0.76
Weld & Heat Treat	4.99 ± .57	15.50 ± 2.03	--	--

Appendix F - Ultrasonic Evaluation of Welds

Objective: To non-destructively measure the geometric features of a spot weld which are to be correlated with various measured strengths.

A resistance spot-weld joint is formed between two or more sheets of material. Visual evaluation to determine weld quality is not effective for determining weld size at the interfaces of the welded sheets. An effective non-destructive test method using an ultrasonic B-scanner designed by *Applied Metrics* was adapted and qualified for accurate quality inspection of resistance spot welds.

The device was first evaluated by comparing the ultrasonic measurement results with those from metallographic sectioning. A low carbon steel and a DP600 advanced high strength steel were used in the comparison. Various welding conditions were created that produced good welds, undersized welds, welds with unfused internal area/voids, stick/cold welds, and welds with expulsion using these two materials. Comparisons show that the difference is within 10% between ultrasonic measurements and cross-sectioning measurements of weld nugget width. After the ultrasonic device was approved, it was used for measuring the geometric features of all impact testing specimens and selected quasi-static tensile-shear specimens. Dimensions measured include surface indentation width and depth, weld thickness, nugget width, internal void width and location. These data were stored and used to link measured strengths of the welds, after destructive testing, to geometric features in order to link the strengths, such as impact energy to the easily measurable geometric quantities such as indentation depth. Certain good correlations have been obtained.

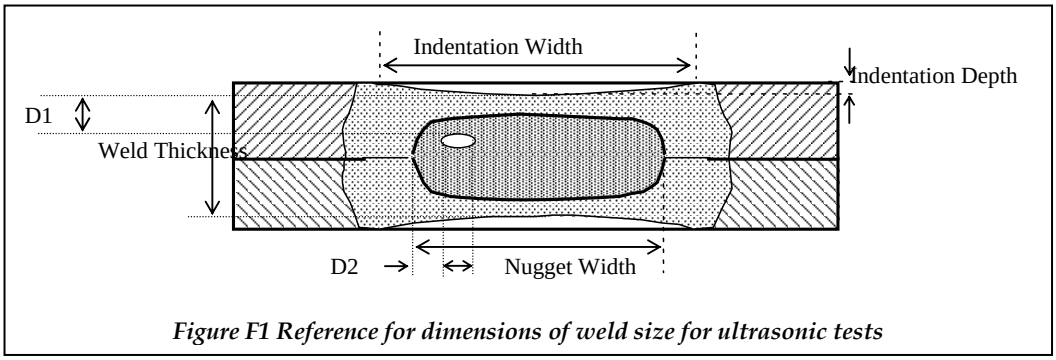

Figure F1 Reference for dimensions of weld size for ultrasonic tests

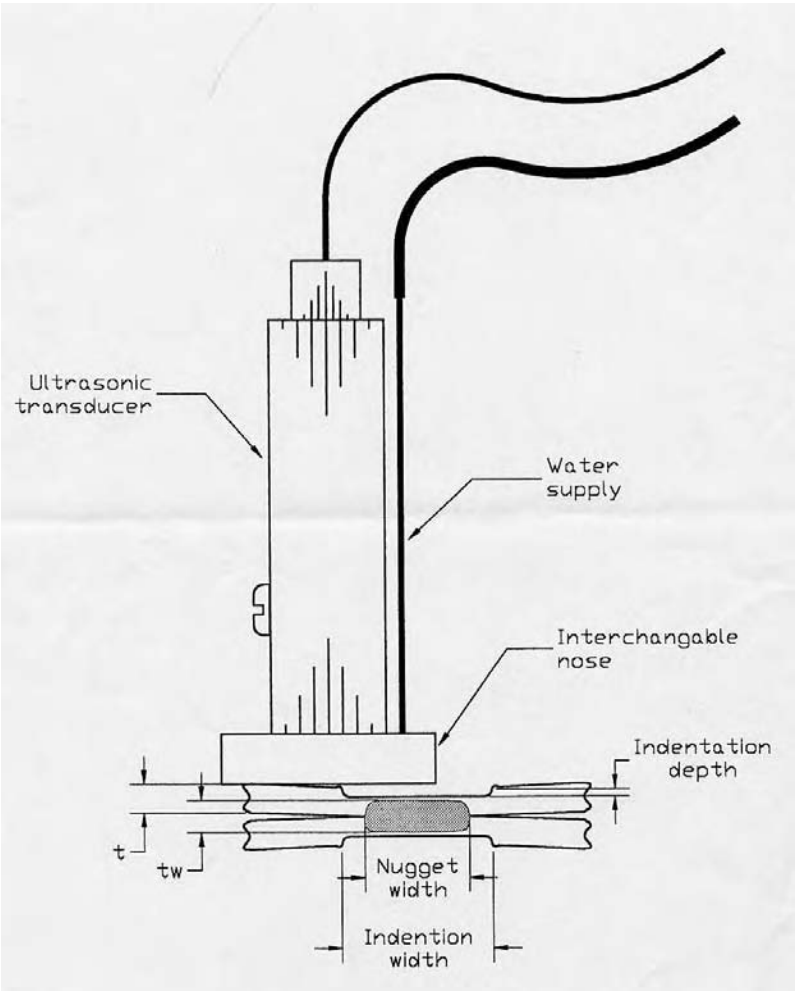

Figure F2 Schematic of ultrasonic transducer placement on sample surface. Transducer is moved across the welded area to acquire the weld data.

Ultrasonic Spot Weld Inspection System (SWIS)

SWIS is composed of three major components: the computer data acquisition system (DAS), a couplant supply system, and a narrow beam scanner.

1. The DAS is located at a distance that provides easy access to the parts to be imaged and is connected to an AC power source.
2. The couplant supply system is located next to the DAS and connected to delivery mechanism.
3. A pencil probe/scanner connected to the DAS as shown in F**igure F2** The couplant (water) supply hose is connected to the couplant supply system.

The system used for acquiring and replicating the weld diameter used and ultrasonic scanning mode known as B-Scan. The difference between A-and B-scan are shown in the graphic s below.

A-scan is a cross-sectional image of a part at one point or transducer location. It produces a plot of signal amplitude *vs.* time on an oscilloscope type screen display. A-Scan is the basic method for displaying ultrasonic beam propagation through material.

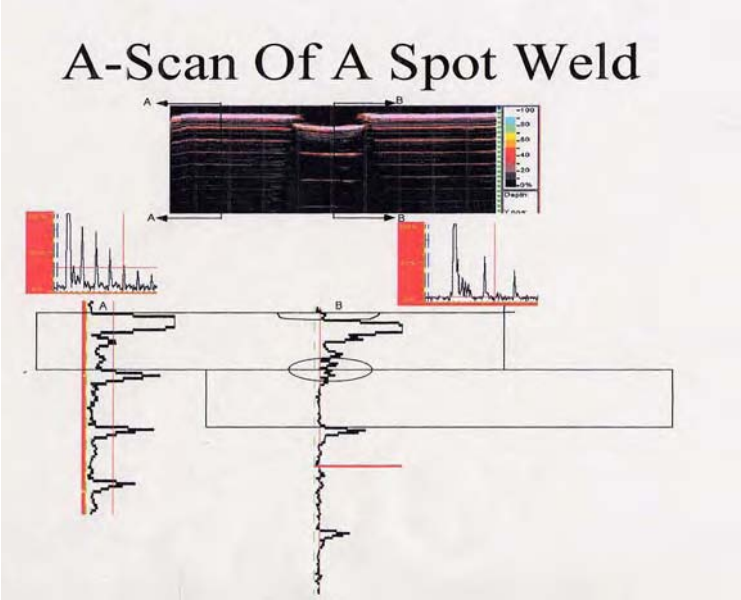

Figure F3 The left echo train shows the attenuation through the base metal sheet in contact with the transducer. The right pulse train shows attenuation through the weld metal in this example.

The B-scan is a cross-sectional image of a part **along a section line** on the surface of the part. It is formed by rotating A-scans into a display and presenting the amplitude of signals with a color code. It is then placed side by side along a line to form the image. B-Scan can be constructed showing all of the A-Scan data or selected portions.

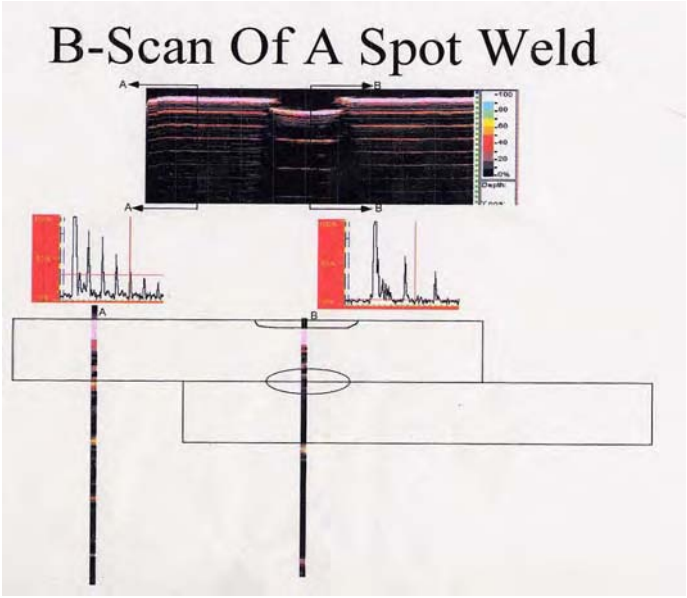

Figure F4 Schematic B-Scan of a spot weld. The echo trains are color coded and stacked for each sample pulse taken as the probe is moved across the sample. Note that sonic beam divergence is not shown in this schematic.

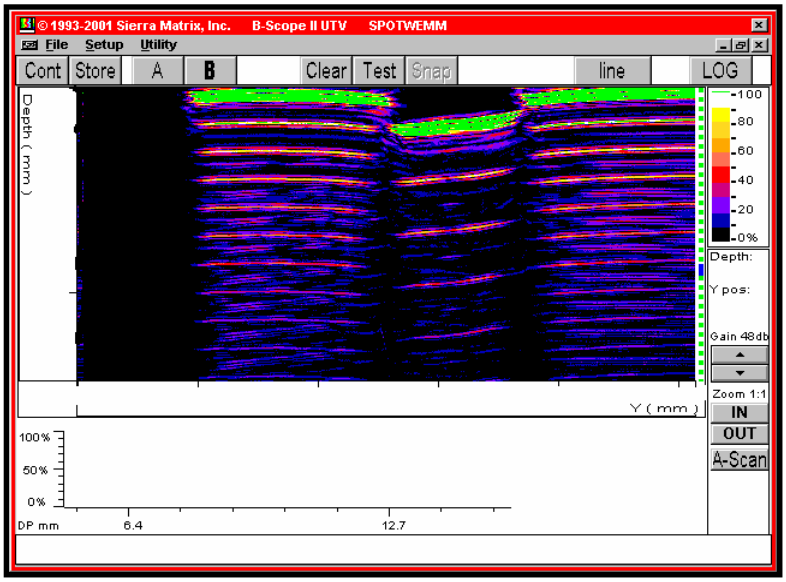

Figure F5 Screen shot of the computer generated B-Scan

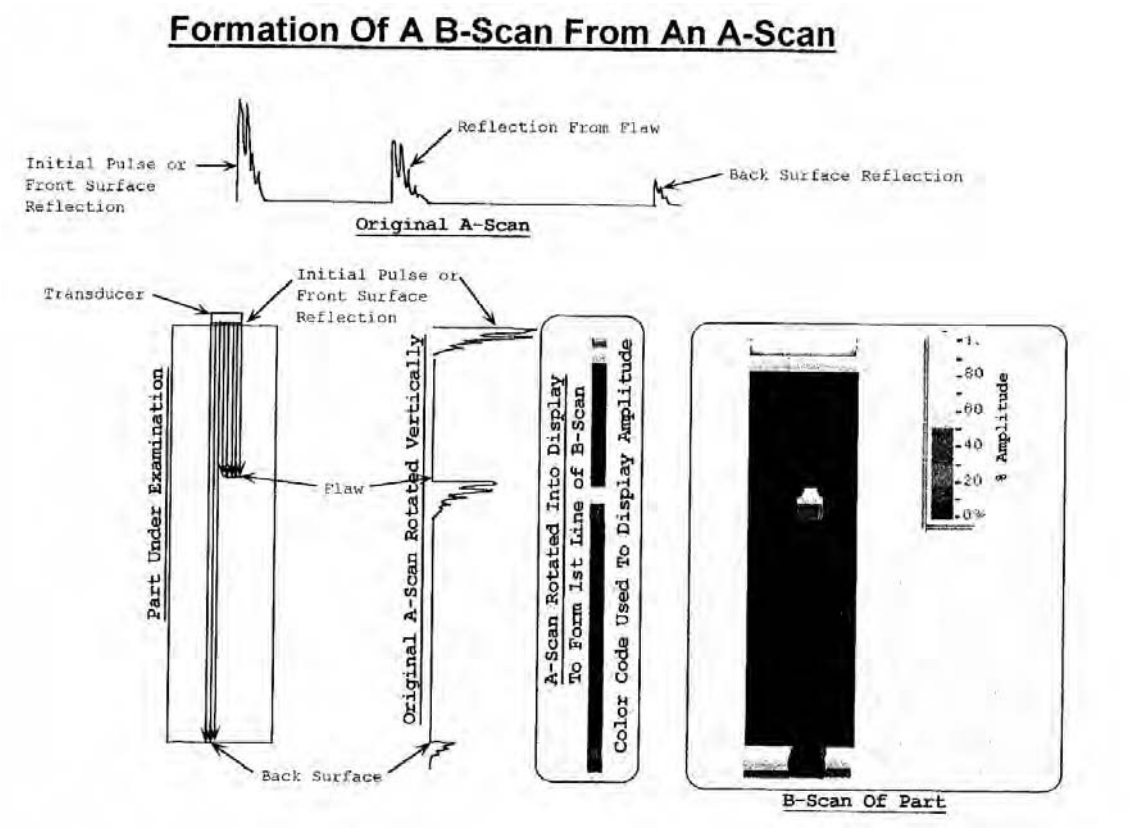

The A-scan provides a overall sonic signature of the column of material covered by the probe. The probe is stationary for the test and the beam diameter is selected to be slightly larger than the minimum acceptable diameter of the weld for the selected material thickness testes.

The B-scan uses a moveable probe and records a cross section through the material in line with the probe movement. The distance the probe moves is recorded by the (DAC?) encoder for use in measurement made from successive waveforms of the weld. The probe is moved across the centerline of the weld and the sonic beam is concentrated over a diameter of 0.030 inches (0.76mm) at the theoretical interface (faying surface) of the two plates. This can measure the weld top surface shape, the heat affected and weld zone and the bottom shape of the weld; all of which provide useful dimensional information about the weld. The fundamental frequency used in this system is 20 MHz, the H2O delay line is 1.7in. (43mm) and the data is recorded on a spacing across the weldment on grid of 0.005 in. (0.13mm).

Determining measurement accuracy

DP600 and Low Carbon Steel were used to make good weld, stick weld, void, undersized, large indentation & expulsion welds.

In this step, several welds of each kind were made by using data from the AHSS weld lobe charts and modifying parameters to obtain variation in quality. , The records of all the welding parameters were kept for later reference. The samples were peeled to determine spot welds produced. After tuning the process of producing weld types, , ten samples for each weld type were made with corresponding parameters.

G90/G90 mild steel and the same welding machine were used to make 25 different degrees of stick welds. Degrees varied from totally separated, slightly sticky, mid sticky, hard sticky until good weld.

For this experiment, 50 samples were scanned, and then the samples with the best image were chosen for each kind to be sectioned in the next step. In addition, 25 stick welds were scanned for further analysis. According to the analysis of internal shape of spot-weld with ultrasonic inspection theory, the measurements were made for each part as shown in figures below. It is noticed that under the indentation part, almost no signal could be found.

Good Weld

A ideal weld is one that is formed by complete fusion of the sheets in contact at the interface. It has a large nugget diameter, shallow indentation marks, and is formed without any expulsion. A peel test on a good weld reveals a button on one of the sheets and a hole on the other sheet.

The B-Scan images of the good weld samples show the following characteristics:

1) Shallow depth of electrode indentation.
2) Reflection from the top sheet surface and the back sheet surface only in the nugget zone.
3) No reflection from the interface in the nugget zone.

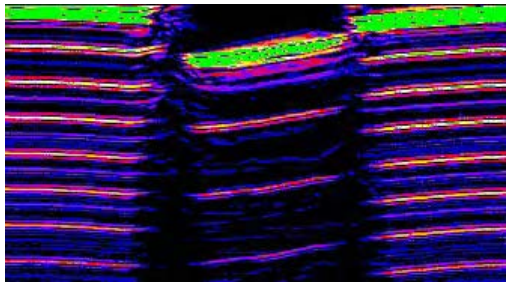

Figure F6 Ultrasonic computer generated section of weld in DP-600, 0.7mm thick

Figure F7 Photograph of cross section of same weld (DP-600), 0.7 mm thick

DP 600 Sheet thickness = 0.7 mm

Nugget diameter = 4.25 mm (B-scan) 3.526mm (measured)

Width of indentation = 4.51 mm (B-scan) 4.048 mm (measured)

Depth of indentation = 0.19 mm (B-scan) 0.093 mm (measured)

*Note: The stray lines of reflection in the nugget zone are the result of the noise present in the environment surrounding the machine. We should only focus on the brightest lines.

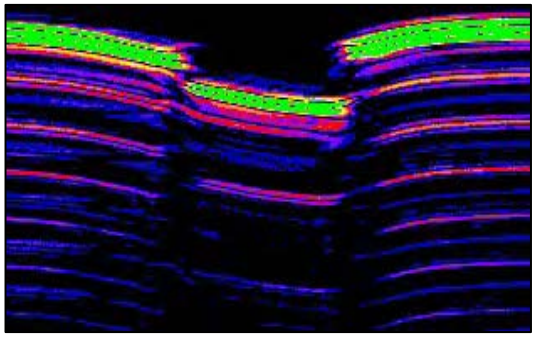

Figure F8 B-scan of acceptable weld in low carbon steel

Figure F9 Cross section of acceptable weld in low carbon steel

Good weld image for low carbon steel

Sheet thickness = 0.75 mm

Nugget diameter = 4.09 mm (B-scan) 3.854 mm (measured)

Width of indentation = 4.66 mm (B-scan) 3.406 mm (measured)

Depth of indentation = 0.09 mm (B-scan) 0.073 mm (measured)

Stick Weld

A stick weld is characterized by partial or semi-fusion of the sheet metal at the interface. There is no nugget formation in this case. The electrode indentation is very shallow. Sheets, which are stick-welded, can be pulled apart easily and do not show the presence of any button on either sheet.
The B-Scan image of stick weld has the following characteristics:

1) Extremely shallow depth of electrode indentation.

2) Reflection from the top surface of the first sheet, partial reflection from the back surface of it.

3) No reflection from the second sheet.

4) Partial reflection from the interface in the electrode zone.

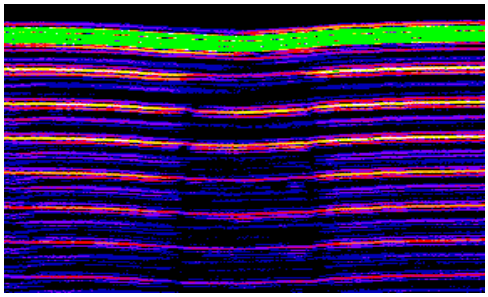

Figure F10 B-Scan of stick weld in DP-600

Figure F11 Cross section of stick weld in DP-600

Stick-weld image for DP600 steel

Sheet thickness = 0.7 mm

Stick diameter = 2.80 mm (B-scan) 2.116 mm (measured)

Width of indentation = 3.16 mm (B-scan) 2.621 mm (measured)

Depth of indentation = 0.03 mm (B-scan) 0.026 mm (measured)

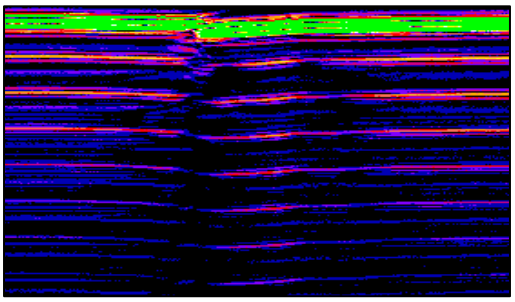

Figure F12 B-Scan of stick weld in low carbon steel

Figure F13 Cross section of stick weld in low carbon steel

Stick weld image for low carbon steel

Sheet thickness = 0.75 mm

Stick diameter = 3.42 mm (B-scan) 3.492 mm (measured)

Width of indentation = 2.83 mm (B-scan) 2.318 mm (measured)

Depth of indentation = 0.05 mm (B-scan) 0.057 mm (measured)

This system was used to record weld size for the impact samples and data is reported in the test record along with the measured weld size determined after impact samples were tested. Some error in measuring the separated impact sample pieces is due to the nature of weld fracture. Fracture modes having full interfacial fracture require estimating the actual fused area. Determining fused area is made difficult by the adjacent bond halo that was not actually fused during the weld process.

Determining Specimen Sizes for Testing AHSS Spot Welds

The objective of this test was to determine suitable sizes of test specimens to obtain consistent testing results.

Specimen geometry plays an important role in a weld's strength measurement, as the mechanical constraint imposed on a weldment from the base metal significantly influences the deformation and loading mode on the weld when a specimen is tested. In order to eliminate the variability in strength measurement induced by specimen sizes, a study was conducted to determine the narrowest specimen widths that produce consistent results when tested in both tensile-shear and impact tests.

Use of flat samples, in place of "C" channel specimens proposed by others, reduced testing cost and simplified sample fabrication. All samples were planned to be the width determined by the highest strength of the materials to be tested. Three tasks were conducted to achieve the objective:

1. Determine coupon sizes which produce the least and critical constraining;
2. Conduct a sensitivity study on specimen width of impact tests; and
3. Determine a unified width for tensile-shear test and impact test.

By testing the impact response for sample width starting at 50 mm wide, optimal specimen sizes were determined. The highest strength material to be evaluated in this test series was MS –1300. Based on this strength, the sample width was determined to be:

For tensile-shear tests: Length = 150 mm; Width = 125 mm; Overlap = 125 mm.

For tensile-shear tests: Length = 208 mm; Width = 125 mm; Overlap = 125 mm.

Constraint test for tensile testing

After determining optimum flat sample width that would be applicable to both impact testing and tensile testing, two other tests were conducted to determine feasibility for using other geometries that potentially would conserve material usage from our limited supply of test material. These designs would not be suitable for impact testing due to the configuration of the impact test fixture. They would, however, be a means to conserve material for the quasi static tensile testing if that became necessary. The designs were a "U" channel design and a bearing or strong back fixture to constrain bending. Data for the tests can be found in RES report ASP-BR-03 r1.doc on the CD.

U-Channel Design

Additional tests were performed to evaluate the effect of sample shape and mechanical constraint. A U-shape channel was formed to provide a tensile specimen that would minimize rotation during testing. The dimensions of the sample are shown in the figure below. The target width after forming was 1 inch (25.4 mm) inside the channel and 0.5 inch (12.8 mm) flange height. Length of individual components was 5 inches (125 mm). The bend radius was 0.18 inch inside (3 x T) which was the minimum radius needed for the some of the AHSS materials. Samples made in the U-channel configuration were tested and compared to specimens constrained by use of a special constraint fixture shown in the following figure. While the channel produced similar results as the 125 mm flat sample configuration and conserved material, other factors made this configuration less desirable than the flat sample design.

Forming the bends in the high strength material was difficult and controlling the finished dimensions proved problematic. Increased cost, increased scrap and issues related to fitting the sample to existing test equipment also made this configuration less desirable than the flat sample design.

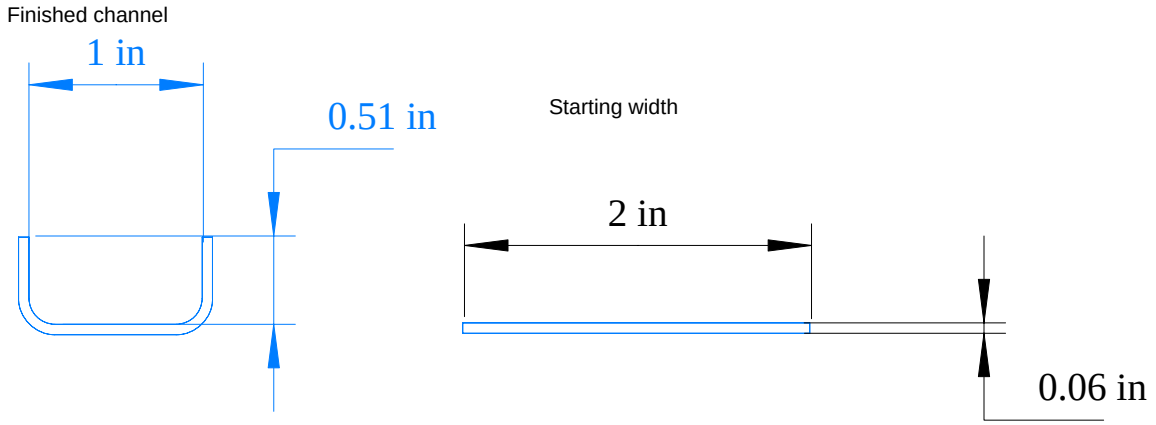

Figure G1 Proposed U- Channel Design for tensile testing. The bend radius had to be controlled to allow forming in the highest strength material in the test series (MS1300)

Bearing Plate – Strong Back Fixture

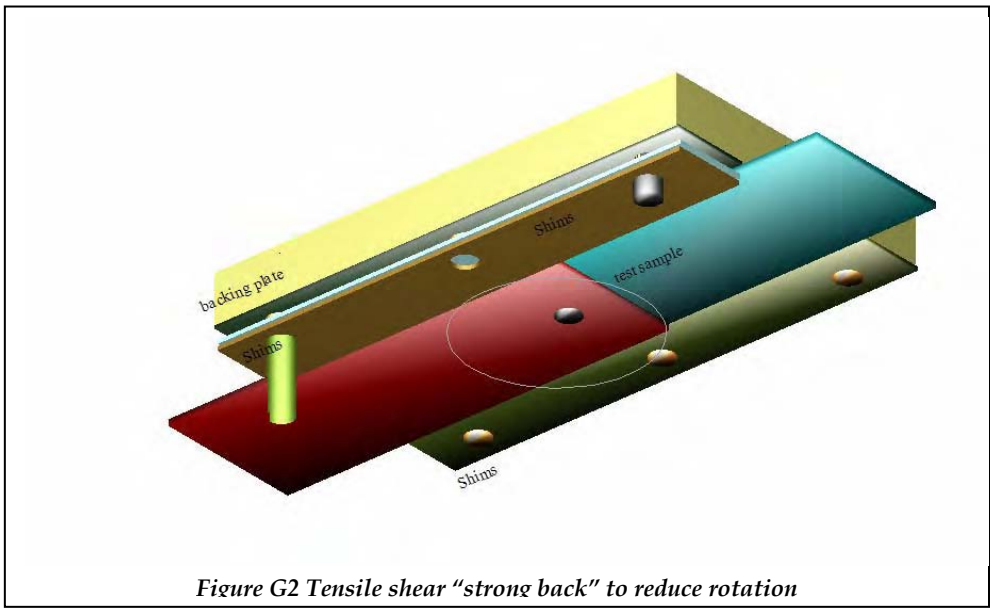

Figure G2 Tensile shear "strong back" to reduce rotation

Bearing plate fixture was evaluated as a means to limit sample rotation during tensile test of 40 mm wide samples. Two plates (only one shown for clarity) are used during testing. The illustration shows the arrangement of the tensile sample and the shims used on each side of the test sample. Shims are stacked to provide clearance between the two strong-back plates and the test sample thus reducing sliding friction. The strong back plates are drilled through with a 12 mm (1/2 inch) hole centered at the spot weld to allow viewing the weld during assembly and to provide clearance for any metal that may be protruding from the weld. A screw is used (not shown in this view) to lightly clamp one end of the sample to the bearing plates to prevent the fixture from sliding off the sample during testing.

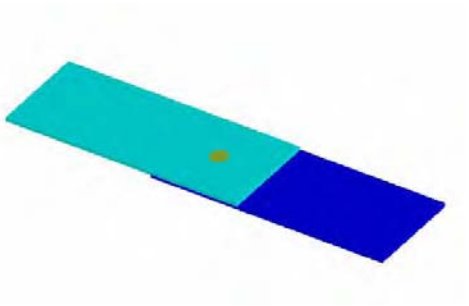

Figure G3 Tensile shear 40 mm wide samples have overlap equal to the width. Length of individual pieces was 125 mm. A finished sample was approximately 210 mm long. Grade and metal gage was equal for the each sample.

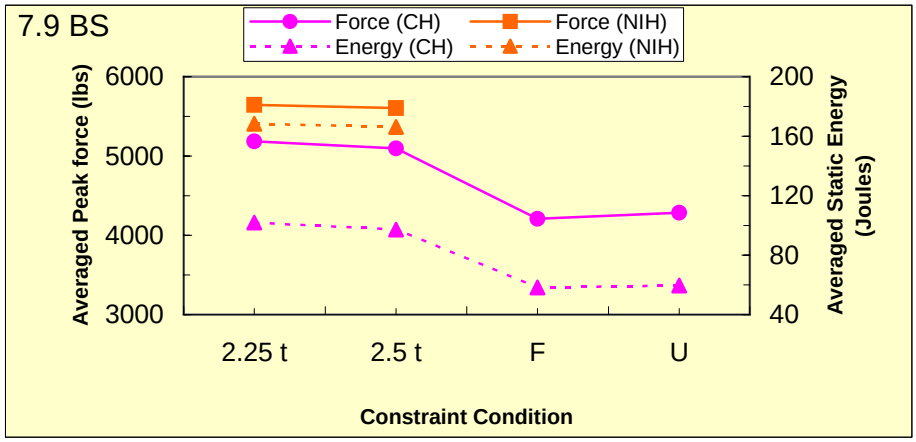

This chart shows the effect of constraint on tensile shear strength and energy for button size of 7.9 mm diameter.

The strong back fixture was tested with two shim arrangements 2.25t and 2.5 t with t being the thickness of the sheet steels welded. The shims provide clearance for sample movement between the bearing plates. The strong back produced the highest of tensile loads. Two conditions for weld location for the strong back fixture were also evaluated. The fixture has a clearance hole drilled through to allow clearance for button rotation. If the hole is not lined up (NIH in the chart legend) with the weld, the breaking loads are higher that when the weld is centered in the hole.

The chart also reports the loads and energy for the Flat 125 mm wide sample (F) and the "U" channel 25 mm wide with 12.5 mm upstanding flanges (U).

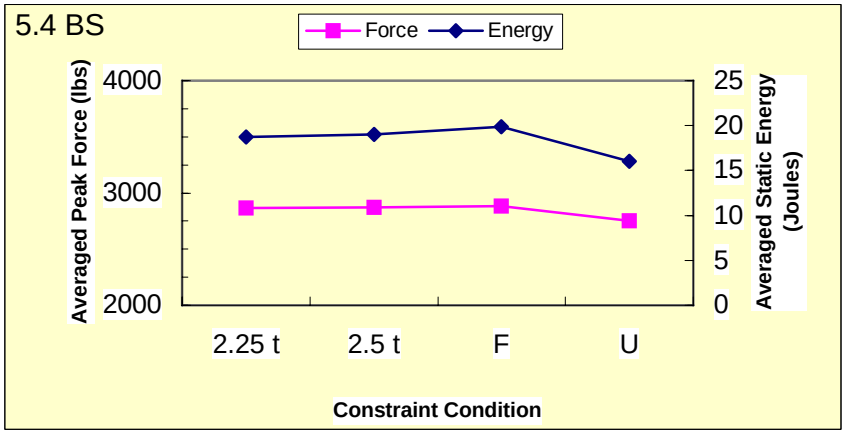

This chart reports strength and energy for a smaller weld size of 5.4 mm diameter. The flat and strong back fixture produced similar results with the "U" channel producing the lowest result.

Impact Testing of AHSS Spot Welds

The objective of this test was to determine the impact strength of various AHSS spot-welds.

The impact strength of a spot weld is an important quality index in the automotive industry as it is directly related to the crashworthiness of spot welded structures. Advanced high strength steels provide a unique opportunity for building lighter automotive body frames for fuel economy and safety. However, the strength of AHSS welds, especially their impact strength is largely unknown. As the impact performance is critical in adopting a new material, the evaluation of a spot weld's impact behavior is of practical importance to material and welding engineers.

The materials tested under impact conditions:

> HSLA 340YGI, HSLA 340YGA, DP 600GA, DP 600 Bare, DP 800GA, DP 980Bare, RA 830 Bare, TRIP 600 Bare, TRIP 800 EG, and MS 1300 Bare.

Impact energy and peak load were monitored during the tests. The testing results show that the impact strength of a weldment is roughly proportional to the ultimate strength of the base material, except in the cases of TRIP 800 which has lower impact strength than DP600GA, and of RA830Bare which is lower than HSLA340YGA. DP980Bare has similar (or slightly lower) impact energy than DP800GA. Another observation is the variability of the impact energies. As the mean values of impact energy increase, the variability also increases in terms of energy units. The variability should be normalized to reflect the strength levels of the material tested. When variability is measured in terms of percent of average strength, a more practical measure is obtained.

The welding schedules have a clear influence on the impact performance of the spot welds. Large welds have larger impact absorption capacity than smaller welds. The effect of hold time is not uniform in all materials tested. For some materials, such as DP600Bare and TRIP600Bare, the hold time has no effect. Other materials, such as TRIP800EG and MS1300CR, a short hold time increase performance, while others, such as DP600GA and DP800GA benefit from a long hold time.

The peak loads have generally a positive correlation to impact energies for the materials tested.

An impact tester used for determining impact data is based on a design developed in the Advanced Technology Program "Intelligent Resistance Welding" . The impact tester allows making impact test a simple, accurate, and affordable test for weldability studies.

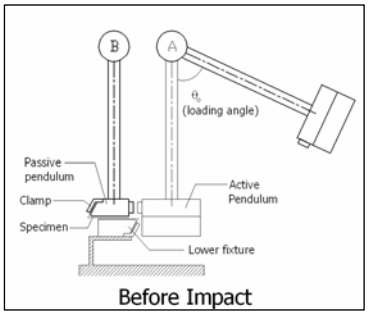

Schematic diagram (before impact)

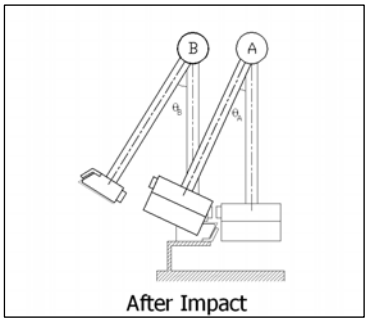

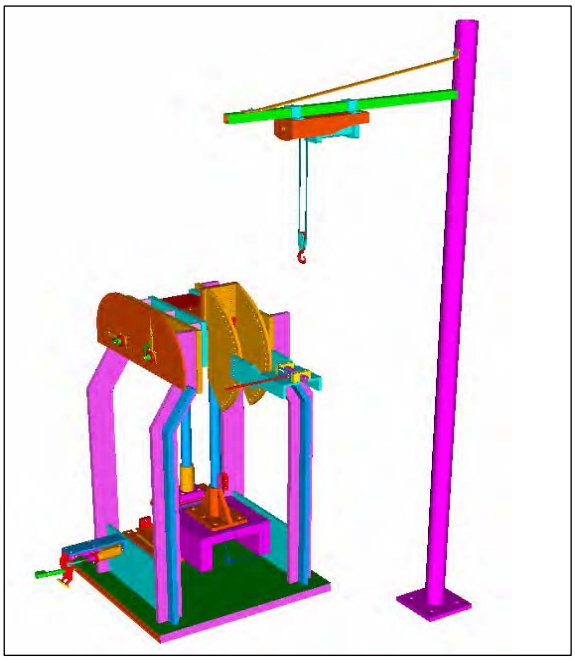

Impact tester

Specification

The *Input Potential Energy* of the active pendulum can be varied from 141 Joules to 2139 Joules by changing the angle of loading (θ_o) of the active pendulum from plus 45 degrees to minus 45 degrees with respect to the horizontal. This enables testing spot welds of very high strength materials that require high input potential energies to achieve fracture.

The adjustable angle of loading enables the *Velocity* of the active pendulum at the instant of impact to be varied. Velocity is a critical factor in impact testing, since many materials exhibit strain-rate sensitivity. This makes the machine versatile in the range of materials handled, the weld geometry tested at the desired input conditions.

The following table lists the detailed machine specifications.

Parameter	*Unit*	*UT Impact Tester*
Mass of Active Pendulum	*kg*	*128*
Mass Center of Active Pendulum from pivot	*mm*	*998*
Mass of Passive Pendulum	*kg*	*36.3*
Mass Center of Passive Pendulum from pivot	*mm*	*818*
Input Energy	*Joules*	*141 to 2139*

Instrumentation

In the impact tester the impact strength of a specimen (in the form of *Impact Energy*) can be evaluated from the dial meter readings for the swing angles for both pendulums in the energy equation without using any electronic devices. This is an important advantage in terms of measurement since a direct correlation between the swing angle on the scale and energy of the pendulums is achieved without complicated intermediate mechanisms.

Detailed information of impact event, such as impact force and its variation with time, are derived from instrumented measurement. The major difference in instrumentation from quasi-static testing is that sensors used in impact testing must have a high response rate. The displacement and force profiles are of particular interest in characterizing the impact process.

On this machine, a set of four force sensors is used to acquire the forces generated in the specimen. These sensors are strain gauge compression load cells. Each load cell has a capacity of 25,000 lbs or 111.5 kN. The output is taken from each sensor and directed to the computer and the profile of impact force and the peak load generated during the test are then derived. A fiber optic sensor was used to measure displacement.

Sensitivity Study

A test was carried out on the impact tester prior to designing the impact specimens. The purpose was to determine the minimum specimen width required to eliminate the specimen width effect.

An infinitely wide specimen permits local nugget "rotation" but eliminates rotation/deformation at the edges of the specimen [17]. This means that the material adjacent to the nugget must not deform significantly, otherwise the energy reading obtained will contain the component of 'base metal deformation', which is difficult to filter out from the energy of fracture of the weld.

The Sensitivity test was carried out by testing specimens of 50 mm, 75 mm, 100 mm, 125 mm, 150 mm and 200 mm widths individually. Five replicates were used for each width. Test Results are shown in the figure G4.

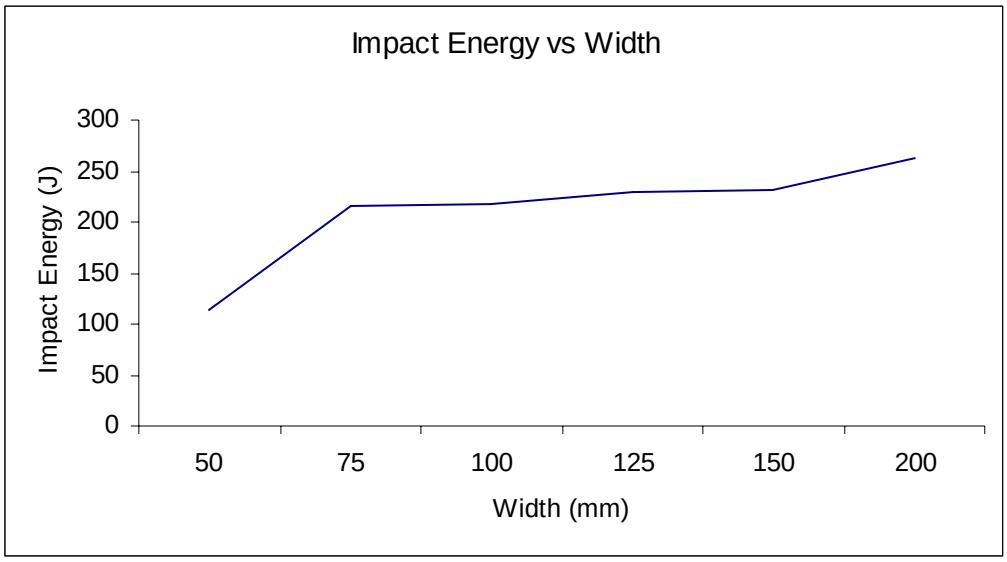

Figure G4 Impact energy versus sample width

The results show that at widths of 50 mm to 75 mm, the failure mode is predominantly interfacial shear and the impact energy absorbed is 112.84 J and 214.75 J, respectively.

The specimens fail mainly in button mode at widths of 100 mm and above. The impact energy absorbed is around 230 J. From the graph, it is concluded that the optimum specimen width is 125 mm.

Calibration

Calibration tests were carried out to determine the magnitude of 'Machine Error' (E_{Error}), before testing actual specimens. It is also important in ensuring repeatability and accuracy of testing. Calibration was done through testing without a specimen, i.e. dry runs. Calibration tests were performed before testing each material.

The active pendulum was loaded to a specific angle (such as 65˚) and then released without mounting any specimen in the machine. After the impact of active pendulum on the passive pendulum, an elastic/stress wave is generated in the head block of the passive pendulum. The passive pendulum does not move until the stress wave reaches the far end of the head block after the strike. The system energy loss E_{Error} was estimated on the basis of calibration from the relation:

$$E_{Error} = M_A g L_A(1 - \cos\theta_0) - M_A g L_A(1 - \cos a_A) - M_B g L_B(1-\cos a_B)$$

Advantages of the Impact Tester

This tester has the following characteristics.

- It is applicable to welded, bonded, weld-bonded, and riveted specimens with equal ease.
- It is capable of testing a large range of materials from polymers, aluminum, low strength steels to advanced high strength steels.
- It can be used for both tensile-shear and peel loading.
- It can be used for impact testing at customized impact speed and input impact energy.
- It makes impact measurement easy, accurate and repeatable.

Photograph of impact and tensile shear samples

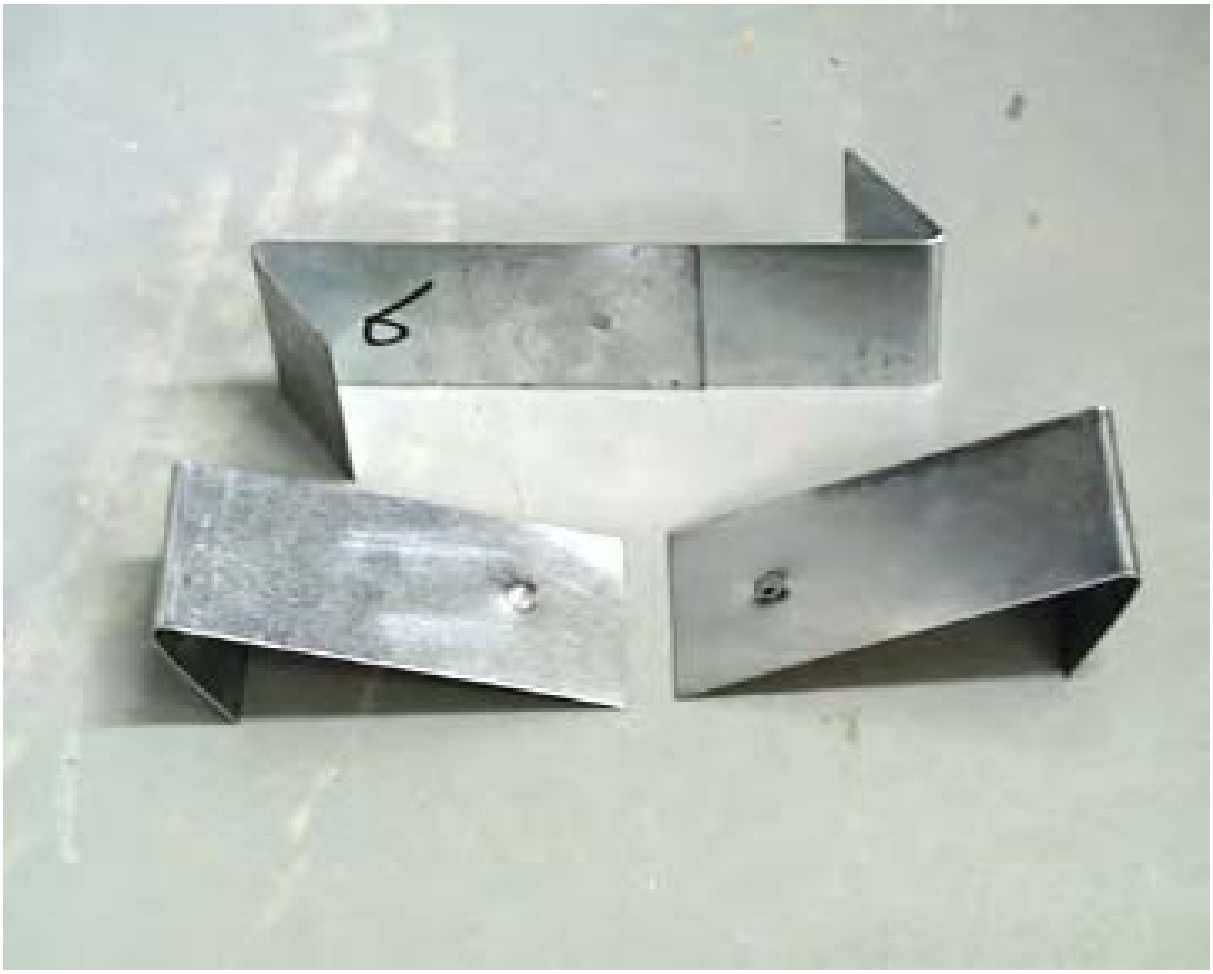

Figure G5 Impact sample before (top) and after testing (bottom)

Figure G6 One lot of samples after testing

One run of samples showing 125 mm wide tensile shear and impact samples after testing. Each material had these tests made.

Appendix H Material Test Matrix - Identification, Chemistry and Physical Properties

MATERIAL- RSW JOINING PROJECT	Mat'l ASP ID	C	Mn	P	S	Si	Cu	Ni	Cr	Mo	Al	V	Cb
HSLA 340Y GI 1.6 MM	001	0.053	0.620	0.008	0.005	0.214	0.052	0.02	0.01	0.000	0.039	0.001	0.016
HSLA 340Y GA 1.5 MM	002A	0.019	0.370	0.009	0.006	0.021	0.040	0.01	0.04	0.000	0.052	0.001	0.037
DP 600 GA 1.6 MM	003A	0.071	1.620	0.011	0.007	0.021	0.036	0.02	0.18	0.170	0.039	0.001	0.003
DP 600 GI 1.45 MM	005	0.081	1.760	0.017	0.006	0.013	0.040	0.02	0.19	0.180	0.048	0.002	0.004
DP 600 Bare 1.15	006	0.086	0.970	0.012	0.012	0.299	0.014	0.01	0.02	0.000	0.030	0.002	0.003
DP 800 GA 1.55 MM	007	0.102	1.830	0.015	0.004	0.022	0.020	0.01	0.24	0.180	0.037	0.002	0.003
DP 980 Bare 1.55 MM	008	0.149	1.380	0.011	0.007	0.293	0.016	0.01	0.03	0.000	0.035	0.002	0.002
RA 830 GI 1.30 MM	009	0.058	1.160	0.010	0.001	0.034	0.023	0.01	0.03	0.010	0.057	0.054	0.073
RA 830 Bare 1.70 MM	010	0.057	1.150	0.010	0.005	0.029	0.023	0.01	0.04	0.010	0.051	0.054	0.065
MS1300 Bare 1.55	011	0.146	0.430	0.005	0.012	0.017	0.018	0.01	0.01	0.000	0.047	0.002	0.003
TRIP 600 Bare 1.55 MM	012	0.101	1.470	0.002	0.001	1.536	0.016	0.02	0.05	0.010	0.027	0.005	0.005
TRIP 800 EG 1.55	013	0.091	1.45	0.019	0.001	0.147	0.015	0.020.	0.05	0.010	0.026	0.005	0.003
DP 600 GA (DC)	003 DC	0.207	1.70	0.014	0.001	1.662	0.009	0.02	0.03	0.000	0.037	0.002	0.003

Material Test Matrix Identification and Physical Properties

Mat'l Description	Mat'l ID	Thickness mm	0.2% offset YS, ksi	UTS, ksi	Uniform Elong %	Total Elong. %	r/Δr
Mat'l 01-HSLA 340Y GI 1.6 mm	1	1.6	53.5	65	15.9	31.7	1.069/ 0.002
Mat'l 02-HSLA 340Y GA 1.5 mm	002A	1.5	53.5	61.5	18.4	32.6	1.053/ -0.249
Mat'l 03A-DP 600 GA 1.6 mm	003A	1.6	48.8	81.8	16.6	28	0.980/ 0.106
Mat'l 05-DP 600 GI 1.45 mm	5	1.45	62.7	97.3	13.6	22.1	0.922/ -0.007
Mat'l 06-DP 600 Bare 1.15 mm	6	1.15	51.7	90.4	15.9	24	0.847/ 0.389
Mat'l 07-DP 800 GA 1.55 mm	7	1.55	60	113.4	12.7	19.5	0.832/ -0.027
Mat'l 08-DP 980 Bare 1.55 mm	8	1.55	101.9	153.3	7.1	11.4	0.845/ 0
Mat'l 09-RA 830 GI 1.30 mm	9	1.3	130.7	129.8	0.8	6.7	0.634/ -0.426
Mat'l 10-RA 830 Bare 1.70 mm	10	1.7	132.1	136.9	4.5	8.7	0
Mat'l 11-MS1300 Bare 1.55 mm	11	1.55	167.7	196.6	3.2	5.1	0
Mat'l 12-TRIP 600 Bare 1.55 mm	12	1.55					
Mat'l 12B- TRIP 600 Bare 1.55 mm	12B	1.55	60.3	98.6	19.6	28.3	1.08
Mat'l 13-TRIP 800 EG 1.55 mm	13	1.55	73.9	121.7	22.3	27.2	0.752/ -0.307

Impact Data Charts

All dynamic testing for the following steels were performed at 12 mph impact velocity. Seven samples were fabricated for impact testing for each weld condition. Weld conditions were: small weld – long hold time, small button- sort hold time, large weld- long hold time, and large weld -short hold time. Some samples of the very high strength materials required retesting due to fractures in the bend attaching the sample to the testing machine. In some instances, this resulted in having to run spare samples allocated in the original test plan. The number of data points collected for each chart is a minimum of 4 with most charts having at least 5 data points for each characteristic measured. The number of data points used to develop the chart is indicated in the legend. The following charts show the high, average and lowest values for both peak load in kN, and energy in Joules. Exceptional conditions are reported below each chart as required.

All data used to generate these charts is contained in the file defined as '1768 TensileStaticReport a 050216 HZ cjo jwd R0. xls " on the CD of this report. The file contains the run-sheet information in Excel files. The data sheets provide all the data obtained to allow thorough data analysis. The following charts generated from the run sheet data convey the significant differences in weld joint performance among the range of steels tested.

All impact and tensile shear data are reported for 125 mm wide samples unless otherwise noted in the charts or text.

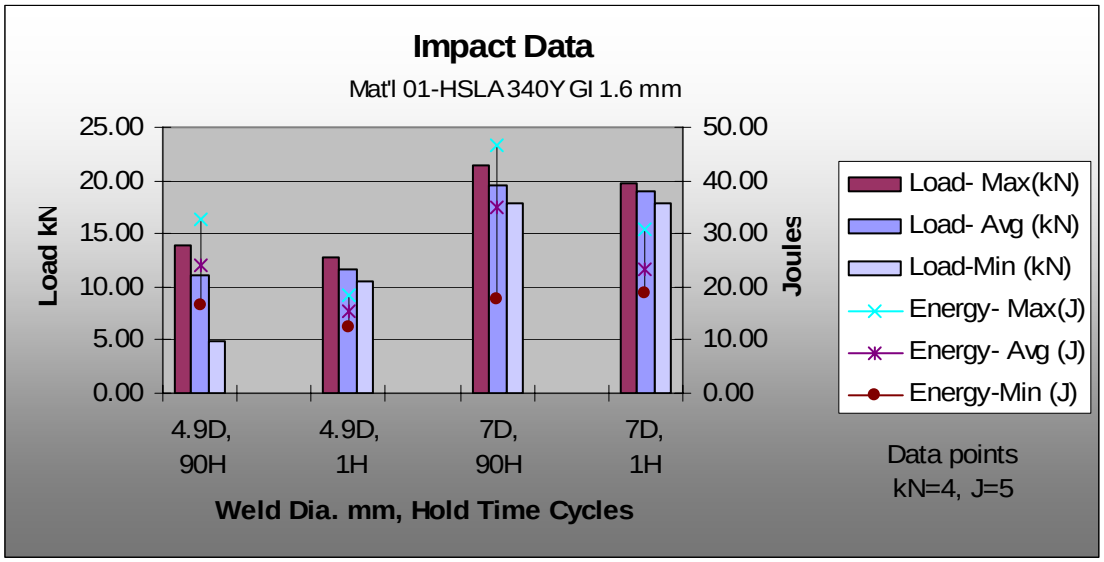
Impact Data
Mat'l 01-HSLA 340Y GI 1.6 mm
Load kN
Joules
25.00
20.00
15.00
10.00
5.00
0.00
50.00
40.00
30.00
20.00
10.00
0.00
4.9D, 90H
4.9D, 1H
7D, 90H
7D, 1H
Weld Dia. mm, Hold Time Cycles
Load- Max(kN)
Load- Avg (kN)
Load-Min (kN)
Energy- Max(J)
Energy- Avg (J)
Energy-Min (J)
Data points
kN=4, J=5

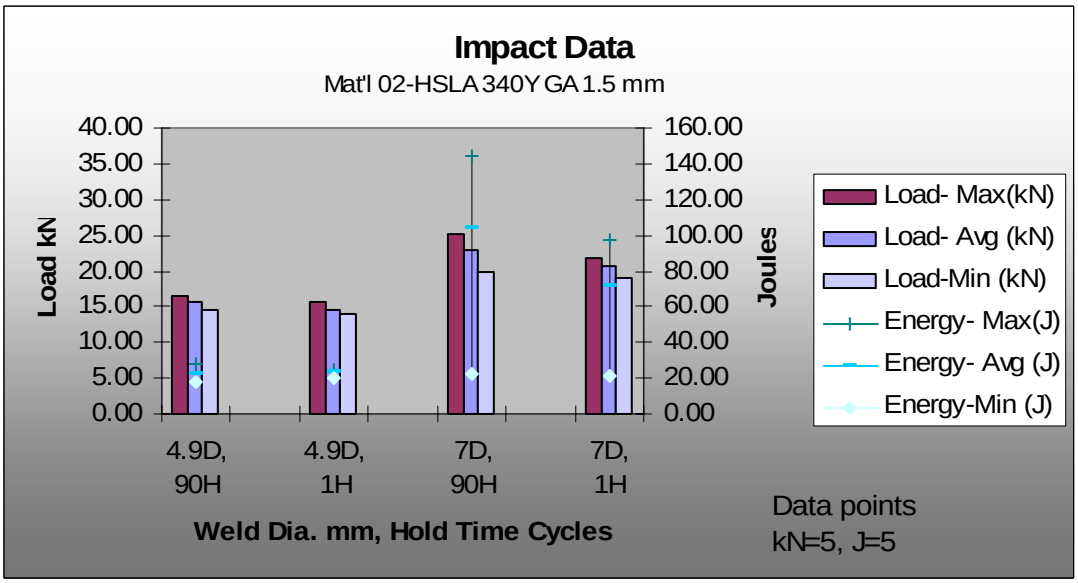
Impact Data
Mat'l 02-HSLA 340Y GA 1.5 mm
Load kN
Joules
40.00
35.00
30.00
25.00
20.00
15.00
10.00
5.00
0.00
160.00
140.00
120.00
100.00
80.00
60.00
40.00
20.00
0.00
4.9D, 90H
4.9D, 1H
7D, 90H
7D, 1H
Weld Dia. mm, Hold Time Cycles
Load- Max(kN)
Load- Avg (kN)
Load-Min (kN)
Energy- Max(J)
Energy- Avg (J)
Energy-Min (J)
Data points
kN=5, J=5

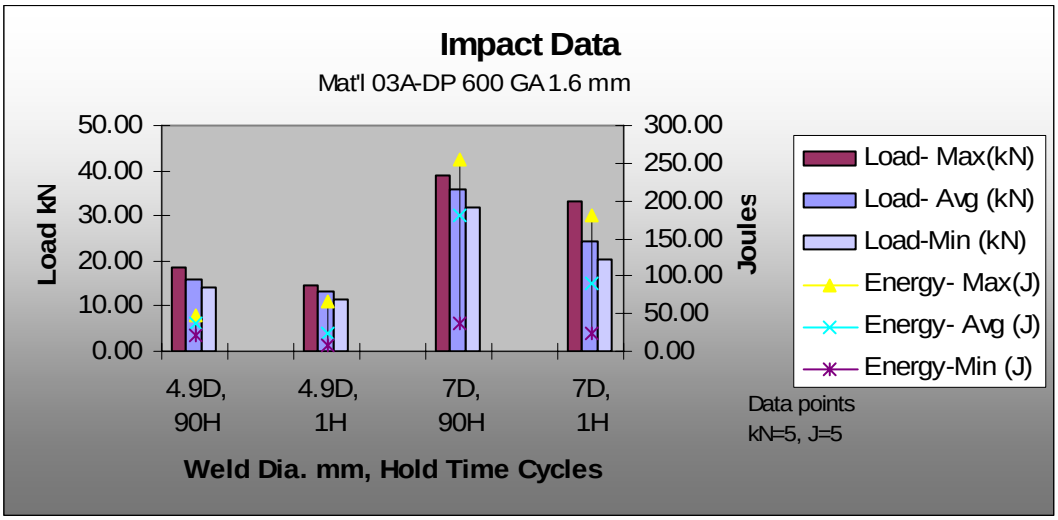
Impact Data
Mat'l 03A-DP 600 GA 1.6 mm
Load kN
50.00
40.00
30.00
20.00
10.00
0.00
Joules
300.00
250.00
200.00
150.00
100.00
50.00
0.00
4.9D, 90H
4.9D, 1H
7D, 90H
7D, 1H
Weld Dia. mm, Hold Time Cycles
Load- Max(kN)
Load- Avg (kN)
Load-Min (kN)
Energy- Max(J)
Energy- Avg (J)
Energy-Min (J)
Data points
kN=5, J=5

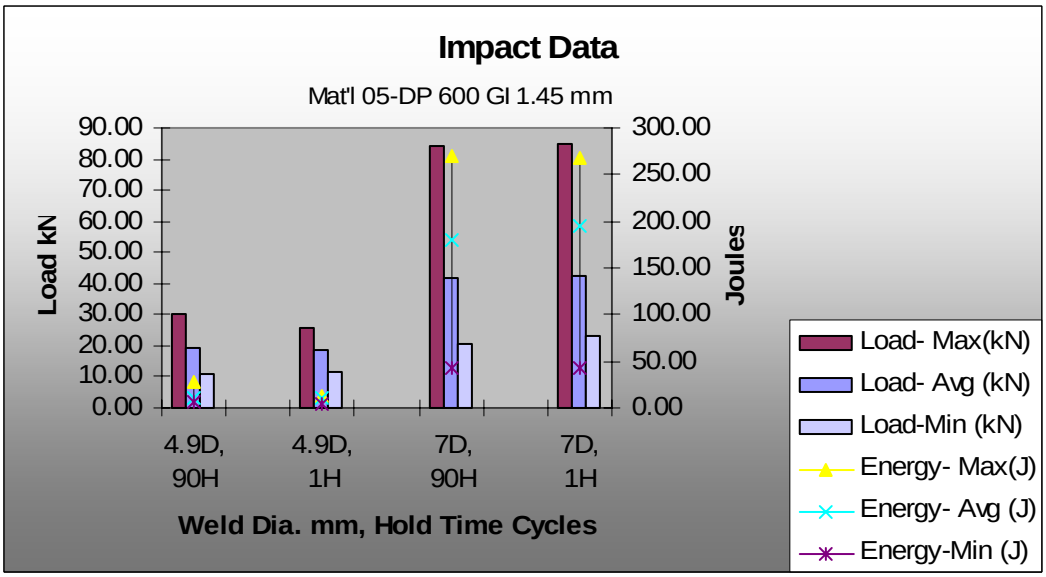
Impact Data
Mat'l 05-DP 600 GI 1.45 mm
Load kN
90.00
80.00
70.00
60.00
50.00
40.00
30.00
20.00
10.00
0.00
Joules
300.00
250.00
200.00
150.00
100.00
50.00
0.00
4.9D, 90H
4.9D, 1H
7D, 90H
7D, 1H
Weld Dia. mm, Hold Time Cycles
Load- Max(kN)
Load- Avg (kN)
Load-Min (kN)
Energy- Max(J)
Energy- Avg (J)
Energy-Min (J)

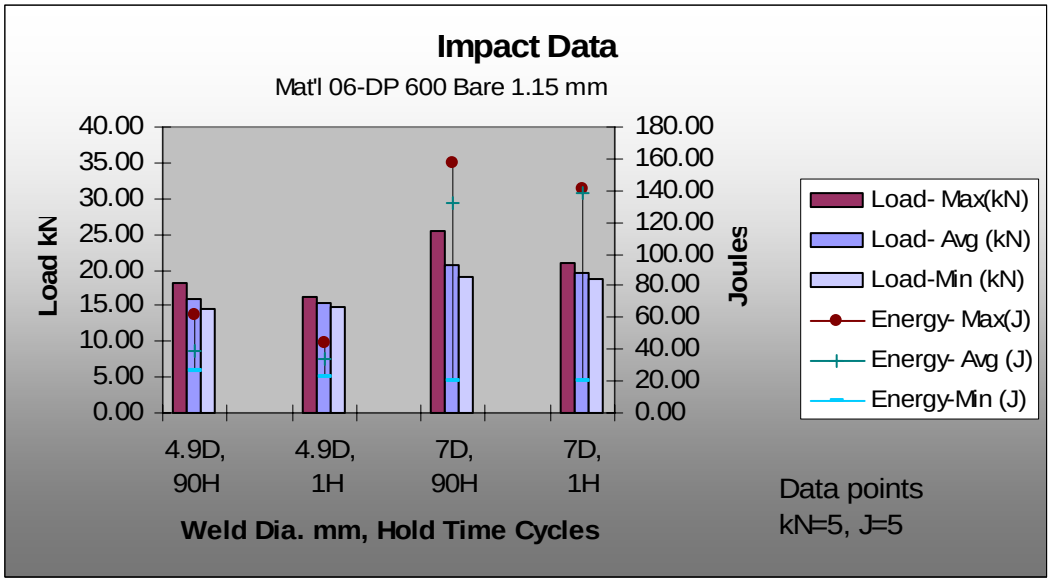
Impact Data
Mat'l 06-DP 600 Bare 1.15 mm
Load kN
Joules
40.00
35.00
30.00
25.00
20.00
15.00
10.00
5.00
0.00
180.00
160.00
140.00
120.00
100.00
80.00
60.00
40.00
20.00
0.00
4.9D, 90H
4.9D, 1H
7D, 90H
7D, 1H
Weld Dia. mm, Hold Time Cycles
Load- Max(kN)
Load- Avg (kN)
Load-Min (kN)
Energy- Max(J)
Energy- Avg (J)
Energy-Min (J)
Data points
kN=5, J=5

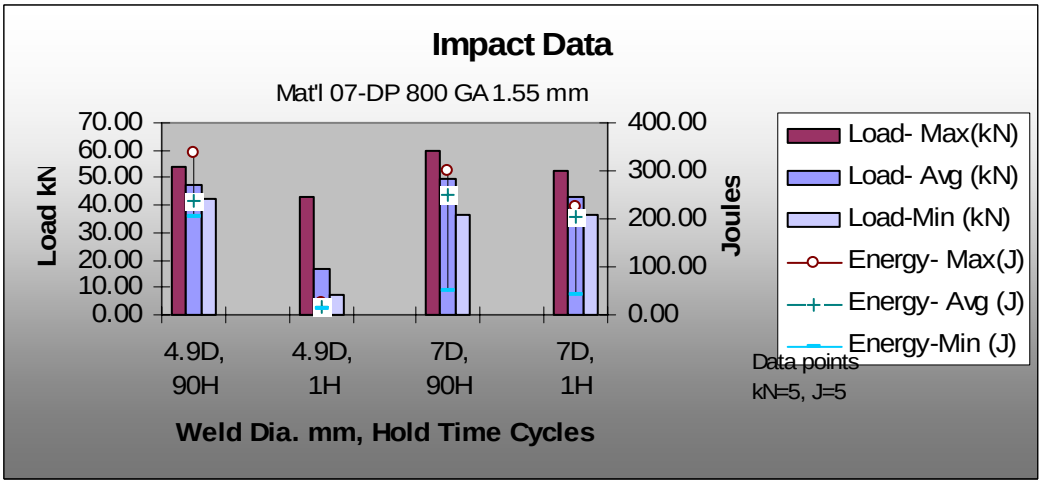
Impact Data
Mat'l 07-DP 800 GA 1.55 mm
Load kN
Joules
70.00
60.00
50.00
40.00
30.00
20.00
10.00
0.00
400.00
300.00
200.00
100.00
0.00
4.9D, 90H
4.9D, 1H
7D, 90H
7D, 1H
Weld Dia. mm, Hold Time Cycles
Load- Max(kN)
Load- Avg (kN)
Load-Min (kN)
Energy- Max(J)
Energy- Avg (J)
Energy-Min (J)
Data points
kN=5, J=5

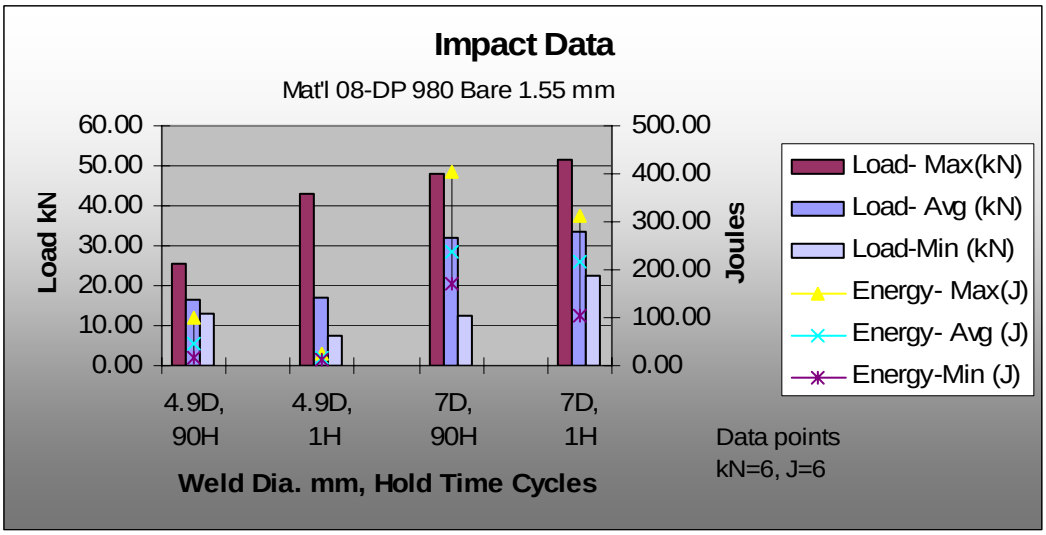
Impact Data
Mat'l 08-DP 980 Bare 1.55 mm
Load kN
60.00
50.00
40.00
30.00
20.00
10.00
0.00
Joules
500.00
400.00
300.00
200.00
100.00
0.00
4.9D, 90H
4.9D, 1H
7D, 90H
7D, 1H
Weld Dia. mm, Hold Time Cycles
Load- Max(kN)
Load- Avg (kN)
Load-Min (kN)
Energy- Max(J)
Energy- Avg (J)
Energy-Min (J)
Data points
kN=6, J=6

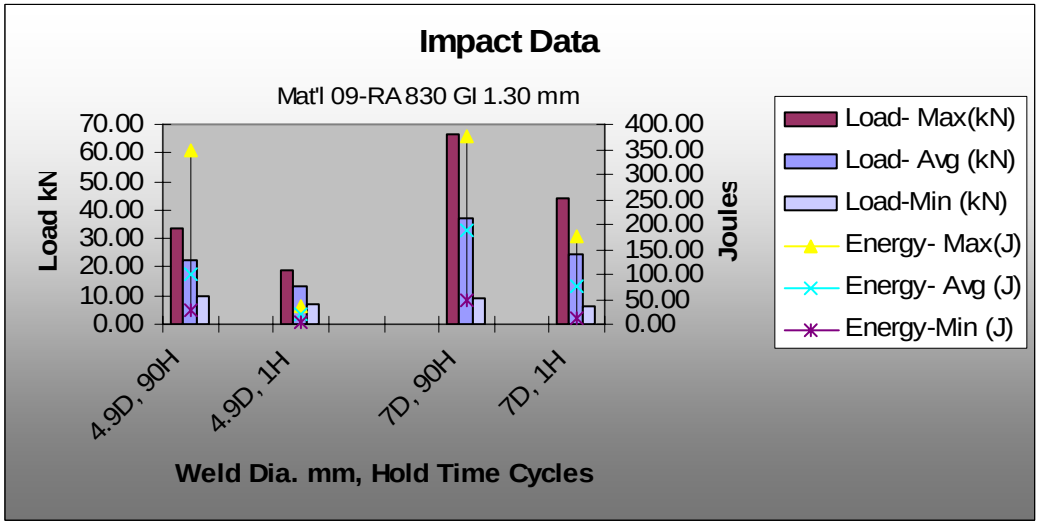
Impact Data
Mat'l 09-RA 830 GI 1.30 mm
Load kN
70.00
60.00
50.00
40.00
30.00
20.00
10.00
0.00
Joules
400.00
350.00
300.00
250.00
200.00
150.00
100.00
50.00
0.00
4.9D, 90H
4.9D, 1H
7D, 90H
7D, 1H
Weld Dia. mm, Hold Time Cycles
Load- Max(kN)
Load- Avg (kN)
Load-Min (kN)
Energy- Max(J)
Energy- Avg (J)
Energy-Min (J)

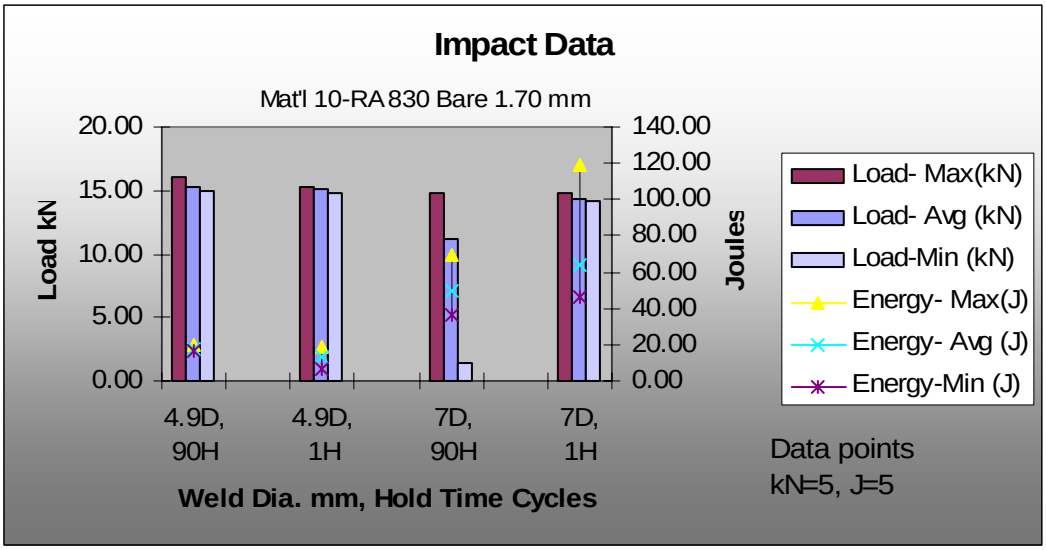

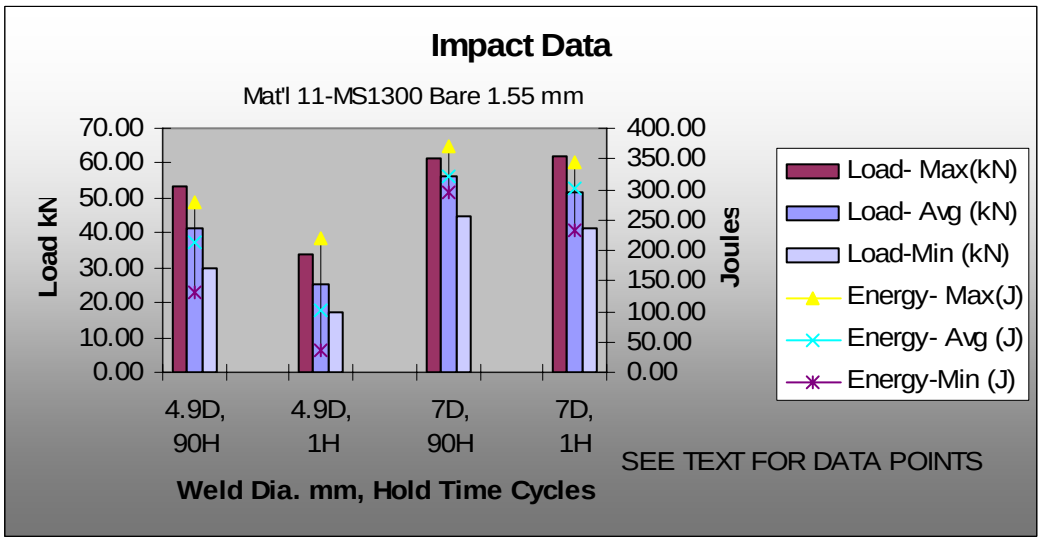

Material 11 had 2 data points for 7D, 1H Peak load (kN). 3 Data points for 7D, 1H Joules (J). All other material 11 chart data contain 4 or more points.

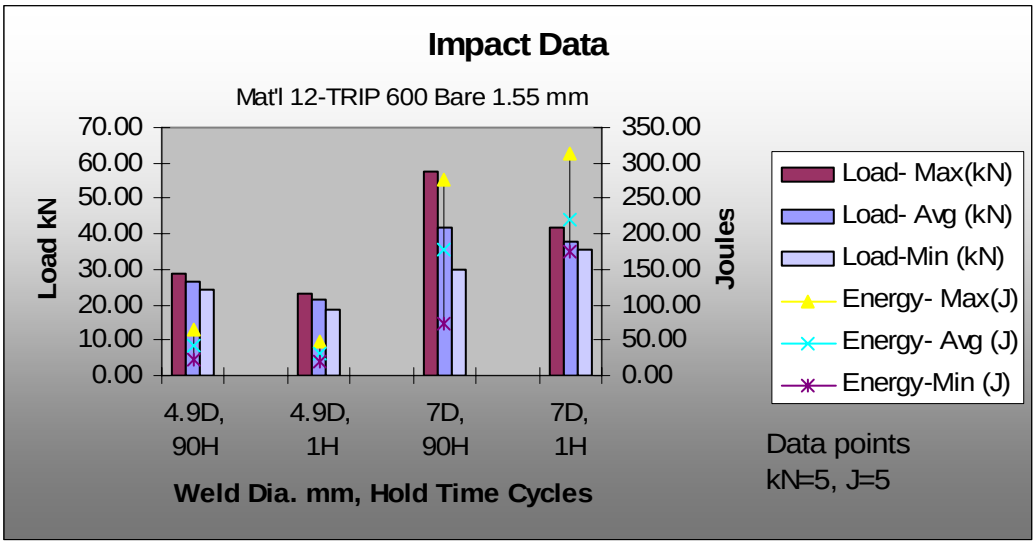
Impact Data
Mat'l 12-TRIP 600 Bare 1.55 mm
Load kN
Joules
70.00
60.00
50.00
40.00
30.00
20.00
10.00
0.00
350.00
300.00
250.00
200.00
150.00
100.00
50.00
0.00
4.9D, 90H
4.9D, 1H
7D, 90H
7D, 1H
Weld Dia. mm, Hold Time Cycles
Load- Max(kN)
Load- Avg (kN)
Load-Min (kN)
Energy- Max(J)
Energy- Avg (J)
Energy-Min (J)
Data points
kN=5, J=5

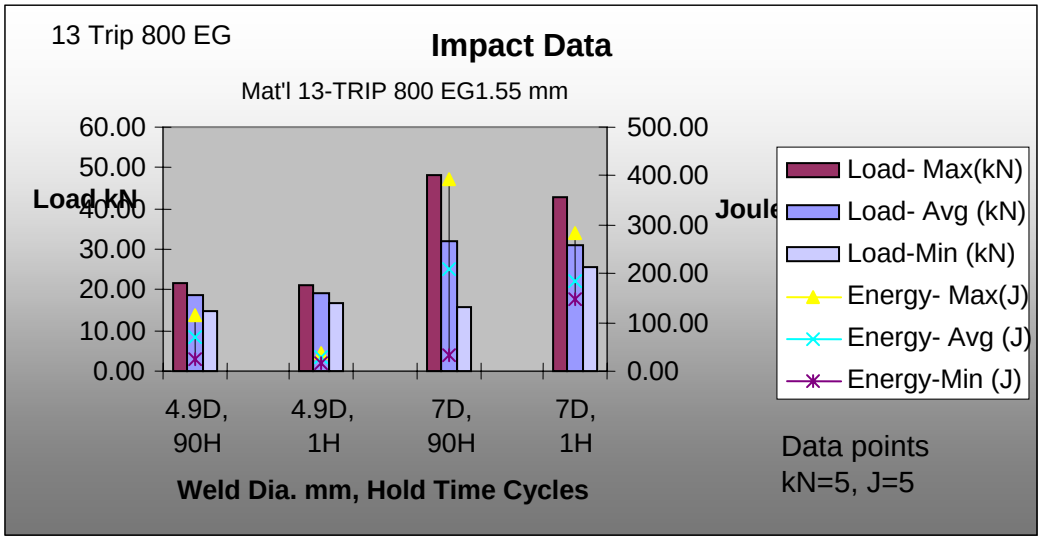
13 Trip 800 EG
Impact Data
Mat'l 13-TRIP 800 EG1.55 mm
Load kN
Joule
60.00
50.00
40.00
30.00
20.00
10.00
0.00
500.00
400.00
300.00
200.00
100.00
0.00
4.9D, 90H
4.9D, 1H
7D, 90H
7D, 1H
Weld Dia. mm, Hold Time Cycles
Load- Max(kN)
Load- Avg (kN)
Load-Min (kN)
Energy- Max(J)
Energy- Avg (J)
Energy-Min (J)
Data points
kN=5, J=5

Static Tensile Shear Charts

The tensile shear charts report data obtained from the DoE run sheets. Each chart reports the measured maximum, average and minimum load. Values in kN are shown on the left axis. The measured energy for maximum, average, and minimum is overlaid with each load group with energy values in Joules shown on the right axis. Charts report results for small weld diameter-long hold, small diameter- short hold, large diameter-long hold, and large diameter-short hold. All metal gage was close to 1.5 mm thick. Actual thickness and chemistry is reported in the material physical sheets.

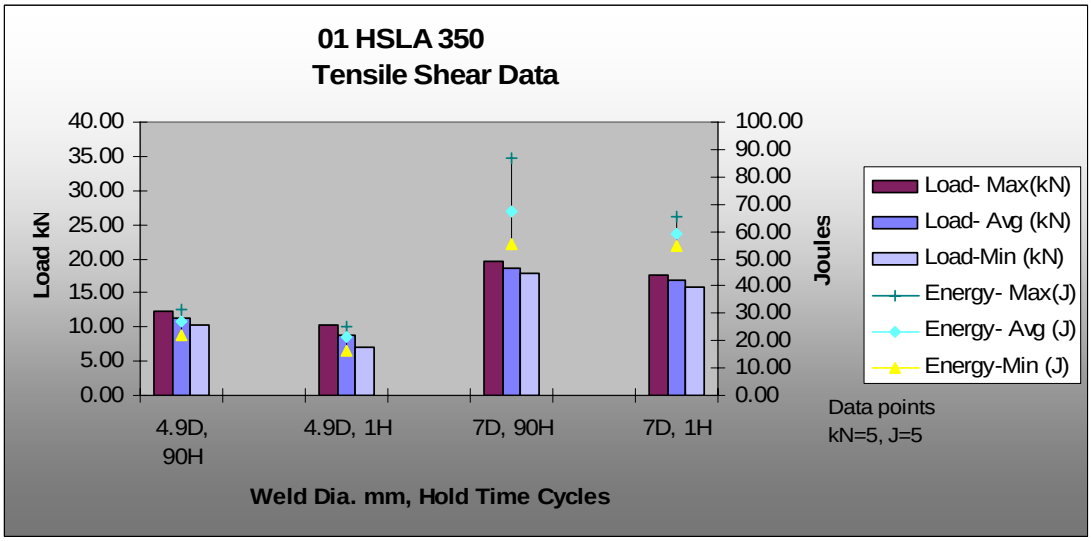

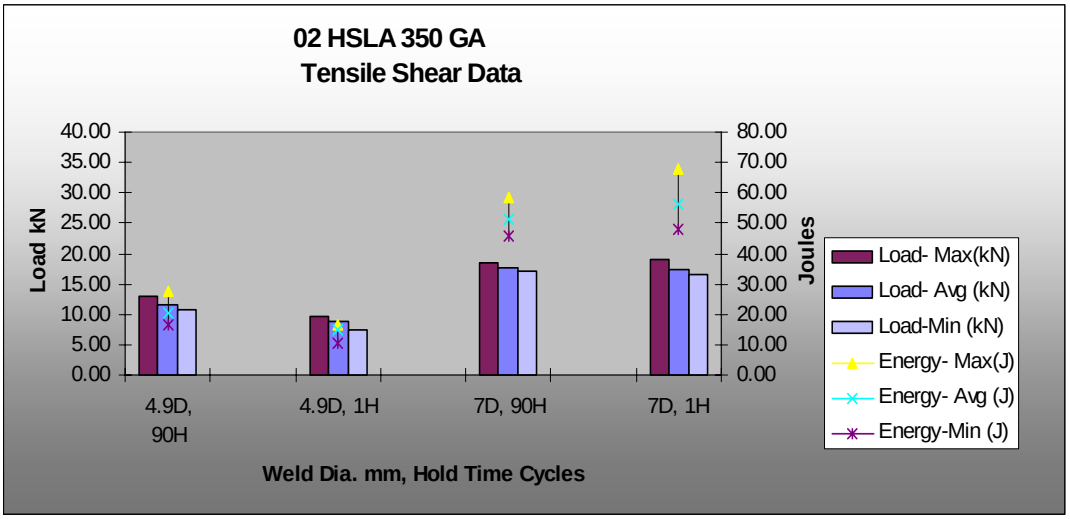
02 HSLA 350 GA
Tensile Shear Data
Load kN
Joules
40.00
35.00
30.00
25.00
20.00
15.00
10.00
5.00
0.00
80.00
70.00
60.00
50.00
40.00
30.00
20.00
10.00
0.00
4.9D, 90H
4.9D, 1H
7D, 90H
7D, 1H
Weld Dia. mm, Hold Time Cycles
Load- Max(kN)
Load- Avg (kN)
Load-Min (kN)
Energy- Max(J)
Energy- Avg (J)
Energy-Min (J)

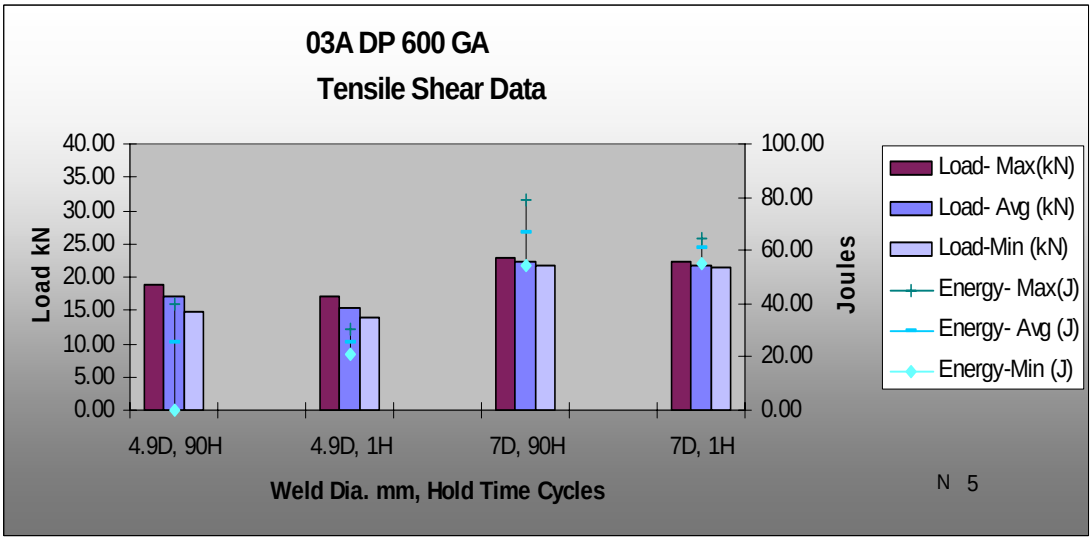
03A DP 600 GA
Tensile Shear Data
Load kN
Joules
40.00
35.00
30.00
25.00
20.00
15.00
10.00
5.00
0.00
100.00
80.00
60.00
40.00
20.00
0.00
4.9D, 90H
4.9D, 1H
7D, 90H
7D, 1H
Weld Dia. mm, Hold Time Cycles
Load- Max(kN)
Load- Avg (kN)
Load-Min (kN)
Energy- Max(J)
Energy- Avg (J)
Energy-Min (J)
N 5

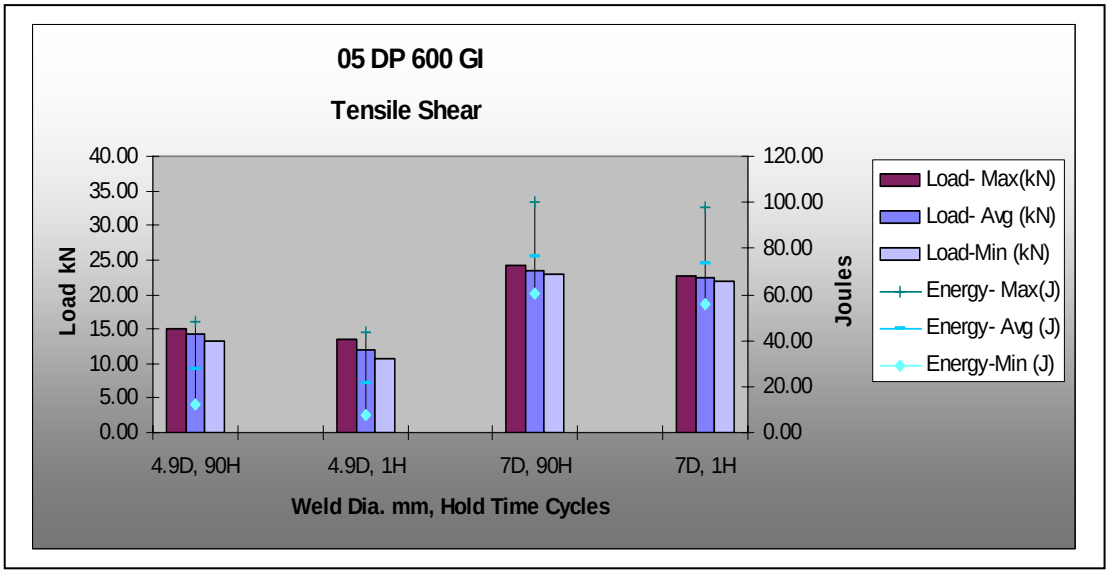
05 DP 600 GI
Tensile Shear
Load kN
Joules
40.00
35.00
30.00
25.00
20.00
15.00
10.00
5.00
0.00
120.00
100.00
80.00
60.00
40.00
20.00
0.00
4.9D, 90H
4.9D, 1H
7D, 90H
7D, 1H
Weld Dia. mm, Hold Time Cycles
Load- Max(kN)
Load- Avg (kN)
Load-Min (kN)
Energy- Max(J)
Energy- Avg (J)
Energy-Min (J)

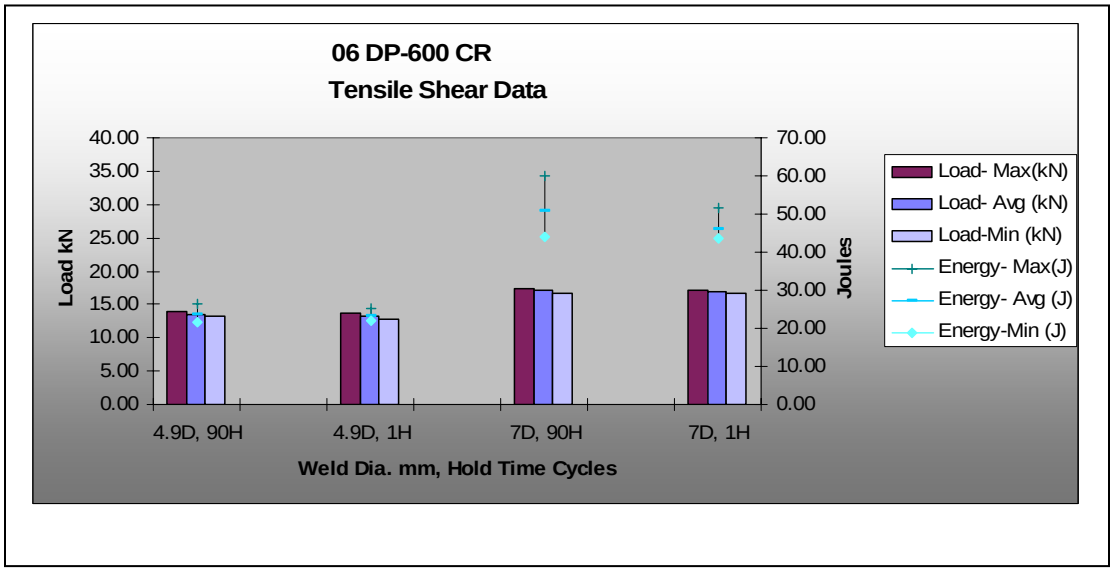
06 DP-600 CR
Tensile Shear Data
Load kN
Joules
40.00
35.00
30.00
25.00
20.00
15.00
10.00
5.00
0.00
70.00
60.00
50.00
40.00
30.00
20.00
10.00
0.00
4.9D, 90H
4.9D, 1H
7D, 90H
7D, 1H
Weld Dia. mm, Hold Time Cycles
Load- Max(kN)
Load- Avg (kN)
Load-Min (kN)
Energy- Max(J)
Energy- Avg (J)
Energy-Min (J)

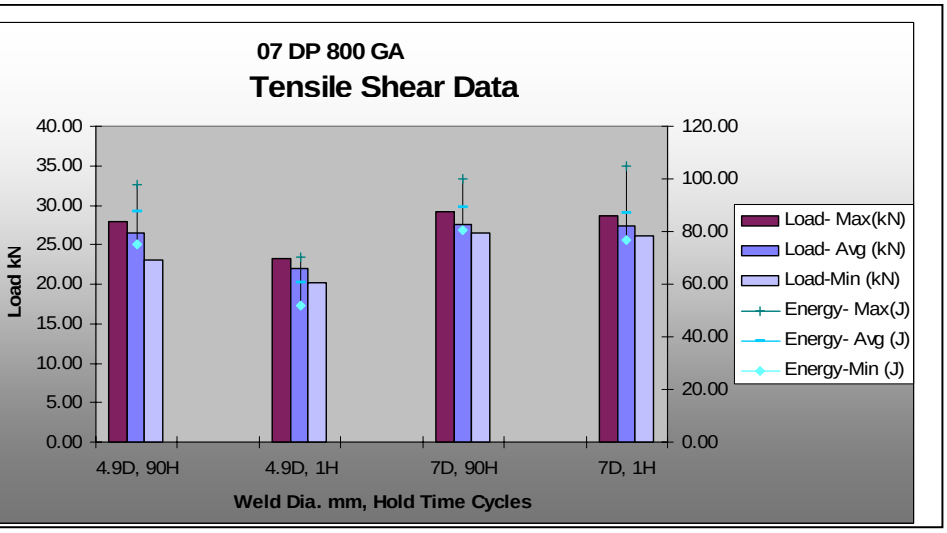
07 DP 800 GA
Tensile Shear Data
Load kN
40.00
35.00
30.00
25.00
20.00
15.00
10.00
5.00
0.00
120.00
100.00
80.00
60.00
40.00
20.00
0.00
4.9D, 90H
4.9D, 1H
7D, 90H
7D, 1H
Weld Dia. mm, Hold Time Cycles
Load- Max(kN)
Load- Avg (kN)
Load-Min (kN)
Energy- Max(J)
Energy- Avg (J)
Energy-Min (J)

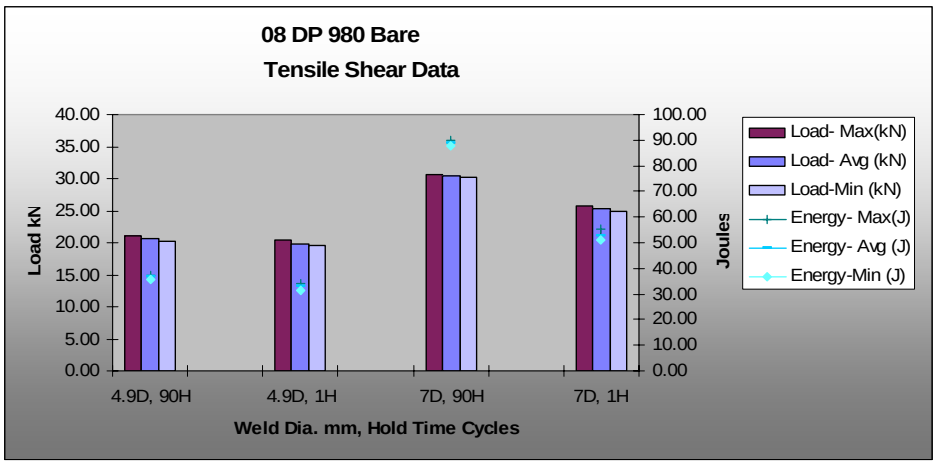
08 DP 980 Bare
Tensile Shear Data
Load kN
40.00
35.00
30.00
25.00
20.00
15.00
10.00
5.00
0.00
Joules
100.00
90.00
80.00
70.00
60.00
50.00
40.00
30.00
20.00
10.00
0.00
4.9D, 90H
4.9D, 1H
7D, 90H
7D, 1H
Weld Dia. mm, Hold Time Cycles
Load- Max(kN)
Load- Avg (kN)
Load-Min (kN)
Energy- Max(J)
Energy- Avg (J)
Energy-Min (J)

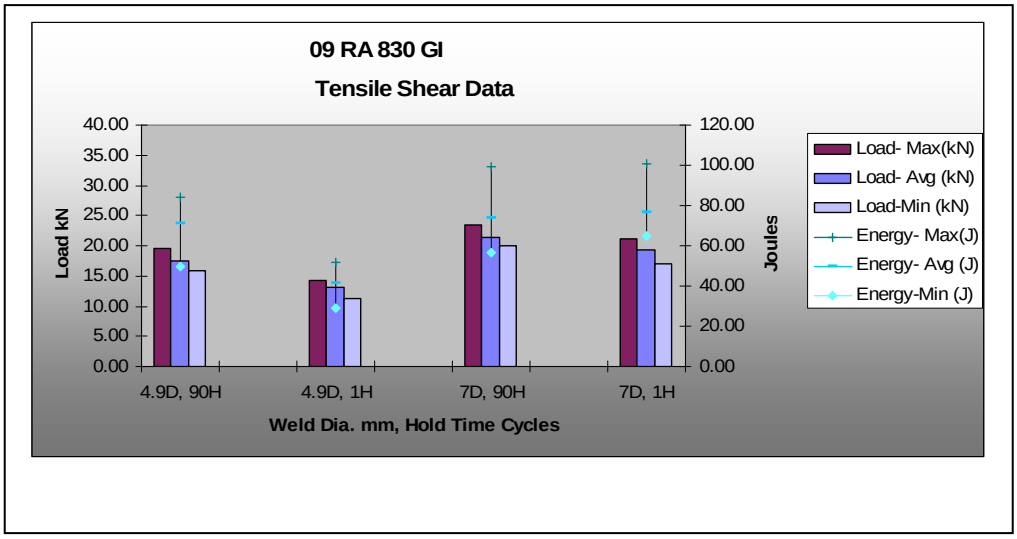
09 RA 830 GI
Tensile Shear Data
Load kN
Joules
40.00
35.00
30.00
25.00
20.00
15.00
10.00
5.00
0.00
120.00
100.00
80.00
60.00
40.00
20.00
0.00
4.9D, 90H
4.9D, 1H
7D, 90H
7D, 1H
Weld Dia. mm, Hold Time Cycles
Load- Max(kN)
Load- Avg (kN)
Load-Min (kN)
Energy- Max(J)
Energy- Avg (J)
Energy-Min (J)

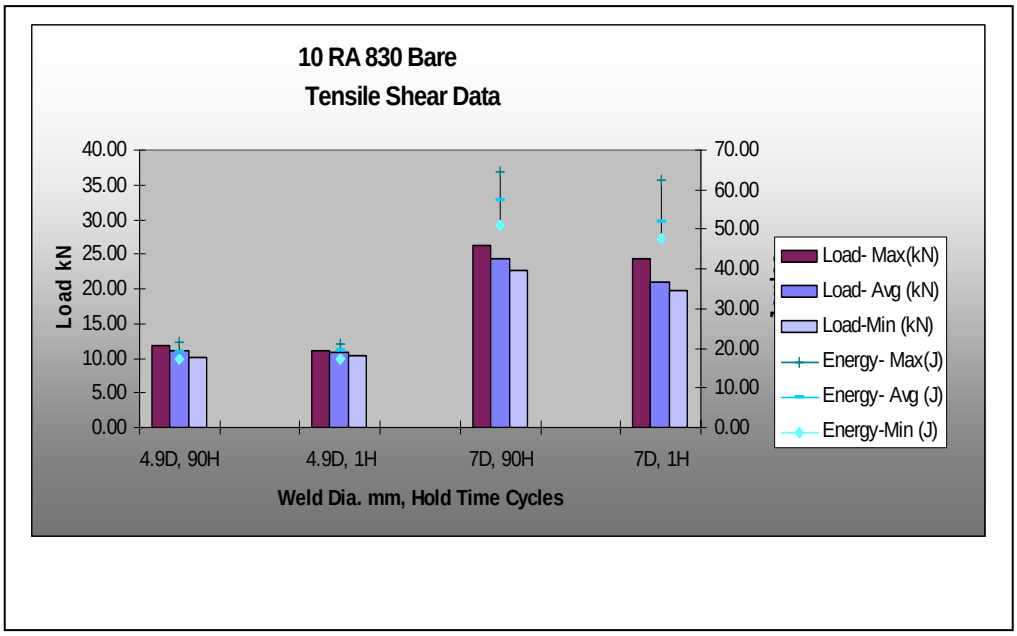
10 RA 830 Bare
Tensile Shear Data
Load kN
40.00
35.00
30.00
25.00
20.00
15.00
10.00
5.00
0.00
70.00
60.00
50.00
40.00
30.00
20.00
10.00
0.00
4.9D, 90H
4.9D, 1H
7D, 90H
7D, 1H
Weld Dia. mm, Hold Time Cycles
Load- Max(kN)
Load- Avg (kN)
Load-Min (kN)
Energy- Max(J)
Energy- Avg (J)
Energy-Min (J)

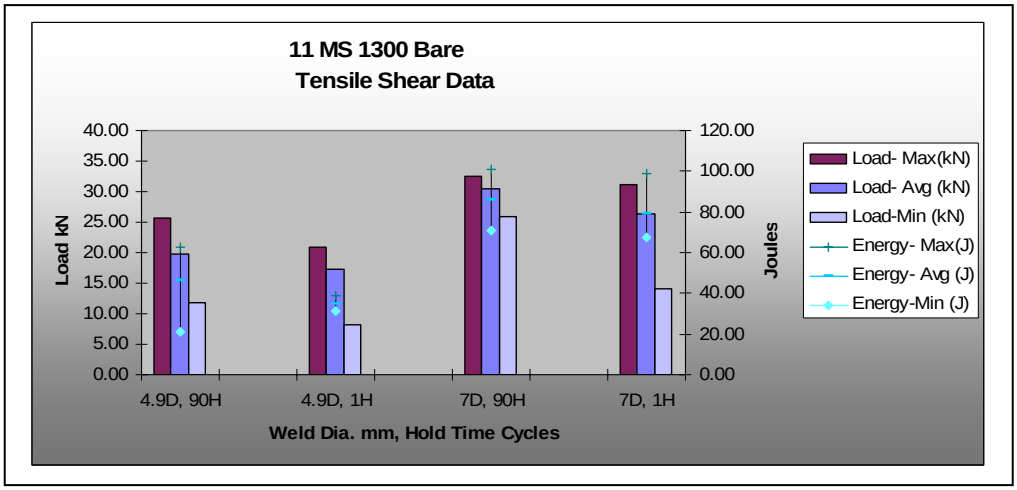
11 MS 1300 Bare
Tensile Shear Data
Load kN
Joules
40.00
35.00
30.00
25.00
20.00
15.00
10.00
5.00
0.00
120.00
100.00
80.00
60.00
40.00
20.00
0.00
4.9D, 90H
4.9D, 1H
7D, 90H
7D, 1H
Weld Dia. mm, Hold Time Cycles
Load- Max(kN)
Load- Avg (kN)
Load-Min (kN)
Energy- Max(J)
Energy- Avg (J)
Energy-Min (J)

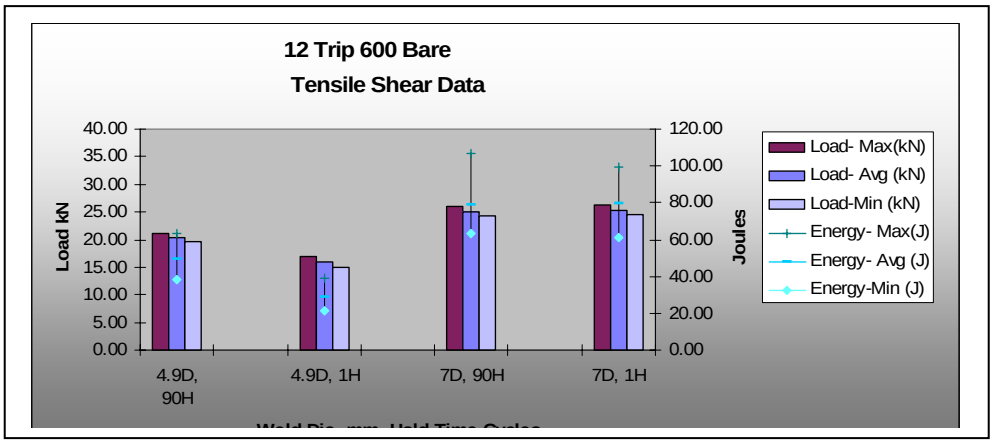
12 Trip 600 Bare
Tensile Shear Data
Load kN
Joules
40.00
35.00
30.00
25.00
20.00
15.00
10.00
5.00
0.00
120.00
100.00
80.00
60.00
40.00
20.00
0.00
4.9D, 90H
4.9D, 1H
7D, 90H
7D, 1H
Load- Max(kN)
Load- Avg (kN)
Load-Min (kN)
Energy- Max(J)
Energy- Avg (J)
Energy-Min (J)

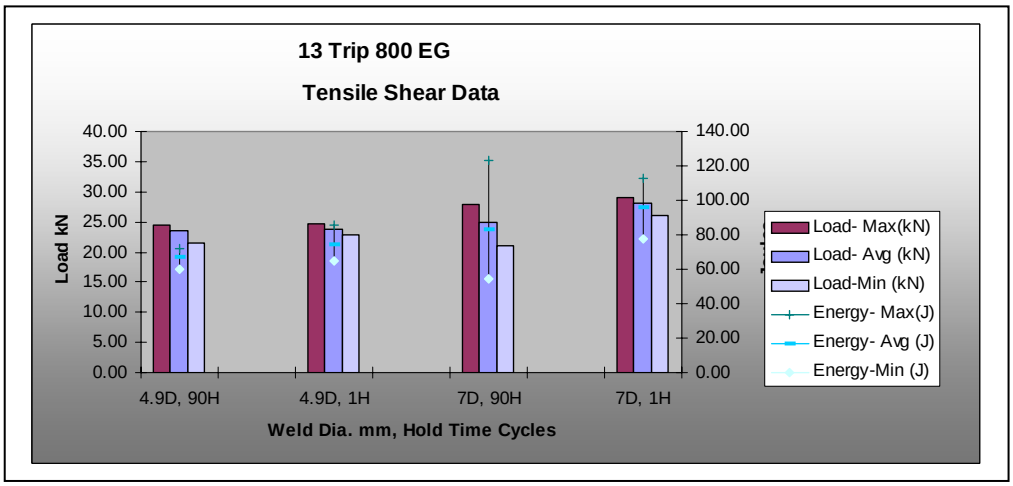
13 Trip 800 EG
Tensile Shear Data
Load kN
40.00
35.00
30.00
25.00
20.00
15.00
10.00
5.00
0.00
140.00
120.00
100.00
80.00
60.00
40.00
20.00
0.00
4.9D, 90H
4.9D, 1H
7D, 90H
7D, 1H
Weld Dia. mm, Hold Time Cycles
Load- Max(kN)
Load- Avg (kN)
Load-Min (kN)
Energy- Max(J)
Energy- Avg (J)
Energy-Min (J)

Plots of consolidated data for tensile strength (from final RSW tensile compare ra1.xls)

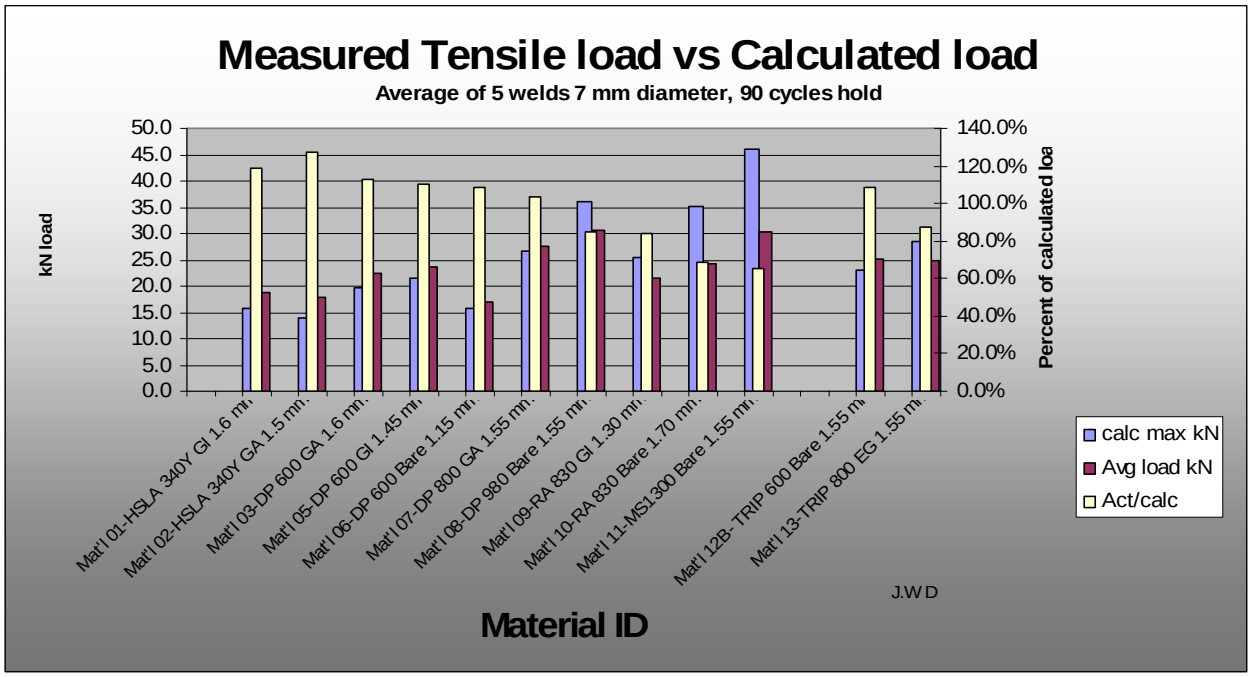

This chart consolidates all materials to show effect of base tensile strength. The values for calculated strength take into account the actual UTS of the material and the actual thickness. This chart shows the estimated breaking load of the 7 .0 mm weld based on a simple estimator for weld strength shown below. Both the estimated strength and the observed breaking tensile load are plotted. The ratio of actual to calculated load is expressed as a percent and is shown on the right axis of the chart. The calculated breaking load is based on the UTS of the sample material obtained from laboratory measurements. For example, the HSLA 340Y GI had a measured UTS of 448 MPa and a thickness of 1.6 mm (obtained from the physical data chart shown earlier in this report)

Generally the breaking load can be estimated to within 20% of actual for these steels. Exceptions are for the RA and Martensite steels that fall below estimates by as much as 30% using the simple estimator.

The estimating formula assumes the sample width is sufficiently large with respect to the weld diameter and little rotation of the sample occurs during tensile testing. The base material sample thickness and width used for these samples provided breaking loads at least five times the anticipated strength of the welds that were tested. The simplified estimator does not address other variables required for a more accurate prediction of maximum strength such as variable uncertainties which include the actual weld diameter, sample rotation, heat affected zone and weld metal strength and stress concentration.

Estimating formula:

Maximum load to failure = weld diameter * K * material base thickness * UTS.

K was set to a value of 3.14 for calculating the charted breaking loads.

Normalized weld tensile strength based on thickness.

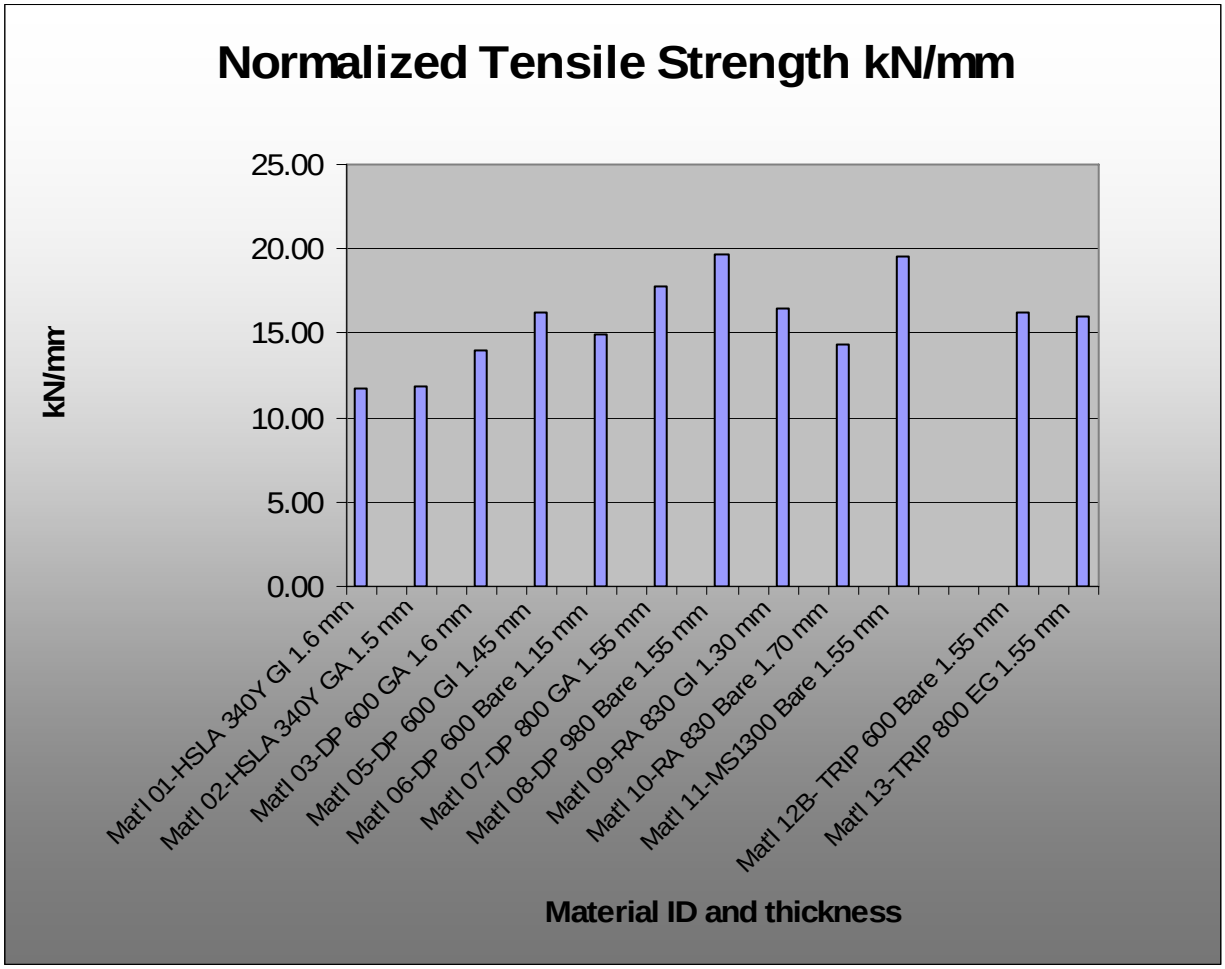

This chart shows the normalized strength of the welds based on the average breaking load of a 7 mm weld in the test material. The average load was divided by the material thickness to provide this data. It is useful for comparing weld performance in the types/grades of steel tested.

Normalized weld strength adjusted for actual material properties

Normalized weld strength accounting for thickness and ratio of purchased UTS/Actual UTS. Note that HSLA is not purchased by a specified UTS, it is specified by yield. In this chart no adjustment was made for the HSLA which had a UTS of approximately 448 MPa. This chart shows the value of weld strength per mm thickness if the grade purchased had the exact UTS specified. The values are adjusted from the breaking loads of 7 mm diameter welds made with 90 cycles hold.

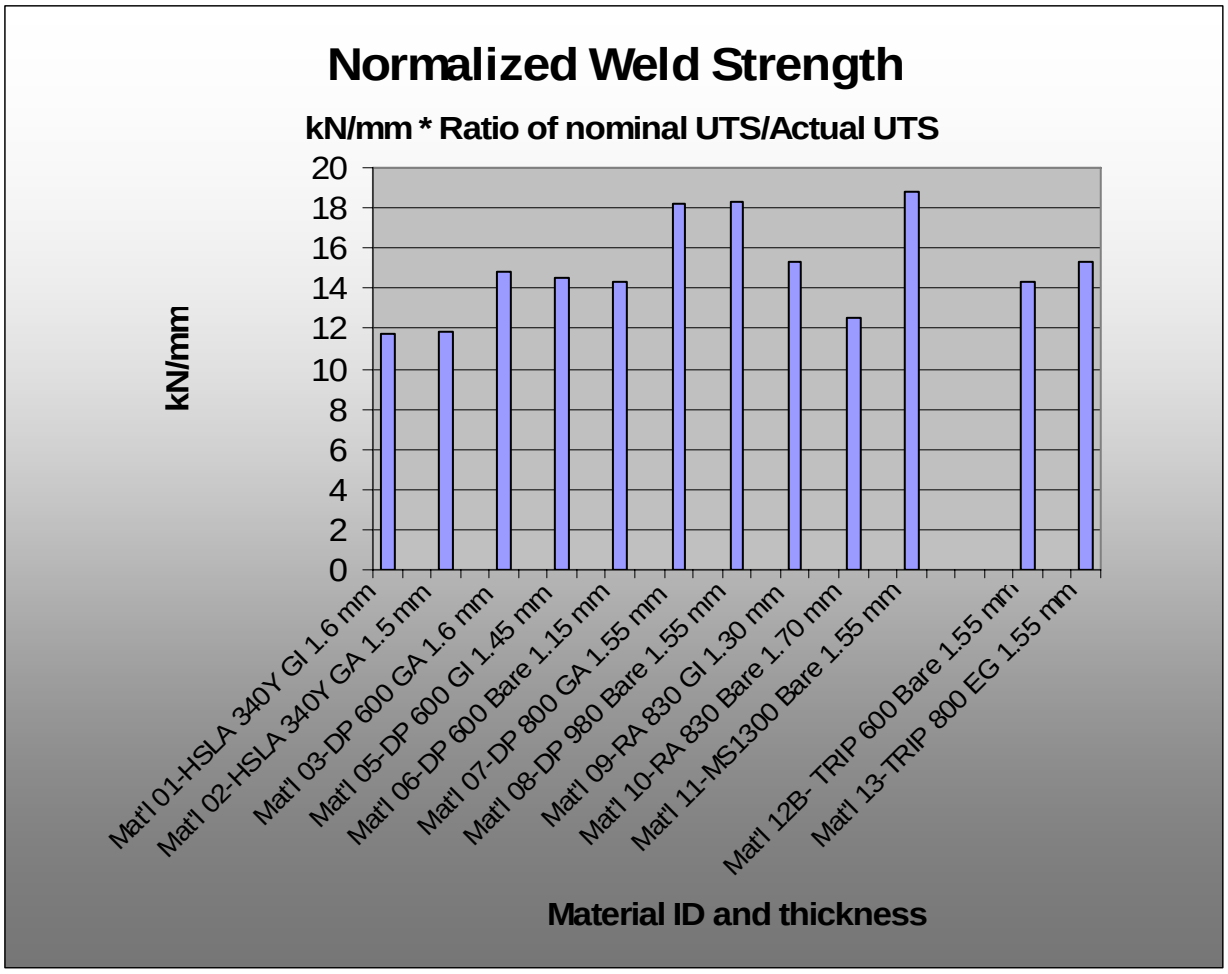

Plots of hold time effect for small and large welds

These charts are from source file "final RSW tensile compare JWD R1a". The data is arranged to show the % difference in breaking loads for long/short hold time for each weld size. With few exceptions tensile loads are improved with longer hold times for both large and small weld sizes. The smaller welds show more change in strength due to hold time in this data set. The chart shows 4.9 mm diameter welds with 90 cycles hold and 1 cycle hold, 7 mm diameter welds with 90 cycles hold and 1 cycle hold. The weld diameters represent the targeted diameters produced by the welding process and verified by destructive peel testing.

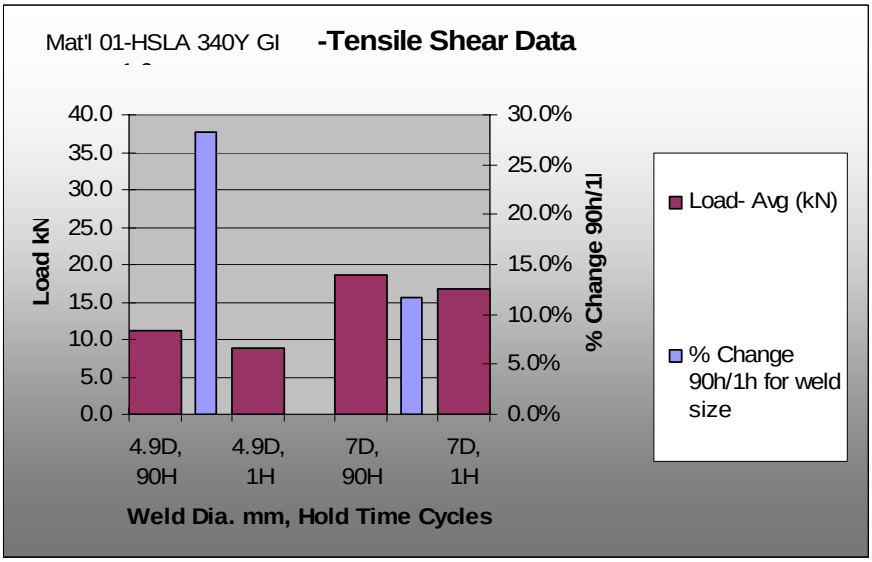

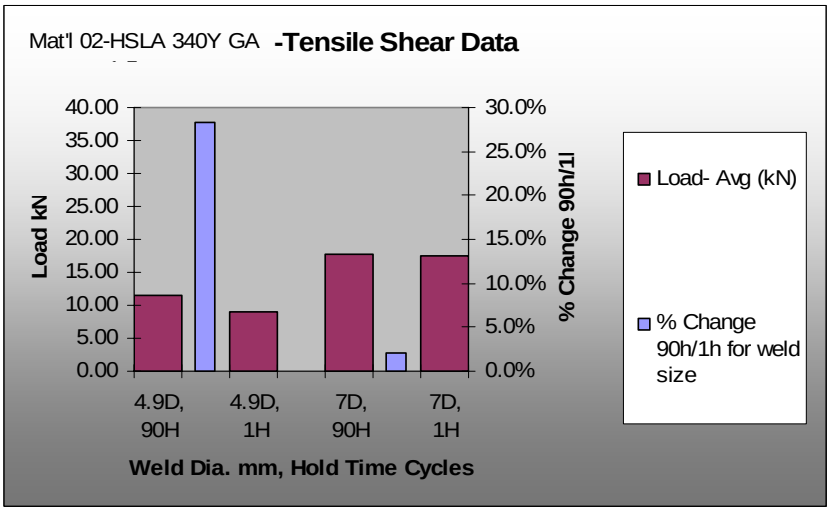

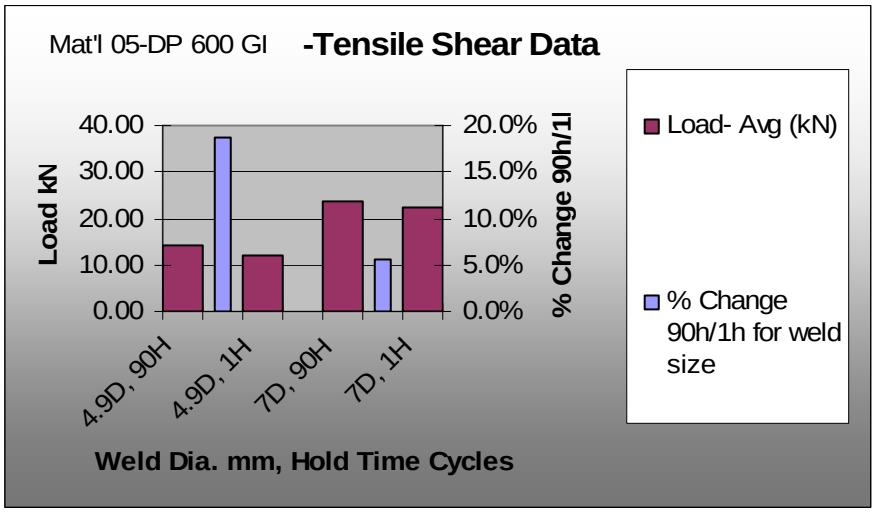
Mat'l 05-DP 600 GI -Tensile Shear Data
Load kN
40.00
30.00
20.00
10.00
0.00
20.0%
15.0%
10.0%
5.0%
0.0%
% Change 90h/1h
4.9D, 90H
4.9D, 1H
7D, 90H
7D, 1H
Weld Dia. mm, Hold Time Cycles
Load- Avg (kN)
% Change 90h/1h for weld size

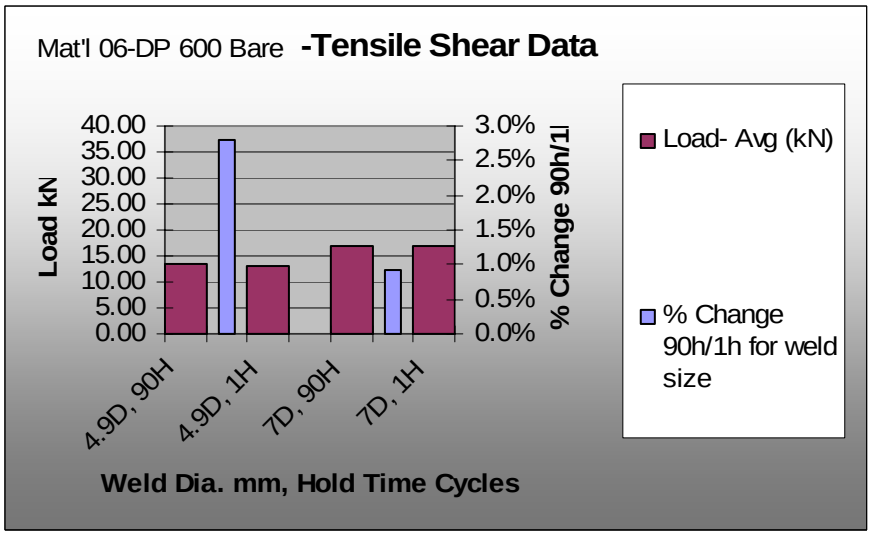
Mat'l 06-DP 600 Bare -Tensile Shear Data
Load kN
40.00
35.00
30.00
25.00
20.00
15.00
10.00
5.00
0.00
3.0%
2.5%
2.0%
1.5%
1.0%
0.5%
0.0%
% Change 90h/1h
4.9D, 90H
4.9D, 1H
7D, 90H
7D, 1H
Weld Dia. mm, Hold Time Cycles
Load- Avg (kN)
% Change 90h/1h for weld size

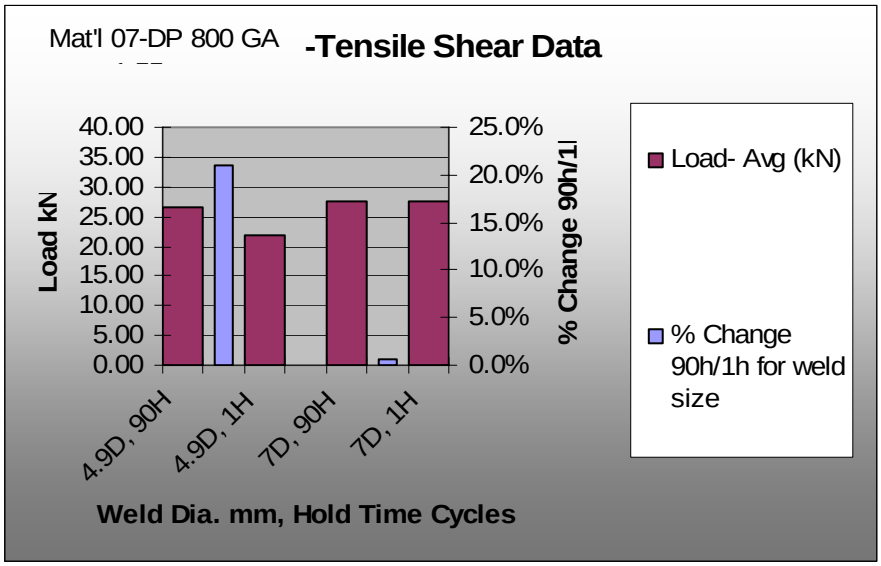
Mat'l 07-DP 800 GA
-Tensile Shear Data
Load kN
% Change 90h/1h
40.00
35.00
30.00
25.00
20.00
15.00
10.00
5.00
0.00
25.0%
20.0%
15.0%
10.0%
5.0%
0.0%
4.9D, 90H
4.9D, 1H
7D, 90H
7D, 1H
Load- Avg (kN)
% Change 90h/1h for weld size
Weld Dia. mm, Hold Time Cycles

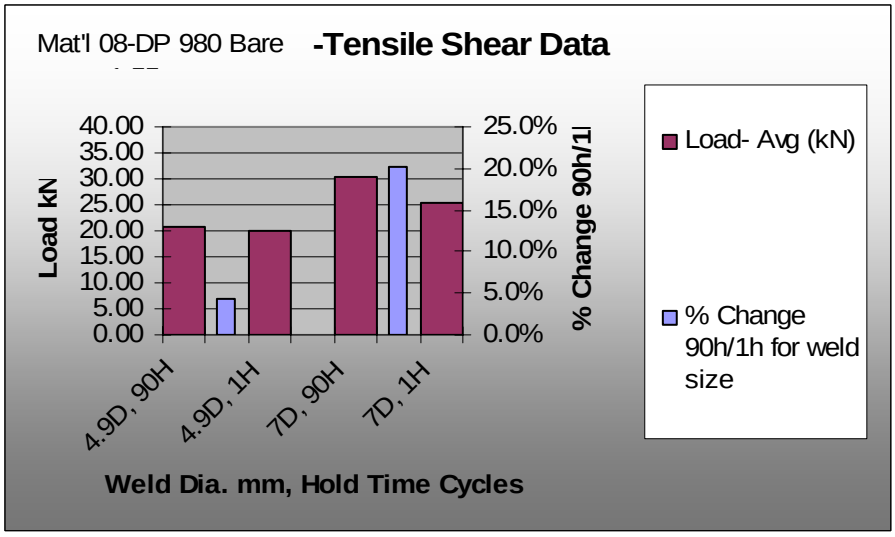
Mat'l 08-DP 980 Bare
-Tensile Shear Data
Load kN
% Change 90h/1h
40.00
35.00
30.00
25.00
20.00
15.00
10.00
5.00
0.00
25.0%
20.0%
15.0%
10.0%
5.0%
0.0%
4.9D, 90H
4.9D, 1H
7D, 90H
7D, 1H
Load- Avg (kN)
% Change 90h/1h for weld size
Weld Dia. mm, Hold Time Cycles

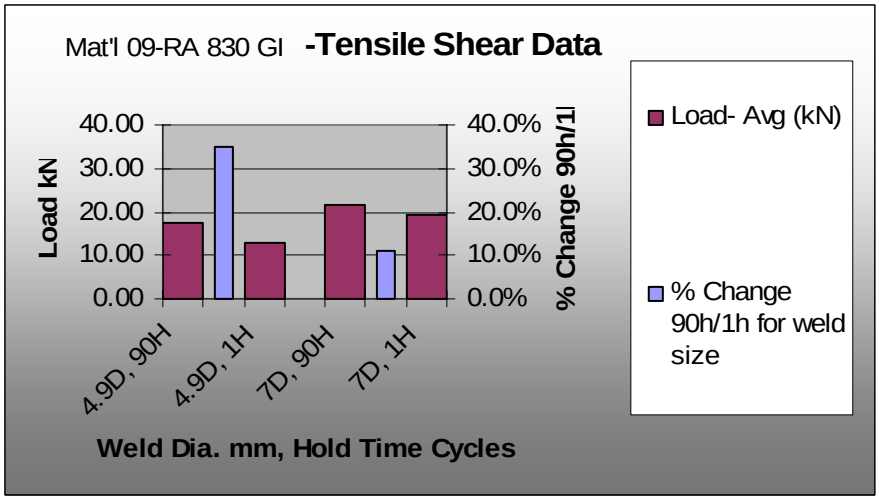
Mat'l 09-RA 830 GI -Tensile Shear Data
Load kN
40.00
30.00
20.00
10.00
0.00
40.0%
30.0%
20.0%
10.0%
0.0%
% Change 90h/1h
4.9D, 90H
4.9D, 1H
7D, 90H
7D, 1H
Weld Dia. mm, Hold Time Cycles
Load- Avg (kN)
% Change 90h/1h for weld size

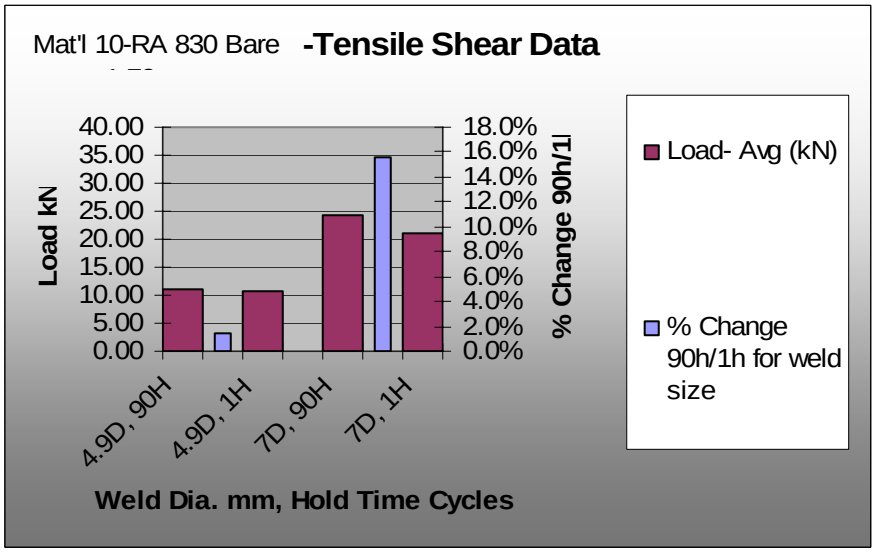
Mat'l 10-RA 830 Bare -Tensile Shear Data
Load kN
40.00
35.00
30.00
25.00
20.00
15.00
10.00
5.00
0.00
18.0%
16.0%
14.0%
12.0%
10.0%
8.0%
6.0%
4.0%
2.0%
0.0%
% Change 90h/1h
4.9D, 90H
4.9D, 1H
7D, 90H
7D, 1H
Weld Dia. mm, Hold Time Cycles
Load- Avg (kN)
% Change 90h/1h for weld size

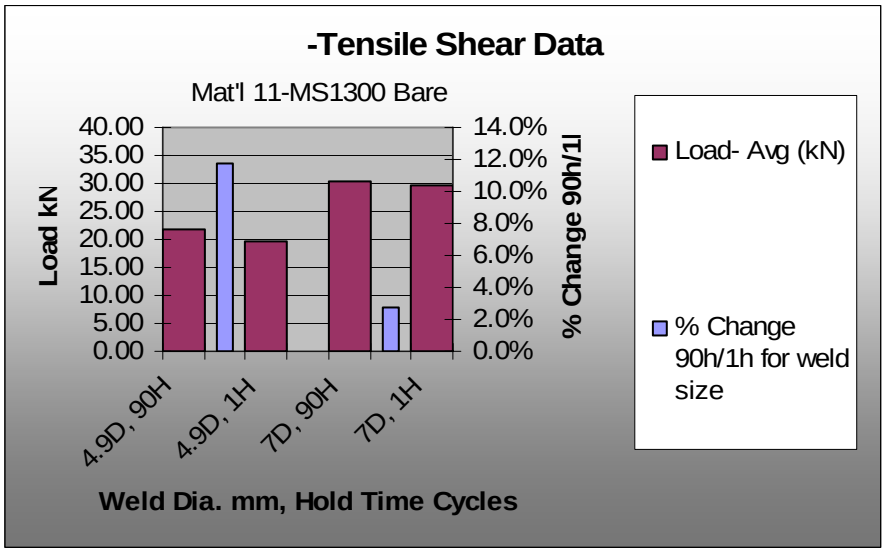
-Tensile Shear Data
Mat'l 11-MS1300 Bare
Load kN
% Change 90h/1l
40.00
35.00
30.00
25.00
20.00
15.00
10.00
5.00
0.00
14.0%
12.0%
10.0%
8.0%
6.0%
4.0%
2.0%
0.0%
4.9D, 90H
4.9D, 1H
7D, 90H
7D, 1H
Weld Dia. mm, Hold Time Cycles
Load- Avg (kN)
% Change 90h/1h for weld size

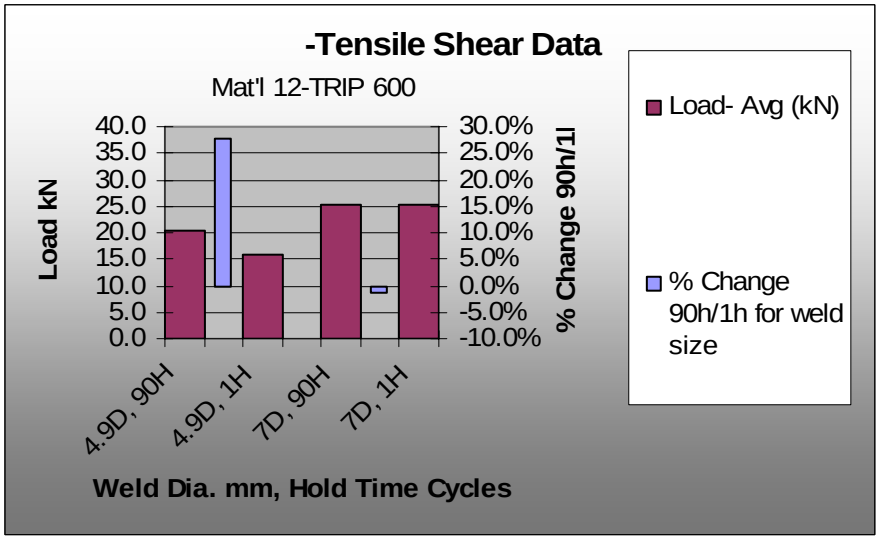
-Tensile Shear Data
Mat'l 12-TRIP 600
Load kN
% Change 90h/1l
40.0
35.0
30.0
25.0
20.0
15.0
10.0
5.0
0.0
30.0%
25.0%
20.0%
15.0%
10.0%
5.0%
0.0%
-5.0%
-10.0%
4.9D, 90H
4.9D, 1H
7D, 90H
7D, 1H
Weld Dia. mm, Hold Time Cycles
Load- Avg (kN)
% Change 90h/1h for weld size

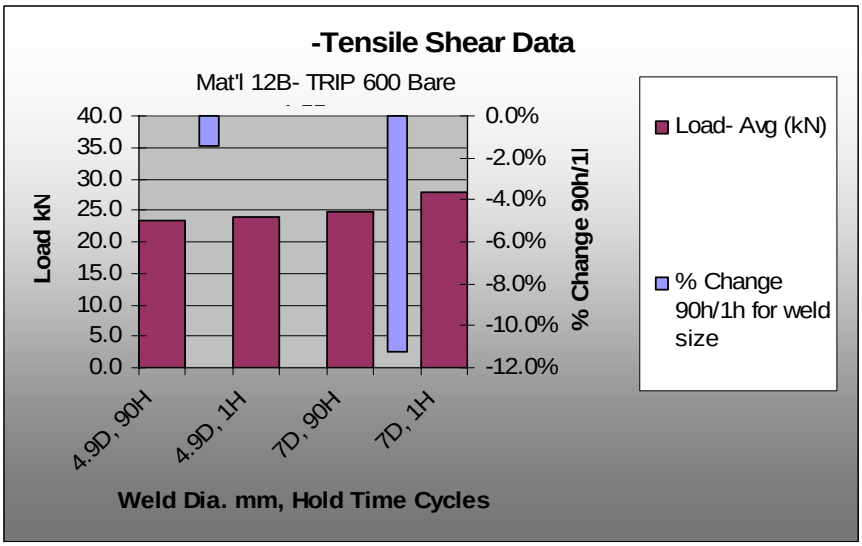
-Tensile Shear Data
Mat'l 12B- TRIP 600 Bare
Load kN
% Change 90h/1h
40.0
35.0
30.0
25.0
20.0
15.0
10.0
5.0
0.0
0.0%
-2.0%
-4.0%
-6.0%
-8.0%
-10.0%
-12.0%
4.9D, 90H
4.9D, 1H
7D, 90H
7D, 1H
Load- Avg (kN)
% Change 90h/1h for weld size
Weld Dia. mm, Hold Time Cycles

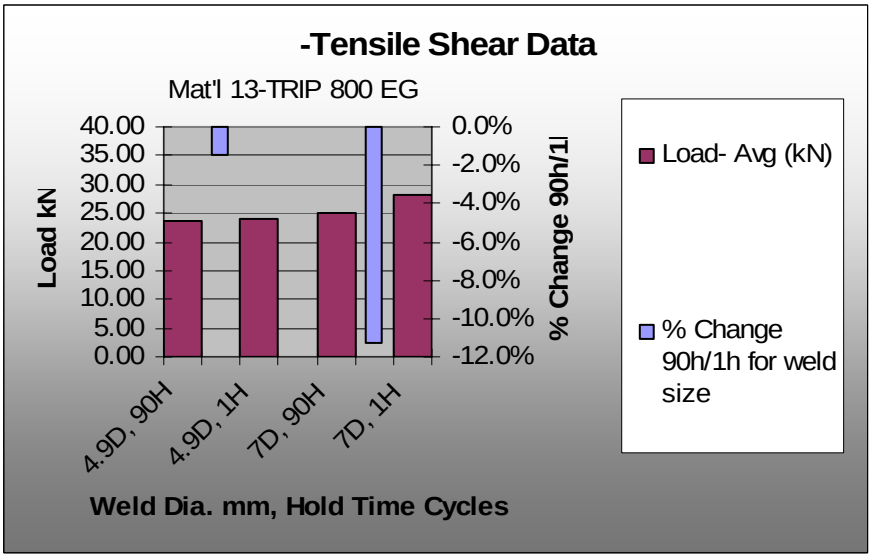
-Tensile Shear Data
Mat'l 13-TRIP 800 EG
Load kN
% Change 90h/1h
40.00
35.00
30.00
25.00
20.00
15.00
10.00
5.00
0.00
0.0%
-2.0%
-4.0%
-6.0%
-8.0%
-10.0%
-12.0%
4.9D, 90H
4.9D, 1H
7D, 90H
7D, 1H
Load- Avg (kN)
% Change 90h/1h for weld size
Weld Dia. mm, Hold Time Cycles

Appendix J - Fracture classification chart

This example of the development phase of the fracture classification chart during the project. Please refer to the AWS D8 standards for released versions of this.

WELD FRACTURE CLASSIFICATION

Fracture Type & Code Number	Weld Fractures - Side View	Weld Fracture Plan View & Code Letter - Bottom Sheet (all may not appear as in side view)					
		A Approximately Round	B Approximately Oval	C With Hollow Area	D Approximately Crescent Shaped	E With Irregular Button/Fused Area	F With Multiple Button/Fused Area
1 Button Pull - Thru sheet button pulled without any evidence of interfacial fracture	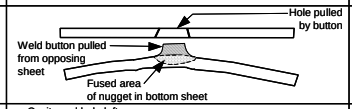			One example of many possible situations	One example of many possible situations	One example of many possible situations	One example of many possible situations
2 Partial Thickness Fracture + thru sheet button	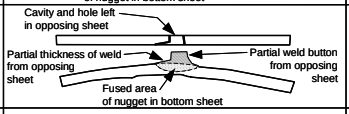	Two examples of many possible situations	Two examples of many possible situations	One example of many possible situations	One example of many possible situations	One example of many possible situations	One example of many possible situations
3 Partial Thickness Fracture - Weld fractures at point partially thru opposing sheet	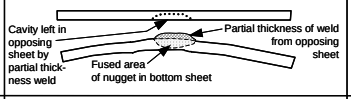			One example of many possible situations	One example of many possible situations	One example of many possible situations	One example of many possible situations
4 Partial Interfacial Fracture + Partial Thickness Fracture + thru sheet button	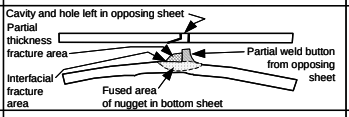	Two examples of many possible situations	Two examples of many possible situations	One example of many possible situations	One example of many possible situations	One example of many possible situations	One example of many possible situations
5 Partial Interfacial Fracture + thru sheet button	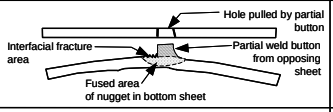	Two examples of many possible situations	Two examples of many possible situations	One example of many possible situations	One example of many possible situations	One example of many possible situations	One example of many possible situations
6 Partial Interfacial Fracture + Partial Thickness Fracture	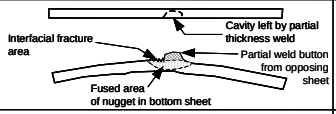	Two examples of many possible situations	Two examples of many possible situations	One example of many possible situations	One example of many possible situations	One example of many possible situations	One example of many possible situations
7 Full Interfacial Fracture- Interfacial fracture exists without evidence of through sheet button pull or partial thickness fracture	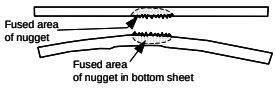			Not Applicable	One example of many possible situations	One example of many possible situations	One example of many possible situations
8 No Fusion - (No evidence of fused area the vicinity where weld current had passed)	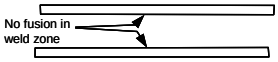			Not Applicable	One example of many possible situations	One example of many possible situations	One example of many possible situations

TWM6@DCX.com FractureD8F+D89Rev7.ppt

2000 Town Center, Suite 320
Southfield, Michigan 48075
Tel: 248.945.4777
www.a-sp.org